SPATIAL DROUGHT RISK ASSESSMENT USING STANDARDIZED PRECIPITATION INDEX AND EFFECTIVE DROUGHT INDEX: EDWARDS AQUIFER REGION

A Thesis

by

GOKHAN YILDIRIM

Submitted to the Office of Graduate and Professional Studies of
Texas A&M University
in partial fulfillment of the requirements for the degree of

MASTER OF SCIENCE

Chair of Committee,	Vijay P. Singh
Committee Members,	Raghupathy Karthikeyan
	Ralph A. Wurbs
Head of Department,	Stephen W. Searcy

May 2015

Major Subject: Biological and Agricultural Engineering

ABSTRACT

Though drought is a recurrent natural disaster in Texas, little attention has been so far paid to the preparedness of drought for spatial drought risk assessment. This study presents a methodology for spatial assessment of drought hazard, vulnerability, and risk in the Edwards Aquifer (EA) region. A conceptual data-based framework for drought hazard and vulnerability was developed in this study. Standardized Precipitation Index (SPI) and Effective Drought Index (EDI) methods were used to identify Drought Hazard Index (DHI) in different time steps, while the GIS environment was used to map the spatial extents of drought hazards. Drought Vulnerability Index (DVI) was identified by using different social and physical consequences of drought and a thematic map was prepared on the county level for vulnerability assessment. The risk, as a result, was computed as the product of intersection between both the DHI and DVI. Very high drought risk was found by 9 and 24-month SPI and EDI in Bexar (9.8% of the area). The highest percentage of the area in high level drought risk was detected by 1 and 12-month SPI as 32.3% of the area and 3-mont SPI found the highest moderate percentage of the area (79.5%). Bexar was found under drought risk based on all time scale SPI and EDI (very high drought risk based on 9, 24-month SPIs and EDI). Medina, furthermore, was detected in high drought risk in terms of all time scale SPI (except 3-month SPI) and EDI. In general, drought risk is higher in counties of the southern part of the area. The results confirmed that higher drought risks are found where both high hazard and high vulnerability coincide.

DEDICATION

This thesis is dedicated to my family who supported me through my time at Texas A&M University

To my parents, Halis and Zeynep Yıldırım

To my siblings, Fadime, Kudret, and Ömer Yıldırım

For their unconditional love. Thank you.

ACKNOWLEDGEMENTS

I would like to express sincere appreciation to my advisor, Dr. Vijay P. Singh, for recommending this research topic and for his guidance, knowledge, patience, and support throughout the study. I also would like to thank my committee members, Dr. Raghupathy Karthikeyan and Dr. Ralph A. Wurbs.

I would like to thank my roommates Mustafa Karabacak and Basri Omac. I also would like to thank Yusuf Turhan for his support and help. Thanks to Abdulkadir Bostanci and Burak Erdogan for their support.

Profound thanks to C. Prakash Khedun for sacrificing his time and kindly providing help vital to completion of this study. I would like to also thank Selim Dogan his support and suggestions.

Finally, thanks to my parents for their encouragement.

TABLE OF CONTENTS

LIST OF FIGURES

Page

LIST OF TABLES

Page

1. INTRODUCTION

1.1 Background

Drought affects more people than any other natural hazard and it is considered by many to be the most complex but least understood of all natural hazards (Hagman, 1984). Even if a universal definition of drought is difficult to specify, the general meaning of drought can be expressed as "deficit of water." Drought is a creeping, slow-onset phenomenon that is normal part of all climatic regimes for all regions in the world. Drought is considered a meteorological fact which is a result of meteorological anomaly (e.g., temperature, moisture, and precipitation) and abnormal water deficiency. Bryant (1991) ranked hazard events by characteristics and impacts, and drought was ranked first among damaging natural hazards (e.g., tropical cyclones, regional floods, earthquakes, tornados, and volcanos). Drought has largely non-structural characteristics and damages larger geographical areas when compared with other natural hazards. The impacts of drought are often categorized as hydrologic, agricultural, economic, social, health, ecological, and environmental. Besides, some of these impacts are difficult to quantify because of the non-structural nature of droughts. Drought preparedness planning should be considered to minimize the effects of drought on people and resources. For this goal, drought components, called hazard and vulnerability, have to be quantified. While hazard is the probability of occurrence of the event, vulnerability refers to the exposure to the hazard. As a result, risk is the product of hazard and vulnerability. In this way, drought

risk assessment is the most essential part of the drought risk management and to response to drought on time.

Drought is a recurring natural phenomenon in Texas that has faced notable droughts since the 1930s. The longest drought event observed in the 1950s in Texas, was as a seven- year drought. However, the drought in 2011 was the driest in the state history. Precipitation was only 267 mm from October 2010 to September 2011. Agrilife Extension economists compiled economic drought losses from 1998 to 2011 as $2.4 billion, $223 million, $1.1 billion, $316 million, $4.1 billion, $1.4 billion, $3.6 billion, $5.2 billion for 1998, 1999, 2000, 2002, 2006, 2008, 2009, 2011, respectively (Agrilife, 2011). Texas also faced a drought which started in 1995 and the drought carried over from western to eastern part in 1996. The losses due to this drought in Texas were reported as $5 billion (Fohn, 1996). The Edwards Aquifer Conservation District issued warnings to cut the water usage by 20 percent because of excessive consumption of groundwater supplies after that drought disaster (U.S. Water News Online, 1996). Cutting water usage was enforced to protect and manage the groundwater which reached a critical level (Edwards Aquifer Authority, 1996). Because Edwards Aquifer (EA) is the most prolific artesian and permeable aquifer in the USA, the Edwards Aquifer Authority (EAA) was established in May 1993 by the 73rd Texas Legislature to manage, protect and enhance the groundwater resource. The water cut or pumping limitation has lasted to the present and now to preserve water resources 30-40 percent water cut (for municipal, agricultural and industrial aims) have been in force since April, 2014 by EAA.

Texas Water Development Board (TWDB, 2014) reports that groundwater provides 60 percent of water used in Texas and this shows that groundwater is a major source of water in Texas. There are 9 major aquifers in Texas (Carrizo–Wilcox, Edwards, Edwards–Trinity, Gulf Coast, Hueco–Mesilla Bolsons, Ogallala, Pecos Valley, Seymour, and Trinity) and the EA is one of the major aquifers in the state. The EA is a crucial water source for municipal, agricultural, and industrial users in the region. Because of the climate change and increasing regional water demand, water storage and also flora-fauna species are under the risk due to the deficit of water. In this regard, meteorological drought risk assessment was addressed in the EA region and the relation of groundwater and rainfall due to drought was examined. This study will help determine which area is more vulnerable to drought and detect the area under risk due to drought. Besides, areal extent, severity, and duration of drought are used for drought preparedness and planning (Mishra and Singh, 2011). Hence, spatial drought risk assessment in the EA region will be the key for mitigation and drought preparedness planning.

1.2 Objectives

The overall objective of this thesis is to quantify the spatial drought risk in the Edwards Aquifer region which is located in the south-central part of Texas by using "standardized precipitation index" and "effective drought index." The thesis will focus on a conceptual risk model which is explained in the "Methodology" section. For this aim, drought hazard assessment and drought vulnerability assessment will be quantified to

identify drought risk by using hydro-meteorological and socio-economic data. In light of the above, the following specific objective will be addressed:

1. Determine the missing precipitation data and fill in the missing data by using the normal ratio method.
2. Calculate the Standardized Precipitation Index (SPI) by using the probability density function (gamma distribution) for seven different time-steps (1, 3, 6, 9, 12, 24, and 36 months).
3. Calculate the Effective Drought Index (EDI) from effective monthly precipitation.
4. Classify drought characteristics (such as duration, magnitude, and intensity) based on SPI and EDI for each rain gauge station.
5. Map the spatial extent of drought characteristics for each SPI and EDI in a GIS environment by using the kriging interpolation method and natural breaks method.
6. Quantify drought hazard by calculating the drought occurrence probability for each station.
7. Determine drought vulnerability factors and calculate drought vulnerability by using local indicators.
8. Quantify drought risk which is the product of hazard and vulnerability and map its spatial extent
9. Depict "drought hazard assessment," "drought vulnerability assessment" and "drought risk assessment" from regional to county level.
10. Determine the relation between meteorological drought and groundwater level in the Edwards Aquifer.

2. LITERATURE REVIEW

2.1 Drought definitions

There is no unique and universal definition of drought. Drought is a stochastic phenomenon that can be interpreted from several perspectives. Even though the central meaning in all of the definitions of drought is the shortage of water, there are more than 150 published definitions of drought (Wilhite and Glantz, 1987). For instance, while the American Heritage Dictionary (1976) defines drought as "a long period with no rain, especially during a planting season," Random House Dictionary (1969) defines drought as "an extended period of dry weather, especially one injurious to crops." Drought definitions have been categorized into conceptual (definitions formulated with general terms) and operational by Wilhite and Glantz (1987). Drought has conceptual and operational meanings, because drought is a complex phenomenon that can be defined from person to person (Hisdal and Tallaksen, 2003). Conceptual definitions-those stated in relative terms (e.g., a drought is a long, dry period), whereas operational definitions, on the other hand, attempt to identify the beginning, severity, and end of a drought. Mostly, the operational definition of a drought can be used to identify drought frequency, severity, and duration for a given return period (Mishra and Singh, 2010). Some of the common definitions of drought are given below:

- Drought was defined as 'Drought as the smallest annual value of daily stream flow' by (Gumbel, 1963).

- Palmer (1965) expressed 'Drought as a significant deviation from the normal hydrologic condition of an area.'
- World Meteorological Organization (WMO) (1986) defines drought as: 'Drought means a sustained, extended deficiency in precipitation.'
- United Nations Convention to Combat Drought (UN Secretariat General, 1994) describes: 'Drought means the naturally occurring phenomenon that exists when precipitation has been significantly below normal recorded levels, causing serious hydrological imbalances that adversely affect land resource production systems.'
- Definition given by Schneider (1996) states that 'An extended period—a season, a year, or several years—of deficient rainfall relative to the statistical multi-year mean for a region.'
- 'Drought is an insidious natural hazard that results from a deficiency of precipitation from expected or "normal" that, when extended over a season or longer, is insufficient to meet the demands of human activities and the environment' (Wilhite and Buchanan-Smith, 2005).

From the above definitions it can be understood that drought is mainly concerned with the considerable deficit of water. Drought has been categorized, to grasp drought phenomenon, in different classes which are discussed below.

2.2 Classification of droughts

Droughts are generally classified into four major categories, based on the nature of water deficit (American Meteorological Society (AMS), 2004; Hennessy et al., 2008; Wilhite and Glantz, 1985) which include:

1. Meteorological drought is the least severe form and occurs as a result of any unexpected shortfall of precipitation. Meteorological drought has been commonly analyzed by using monthly precipitation data.
2. Hydrological drought occurs when natural stream flows or groundwater levels are sufficiently reduced to adversely impact water resources. Hydrological drought is assessed by using surface water area and volume, streamflow, infiltration, and groundwater level fluctuations.
3. Agricultural drought, usually, refers to a period with declining soil moisture and consequent crop failure without any reference to surface water resources. The severity of agricultural drought has been commonly assessed, based on soil moisture or as indirectly by PDSI.
4. Socio-economic drought is associated with the failure of water resources systems to meet the water demands, thus associating droughts with supply of and demand for an economic good (water).

While the socio-economic drought is considered as a water resources systems drought, the first three categories are referred to as environmental droughts (Wilhite, 2000)

2.3 Impacts of drought

Drought causes a complex web of impacts that traverse many sectors of economy and reaches well beyond the area experiencing physical drought. The impacts of drought are generally classified as economic, environmental, and social (Wilhite, 1992). Effects of a drought can be categorized as direct or indirect because of the dynamic nature of drought. Some direct impacts of drought can be given, such as reduced crop, forest productivity, increased fire hazard, reduced water levels, increased livestock and wildlife mortality rates, and so forth. Indirect impacts are the consequences of these direct impacts. As an illustration, reduced income for farmers and agri-business, increased prices for food and timber, unemployment, increased crime, migration and so on are the indirect impacts of drought phenomenon. Figure 1 shows the relationship between different types of drought and their impacts.

2.4 Drought indices

Drought indices are used to characterize and quantify drought severity by assimilating data from one or several variables, such as precipitation and soil moisture. The number of drought indices which have been proposed so far are more than one-hundred. Drought indices are commonly categorized, based on types of drought impacts, such as meteorological, agricultural, and hydrological. Drought Preparedness Council (DPC) has developed three types of functional assessment in State of Texas Drought Preparedness Plan which was released in 2005: climatological assessment, agricultural, and water availability assessment. The DPC uses twelve different drought indices for

climatological, agricultural, and water availability assessments. Some popular drought indices which are used for meteorological, agricultural and hydrological droughts can be listed as follows:

- Standardized precipitation index (SPI)
- Palmer drought severity index (PDSI)
- Effective drought index (EDI)
- Crop moisture index (CMI)
- Surface water supply index (SWSI)
- Vegetation condition index (VCI)
- Standardized runoff index (SRI)
- Percent of normal (PN)
- Rainfall decile based drought index (RDDI)
- Normalized difference water index (NDWI) (remote sensing based)
- China-Z index (CZI)

In this work, SPI and EDI were used to characterize drought and quantify drought hazard and for risk assessment. Therefore, the following section discusses the SPI and the EDI and their limitations and advantages.

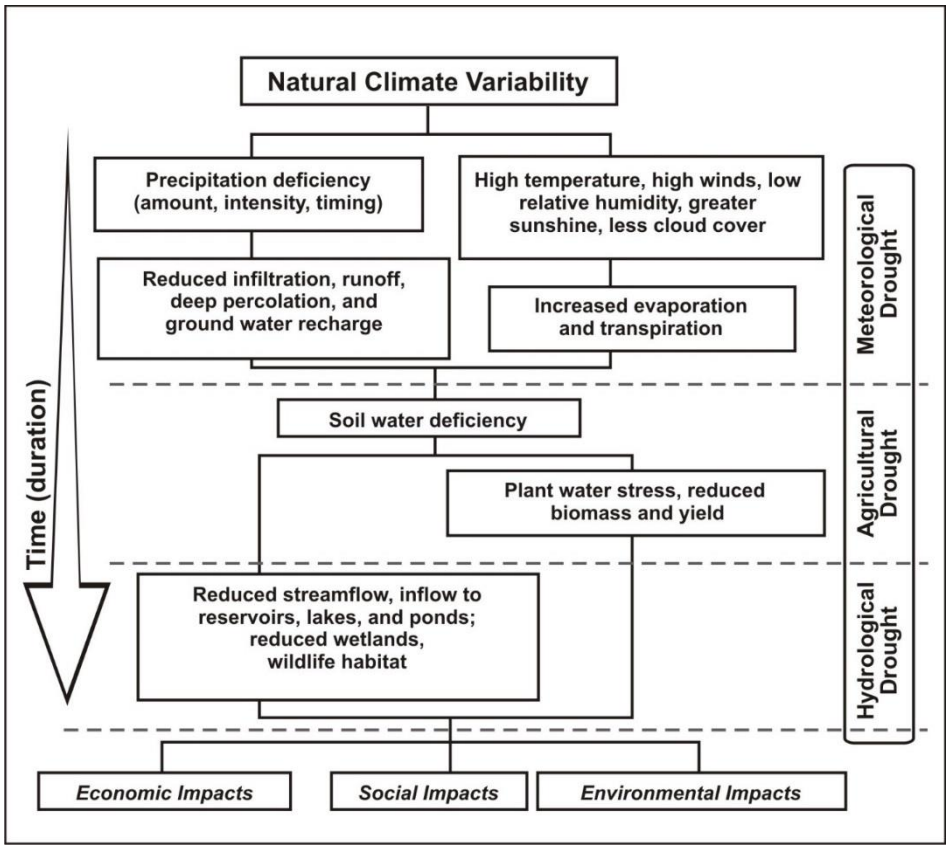

Figure 1. Relationship between various types of drought and duration of drought events, data source: (National Drought Mitigation Center, University of Nebraska-Lincoln, U.S.A.)

2.4.1 Standardized precipitation index

The Standardized Precipitation Index (SPI) was developed by McKee et al. (1993) to identify and monitor local droughts. The SPI is based on the probability of precipitation for multiple time scales. Short-term or long-term drought and dry or wet conditions can be defined by using the SPI for different timescales (1, 3, 6, 9, 12, 48 month SPI, etc.). At least 20-30 years of data are required to calculate the SPI (Guttman, 1994). Long-term precipitation record for any desired time scale is fitted to a gamma probability distribution and then transformed into a normal distribution. As a result, the SPI reflects the number

of standard deviations that a particular event deviates from the normal conditions. The SPI is one of the most popular drought indices used worldwide: Turkey, Greece, China, Italy, North Africa, India, Spain, Europe and so forth. The U.S. National Drought Mitigation Center and the U.S. Western Regional Climate Center compute the SPI for monitoring drought and they advocate the SPI over the traditional PDSI (Redmond, 2000).

2.4.2 Effective drought index

The Effective Drought Index (EDI) was developed by Byun and Wilhite (1999) for the purpose of defining and monitoring drought and its onset, end, and accumulated stress. Effective precipitation concept was defined to calculate the EDI. The EDI is calculated originally at a daily timestep (Akhtari et al., 2009; Kim et al., 2009). However, it can be calculated from monthly rainfall data, even though its original form is computed from daily data (Dogan et al., 2012; Pandey et al., 2008). The EDI is not as popular a drought index as is the SPI. Its calculation has some complexity and difficulties in calculation. Dogan et al. (2012) state that the EDI is preferable for monitoring long term droughts, even if the input data is monthly rainfall.

2.4.3 Strengths and limitations of the EDI and the SPI

The only input parameter is precipitation for the SPI. This can be a strength or a limitation of the SPI based on different points of view. The SPI can be computed on a monthly or yearly time scale, provides monitoring of drought and helps assess the drought severity. The SPI is less complex than many other drought indices like the Palmer drought

severity index. It is flexible for multiple timescales and easy to compute. However, soil water-balance component and evapotranspiration (or potential evapotranspiration) are not used to calculate and this can be viewed as a weakness of the SPI. Furthermore, the probability distribution due to the length of data plays an important role for the calculation of the SPI (Mishra and Singh, 2010).

The EDI is a time independent index and can computed both daily and monthly. The EDI overcomes to identify the onset and end of a drought and calculates drought duration (Byun and Wilhite, 1999). Similar to the SPI, long term precipitation is the only input data for the EDI.

2.5 Drought risk assessment

Risk assessment of a natural hazard is often difficult and complicated. Although some studies have attempted to address risk assessment, they are still limited in literature. A methodology to identify and measure disaster risk has not yet been developed (Du and Lin, 2012). In a seminal work Kates and Kasperson (1983) worked on risk assessment that has corroborated later by Smith (1996), Wilson and Crouch (1987), and O'Brien (2000). Risk assessment is composed of three components:

(i) Identification of hazard,
(ii) evaluation of social consequences, and
(iii) estimation of risk and vulnerability

Hazard and vulnerability components can be used to identify drought risk (Wilhite, 2000). Although drought risk is difficult and complex, it can be quantified from both

"hazard" and "vulnerability." Hazard analysis mainly determines the probability of a natural disaster occurrence, while vulnerability analysis focuses on environmental, social, or physical factors. Even though, hazard and vulnerability assessments have been made by some researchers, there are still considerable shortcomings in their combinations (Du and Lin, 2012).

Kim et al. (2013) worked on drought a risk concept in South Korea by using the EDI. They focused on the combination of drought hazard and vulnerability to quantify drought risk. Drought hazard was detected from the probability of occurrence by using daily EDI. Vulnerability was analyzed using various inflation factors to normalize vulnerability indicators which were selected for the study area. An index was generated for each hazard and vulnerability to obtain a drought risk index by multiplying both hazard and vulnerability.

Sonmez et al. (2005) analyzed spatial and temporal dimensions of meteorological drought vulnerability in Turkey by using 3, 6, 12, and 24 month SPI. The SPI was computed by the classical gamma distribution approach which is explained by Guttman (1999). The frequency of drought occurrence and its spatial distribution were used to identify drought- prone areas and vulnerability. The study defined a threshold rainfall to determine the minimum moisture input required for non-drought conditions.

Chen et al. (2001) addressed a regional model, based on both hydrological and economic activities, and water resource availability in the San Antonio EA region. The Canadian Climate Center Model (CCC) and the Hadley Climate Center Model (HAD) were run by using greenhouse gas and sulfate emission scenarios published by

Intergovernmental Panel on Climate Change. Historical temperature and precipitation data from period 1966 to 1995 were used. Climate conditions in the EA were forecasted for the period 2001 to 2100 by using the CCC model and the HAD model. Results showed that changing climatic conditions reduced the water source and increased water demand in the EA region. Besides, regional welfare loss of $2.2-$6.8 million per year arose due to the climate change and pumping could be reduced by 9-20 % to maintain the desired level for spring flows.

Zelenakova et al. (2012) investigated precipitation-temperature trends by using the non-parametric Mann-Kendall test for drought risk. They claim that there is high correlation between drought and these parameters. Meteorological drought was assessed by the non-parametric Mann-Kendall test. This test is simple, robust and copes with missing values and values below a detection limit. Ferrier and Haque (2003) proposed a standardized framework for hazards risk assessment for mitigation of natural hazards. The framework includes numerical ranking of the frequency of the event in a specific community, based on the potential impact characteristics of a worst scenario. Dilley et al. (2005) projected relative levels of risks of disaster-related mortality, and economic losses were calculated for the population and gross domestic product (GDP) (based on 2.5' x 2.5' latitude-longitude grid cells). Results showed that drought risk areas were much more spatially extensive, with mortality risks and risks of economic losses in proportion to GDP.

3. METHODOLOGY

In this study, setting a conceptual risk model was aimed for regional drought that separates assessment into three sections: hazard analysis, vulnerability assessment, and risk assessment based on Standardized Precipitation Index (SPI) and Effective Drought Index (EDI). This section outlines the methodology used in the study. Drought risk assessment consists of two parts: drought hazard analysis and vulnerability analysis. Drought hazard index (DHI), in this study, was determined separately for two different drought indices which are the SPI and the EDI. A schematic presentation of the methodology that has been followed as shown in Figure 2.

3.1 Drought characteristics

Some quantities of drought need to be analyzed in order to monitor, quantify, and interpret a drought. These quantities are known as duration (D), severity, magnitude (M), frequency, and intensity (I). There is not a universal usage of these terms. Meaning and usage of these terms have been switched at one time or another. For instance, while Yevjevich (1967) uses the terms of run-sum, run-length, and run-intensity, Dracup et al. (1980) use severity, duration, and magnitude. In this study, the mostly adopted terminology was used, such as duration, magnitude, and intensity. A drought begins any time when the drought index (DI) (the drought index, in this section, refers to the SPI or the EDI) is continuously negative and reaches an intensity of -1.0 or less.

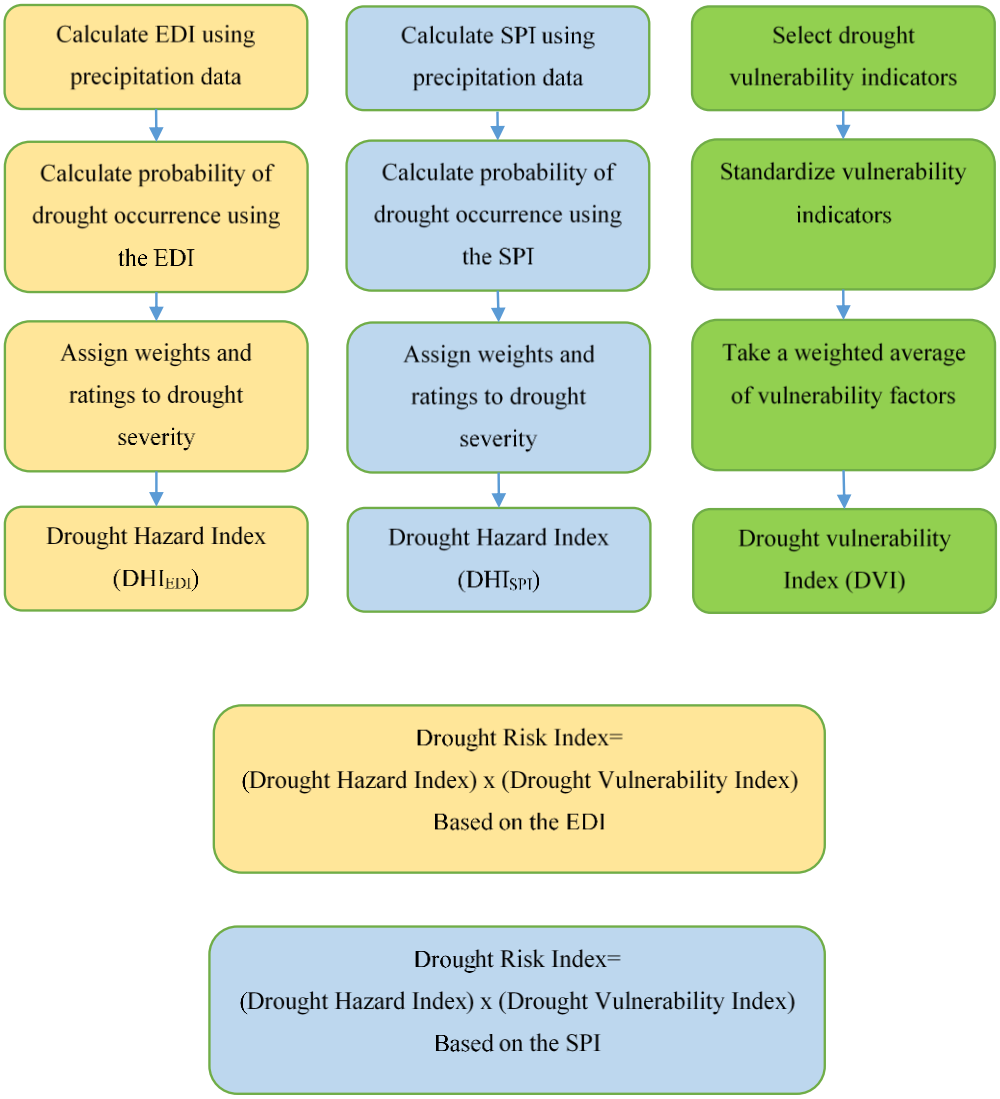

Figure 2. Procedure for calculating hazard-vulnerability and risk index

Drought ends when the DI becomes positive. Duration is defined as the period between drought onset and end time. Magnitude is the accumulated deficit of water (e.g. precipitation) during the drought. In other words, magnitude is defined as the positive sum of the DI for all the months within a drought event. Intensity is defined as the drought

magnitude by dividing the duration. Return period (R) is the duration between two consecutive drought events and interarrival time (T_1 and T_2) refers to the period of time from the onset of a drought to the onset of a next drought event, as shown in Figure 3. Drought classifications of drought indices are shown in Table 1 (Dogan et al., 2012; Kim et al., 2009).

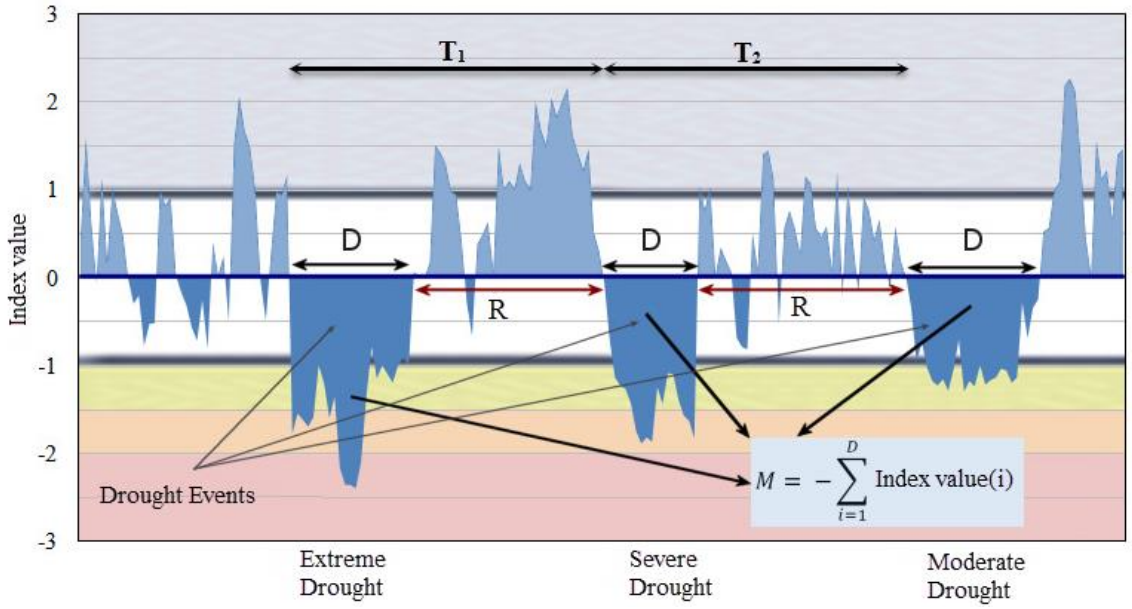

Figure 3. Drought characteristics and drought terms (source: modified from Dogan, S., Ph.D. Thesis (2013)

Table 1 Drought category according to drought indices

Drought Index	Extreme Drought (ED)	Severe Drought (SD)	Moderate Drought (MD)	Near Normal (NND)
SPI	≤ -2.00	(-1.99) - (-1.50)	(-1.49) – (-1.00)	(-0.99) – (0.99)
EDI	≤ -2.00	(-1.99) - (-1.50)	(-1.49) – (-1.00)	(-0.99) – (0.99)

*Wet condition is not shown.

3.1.1 Calculations of drought indices

In this chapter, the method of calculations of drought indices which are used in the thesis study will be shown. There are 31 rain-gauge stations located in the EA. The SPI and the EDI analysis was addressed, based on these rain-gauge stations. The SPI and the EDI calculations constitute the first part of the risk assessment model which is called the hazard assessment.

3.1.1.1 Standardized precipitation index

The SPI calculation is based upon the long-term precipitation data for different time steps (the time steps used in this study are 1, 3, 6, 9, 12, 24, 36 months). In the classical approach of obtaining an SPI, the cumulative distribution function of precipitation totals is formed from the fitted frequency distribution. Then the probabilities from the fitted cumulative distribution function are transformed to the standard normal distribution by using the inverse standard normal distribution. The method, therefore, consists of a transformation of one probability distribution (e.g., gamma or Pearson type III) to another (standard normal distribution).

This study used the gamma distribution which is defined by its probability density function:

$$g(x) = \frac{1}{\beta^{\alpha}\Gamma(\alpha)} x^{\alpha-1} e^{-x/\beta}, \quad \text{for } x > 0 \tag{1}$$

where $\alpha > 0$ is α shape parameter, $\beta > 0$ is a scale parameter, and $x > 0$ is the amount of precipitation. $\Gamma(\alpha)$ is the gamma function. Fitting the distribution to the data requires α

and β to be estimated for each station, for each time-scale of interest (1, 3, 6, 9, 12, 24, and 36 months). Using the approximation (the maximum likelihood method) of Thom (1958), these parameters were estimated as follows:

$$\alpha = \frac{1}{4A}\left(1 + \sqrt{1 + \frac{4A}{3}}\right) \; and \; \beta = \frac{\bar{x}}{\alpha} \tag{2}$$

$$A = \ln(\bar{x}) - \frac{\sum_{i=1}^{n} \ln(x_i)}{n} \tag{3}$$

where n is the number of observations, and $\bar{x}$ is the mean of observed values. These parameters were then used to find the cumulative probability of an observed precipitation for the given time scale. Integrating the probability density function with respect to x yields the following expression G(x) for the cumulative probability:

$$G(x) = \int_0^x g(x)dx = \frac{1}{\beta^{\alpha}\Gamma(\alpha)} \int_0^x x^{\alpha-1} e^{-x/\beta} dx \tag{4}$$

Equation (4) is the incomplete gamma function. Thom (1966) used tables of the incomplete gamma function to define G(x), the cumulative probability. It is possible to have several zero values in a sample set and the gamma distribution is undefined for zero values. Thus, the cumulative probability was defined as

$$H(x) = q + (1 - q)G(x) \tag{5}$$

where q is the probability of a zero precipitation value. If m is the number of zeros in a given dataset of n values, then q can be estimated by m/n (Thom, 1966). H(x), the cumulative probability, was transformed to the standard normal random variable Z (or the SPI value). The SPI value, which is obtained from the standard normal distribution has 0 mean and variance of 1. This transformation is illustrated in Figure 4. Besides, the standard normal distribution has to be defined to understand the transformation concept and the relation between the SPI and the z-score. Abramowitz and Stegun (1965) provided an approximation to convert the cumulative probability to the standard normal random variable Z as

$$Z = -\left(t - \frac{c_0 + c_1 t + c_2 t^2}{1 + d_1 t + d_2 t^2 + d_3 t^3}\right) \quad \text{for } 0 < H(x) \leq 0.5 \tag{6}$$

$$Z = +\left(t - \frac{c_0 + c_1 t + c_2 t^2}{1 + d_1 t + d_2 t^2 + d_3 t^3}\right) \quad \text{for } 0.5 < H(x) \leq 1.0 \tag{7}$$

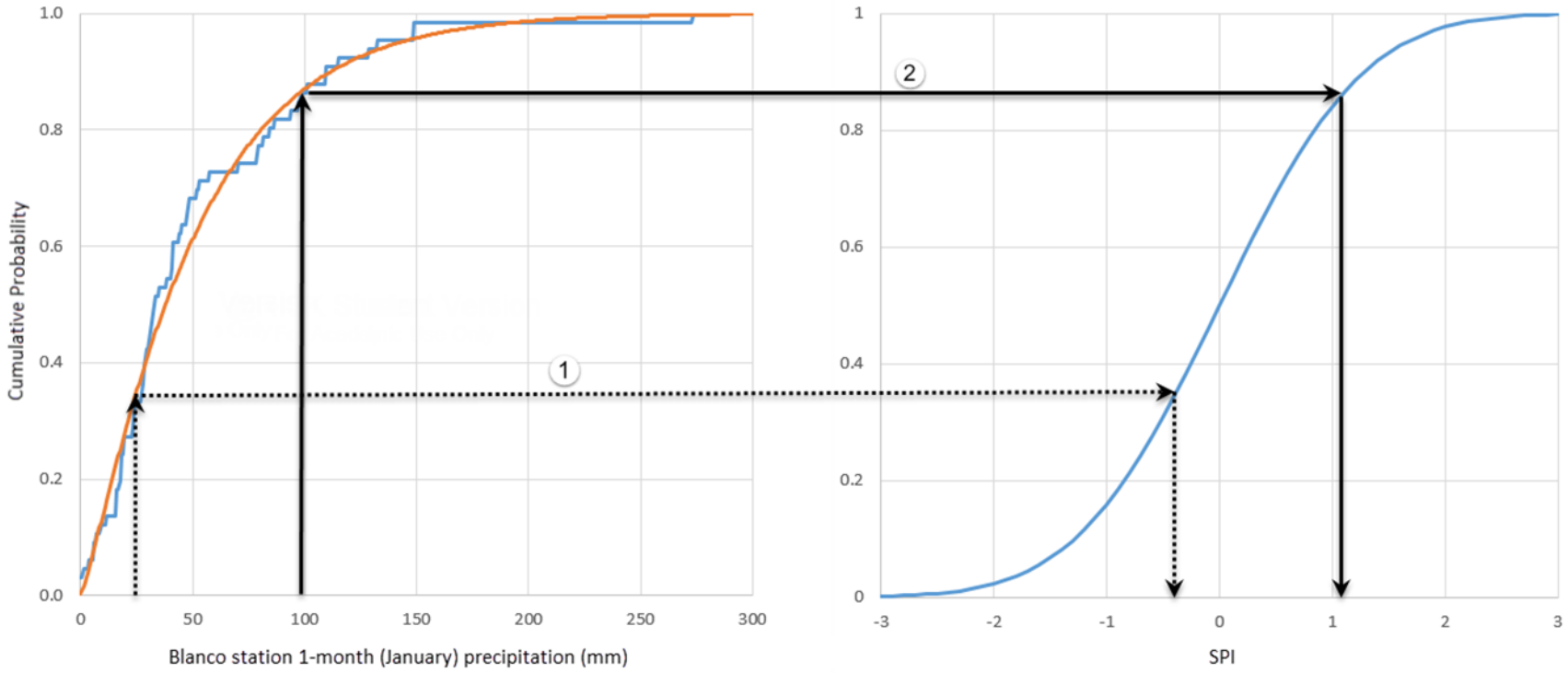

Figure 4. Example of equiprobability transformation from fitted gamma distribution to the standard normal distribution

where

$$t = \sqrt{ln\left(\frac{1}{(H(x))^2}\right)} \qquad \text{for } 0 < H(x) \leq 0.5 \tag{8}$$

$$t = \sqrt{ln\left(\frac{1}{(1 - H(x))^2}\right)} \qquad \text{for } 0.5 < H(x) \leq 1.0 \tag{9}$$

$$\begin{aligned} c_0 &= 2.515517 \\ c_1 &= 0.802853 \\ c_2 &= 0.010328 \\ d_1 &= 1.432788 \\ d_2 &= 0.189269 \\ d_3 &= 0.001308 \end{aligned} \tag{10}$$

Z in equations (6) and (7) refers to the SPI value. Figure 5 shows the standard normal distribution for the SPI with mean of zero and variance of 1. 1-month (January) SPI for the Blanco station was calculated to illustrate and explain the SPI calculation which is detailed above. First of all, all January average rainfall values were picked out from between 1948 and 2013. Then, A, α, and β parameters were estimated. In this way, to compare the results for this estimation, three different tools were used: MATLAB programming, @RISK software, and by formula. The results for the shape and scale parameters of gamma distribution are as follows:

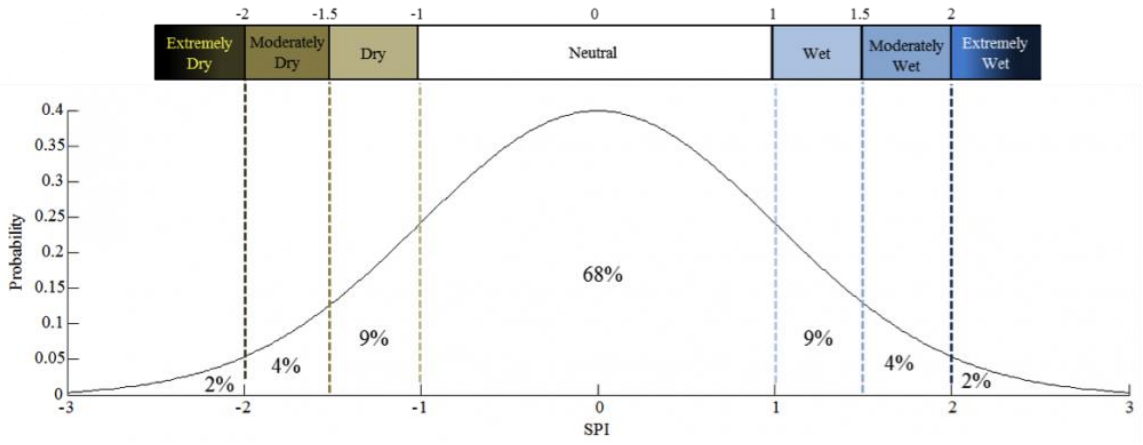

Figure 5. Standard normal distribution for the SPI (expected value and variance are 0 and 1, respectively) (source: contributed by Keyantash)

Table 2 Parameter estimation of gamma distribution

Parameters	MATLAB	@RISK	Formula*
α (shape)	1.1627	1.2314	1.2337
β (scale)	43.7302	41.5780	41.2174

*Parameters for formula: mean=50.85 mm, n=66 (years), A=0.46

Then, to obtain results, the incomplete gamma function has to be solved, based on the estimated parameters. Matlab programming, for this goal, was used to solve incomplete gamma function. After the cumulative probability G(x) was obtained, the cumulative probability H(x) values were found for transforming to the standard normal distribution.

Figure 4 illustrates the transformation from the fitted gamma to the standard normal distribution to obtain the SPI values. In this example, 1-month SPI (January) was calculated for 66 years between 1948 and 2013. Two transformation examples are shown

in Figure 4. The numbers are given 1 and 2 for the rows, line dash and solid, respectively. 25 mm and 99.1 mm observed precipitation values were used to determine the SPI values. Finding the SPI value for the 25 mm precipitation, go vertically upwards from the 25 mm mark on the x-axis on the left of Figure 4 until the curve is intersected. Then go horizontally to the right until the standard normal cumulative distribution curve is intersected. Then, keep on vertically downward to the x-axis on the right of Figure 4. Results of this transformation are roughly -0.42 and +1.13 for the 25 mm and 99.1 mm precipitation observation, respectively. Other time-scales were calculated by moving average in the same way. For instance, 3-month SPI for March: January, February, and March precipitation amount was used. 6-month SPI for March: October, November, December, January, February, and March.

3.1.1.2 Effective drought index

Long term precipitation data was used to calculate the EDI like the SPI. The EDI, however, is calculated only once, because the EDI is a time step independent index. The EDI is a function of the precipitation necessary to the return to normal condition (PRN). The EDI is calculated as follows. The first step is to compute the monthly effective precipitation (EP):

$$EP = \sum_{m=1}^{N} \left[\left(\sum_{i=1}^{m} P_i \right) / m \right] \tag{11}$$

where P_i is the precipitation and N is the duration of the preceding period.

Then the mean EP ($\overline{EP}$) is calculated to compute the deviation of effective precipitation (DEP)

Mean EP ($\overline{EP}$) is an EP calculated by using the averaged precipitation for 30 years.

$$DEP = EP - \overline{EP} \tag{12}$$

PRN is determined from

$$PRN = DEP \Big/ \sum_{i=1}^{N} \frac{1}{i} \tag{13}$$

Finally, the EDI is calculated as

$$EDI = PRN/\sigma_{PRN} \tag{14}$$

where σ_{PRN} is the standard deviation of the PRN values (for relevant months). EDI was developed normally for the daily time-steps. Therefore, monthly EDI program code was used for calculation of monthly time-step EDI.

3.2 Mapping and auxiliary tools

Mapping is an essential part of the illustration of spatial drought as a visual and effective tool to compare and depict how drought is distributed in a region. All drought

maps in this study, based on SPI and EDI, were created by using the Arc GIS 10.1 (ArcMap, ArcCatalog, ArcView) software. Three techniques, such as kriging interpolation method, natural breaks method and the Thiessen polygon method, were used to generate drought mapping in hazard assessment, and vulnerability analysis.

3.2.1 Kriging interpolation method

The kriging interpolation method used in hydro-science for interpolation and spatial analysis has proven quite accurate (Delhomme, 1978). Kriging is a useful spatial statistical technique, such as a point interpolation technique, to evaluate groundwater levels, estimate missing precipitation values, and so on. The kriging method is used mostly in geology and soil science. An example of kriging, which was created by using ArcMap 10.1 is shown in Figure 6.

3.2.2 Natural breaks method

The natural breaks method (NBM) is a classification method and generates a best arrangement of data for different classes. The NBM counts similar values and classifies similar arrangements. The NBM method works as an iterative process. The process uses some steps, such as calculation of the sum of squared deviations between ranges and calculation of the sum of squared deviations from the array mean. An accurate classification can be generated by using the NBM.

3.2.3 Thiessen polygon

The Thiessen polygon approach is probably the most common method used in hydrometeorology. Polygons are generated from a set of sample points. Each Thiessen polygon defines an area of influence around its sample point, so that any location inside the polygon is closer to that point than any other sample points. The GIS environment was used to determine the spatial extent of each rain gauge station. The Thiessen polygon method, in this study, was used to obtain the effective area of each rain gauge station. This effective area of each station was used to obtain the DHI as an auxiliary tool.

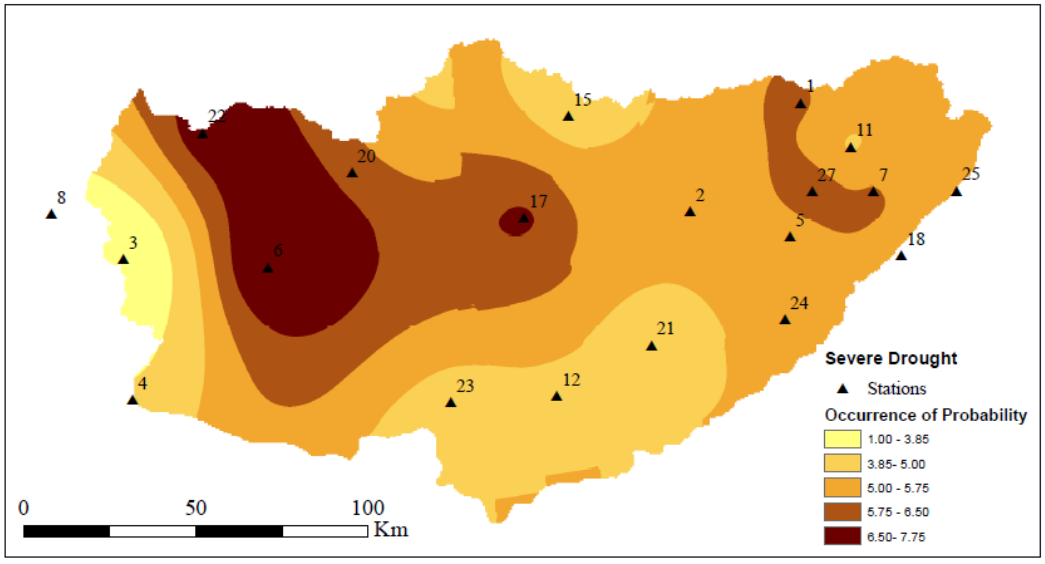

Figure 6. Probability of severe drought occurrence based on the EDI

3.2.4 Spatial variation

The EA region includes 12 counties and only one county (Bandera) is totally within the EA while Medina, Kendall, Kerr, Real, and Comal counties are mostly located in the EA. In this study, therefore, creating three spatial variations was aimed at by using the NBM to generate the hazard map. The EA was divided into 3 regions, based on the rainfall distribution, by using the NBM. In this way, each region has an accurate average rainfall range which is created by using an algorithm (the natural breaks method). Figure 7 illustrates the EA regions which are created by using the NBM. While the east of the EA has the highest average precipitation, the west of the EA has the lowest average rainfall distribution.

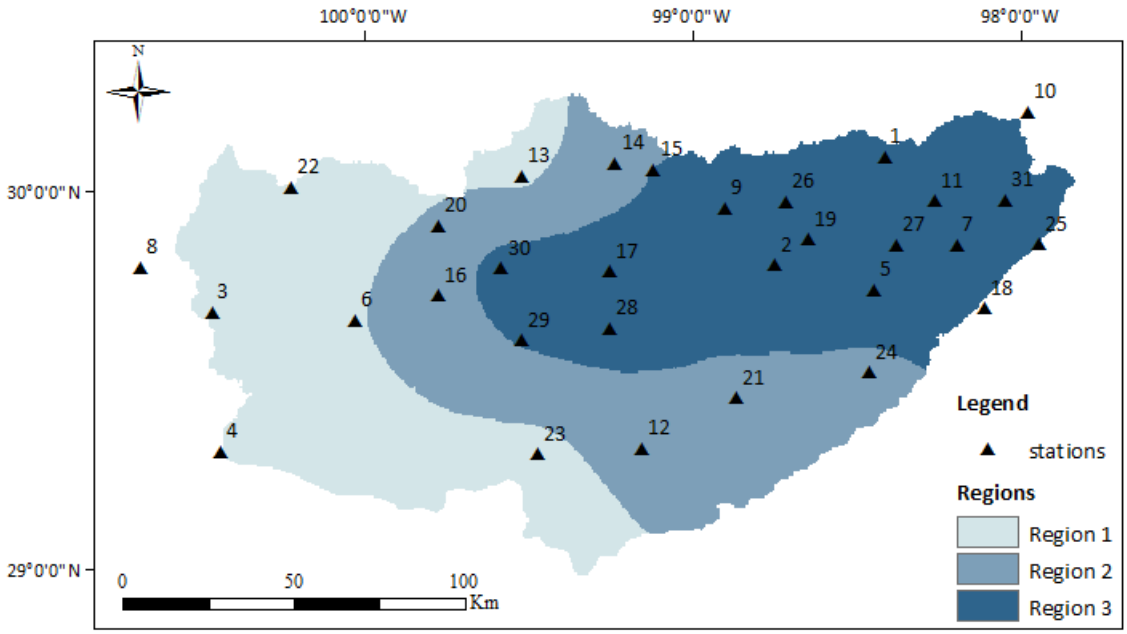

Figure 7. Spatial variations of the Edwards aquifer region

3.3 Drought hazard assessment

After the calculation of the SPI and the EDI, the next step is to determine the drought occurrence probability and then to define the weights and the ratings to create the drought hazard index (DHI). In this study, drought occurrences in the EA were examined, based upon the frequencies of events for each drought category for different time steps. "The percentages of drought occurrence are obtained by taking the ratio of drought occurrences in each time step to the total drought occurrences in the same time step and drought category" (Sonmez et al., 2005). The drought occurrence probabilities were calculated by using each drought event for all stations in the EA.

In this study, to quantify drought hazard by using the occurrence probability and severity, ratings and weights were assigned. First, the weights, from 1 to 4, were assigned according to the SPI and the EDI, based on Table 1. The assigned weights for the DIs are shown in Table 3.

Table 3 Assigned weights for the SPI and the EDI

Drought Index	Extreme Drought (ED_w)*	Severe Drought (SD_w)	Moderate Drought (MD_w)	Near Normal (NND_w)
SPI	4	3	2	1
EDI	4	3	2	1

* "w" is abbreviation the weight as shown subscript

Second, the ratings were assigned from 1 to 4 by evenly dividing the range of occurrence probabilities. Finally, DHI was calculated by combining the weights and the ratings as follows:

$$DHI = (NND_r \times NND_w) + (MD_r \times MD_w) + (SD_r \times SD_w) + (ED_r \times ED_w) \quad (15)$$

This formulation was applied to both the SPI and the EDI in order to calculate the DHI. Then, the DHI based on the SPI and the EDI was abbreviated as DHI_{SPI} and DHI_{EDI}, respectively. All drought categories, which are shown in Equation 15, were abbreviated with drought category and subscript denoting ratings and weights, for example, rating of near normal was abbreviated as NND_r and weight of severe drought as SD_w. If the rating is 1 for all drought conditions, NND, MD, SD, and ED, the minimum DHI would be 10 (=1x1+1x2+1x3+1x4). If the rating is 4 for the all conditions, the maximum DHI would be 40 (=4x1+4x2+4x3+4x4). Then, DHI was re-scaled throughout the normalization method from 10-40 range to 0-1, as shown in Equation 16:

$$Normalized(e_i) = \frac{e_i - E_{min}}{E_{max} - E_{min}} \quad (16)$$

where

E_{min} = the minimum value for variable E
E_{max} = the maximum value for variable E
e_i = normalized value

Then, the DHI was classified into four classes, such as “Low”, “Moderate”, “High”, and “Very High” as shown in Table 4.

Table 4 DHI classification by range

DHI range	DHI classes
0≤DHI<0.25	Low
0.25≤DHI<0.50	Moderate
0.50≤DHI<0.75	High
0.75≤DHI<1.0	Very High

3.4 Drought vulnerability assessment

Vulnerability has different definitions like drought for different communities and disciplines. International Strategy for Disaster Reduction (UN/ISDR) defines vulnerability as 'The conditions determined by physical, social, economic, and environmental factors or processes, which increase the susceptibility of a community to the impacts of hazards.' Vulnerability is difficult to define because of its dynamic character and its changing nature from region to region. Therefore, vulnerability indicators are defined, based on local context and the particular hazard (United Nations Development Programme, 2004). Seven drought vulnerability indicators were selected based on socio-economic and physical effects after careful consideration of obtainable and quantifiable indicators in the EA region. The indicators which were defined for the study area are population density, poverty level, irrigated land, municipal water, industrial water, agricultural water, and market value of products.

The assumptions regarding vulnerability to each of the indicators are described as follows:

1. **Population density (PD):** Population density represents a measurement of population per square mile. Natural disasters will affect more people when they happen in high population areas compared to less populated areas.
2. **Poverty level (PL):** Poverty level, in this study, is defined as the percentage of people who live below the lower poverty level in the area. There is a high link between poverty level and vulnerability. When poverty level decreases, vulnerability of people who have lower poverty level would increase.
3. **Irrigated land (IL):** Irrigated land is the area in acres used by farmers in each county. There is a high correlation between irrigated land and water demand. In the EA region, groundwater and surface water are used for irrigation, and the availability of these water resources is related to the meteorological drought.
4. **Municipal water (MW):** Municipal water is supplied from the Edwards Aquifer for the people who live in the region. Therefore, fluctuation in water resources due to drought is crucial for the people who live in that area.
5. **Industrial water (IW):** Industrial water, in this study, represents the total of manufacturing, mining, and steam electric power water uses in the region.
6. **Agricultural water (AW):** Agricultural water represents the sum of irrigation and livestock water usage. Water availability is directly related to agricultural use and water scarcity affects the crop yield. That means that the area, which demands more water use for agriculture, is more vulnerable than others.

Note: Total water (groundwater + surface water) input data was used for municipal, industrial, and agricultural water vulnerability indicators. The total water use in the region is 81 % groundwater and 19 % surface water

.

7. **Market value of products (MVOP):** The market value of products illustrates the livestock sales and crop sales in the US Dollars. While some counties have higher livestock sales (e.g., Bandera livestock sales: 89%-$9,925,000, crop sales: 11%-$1,263,000), others can be have higher crop sales as a percentage (e.g., Bexar county livestock sales: 24%-$17,682,000, crop sales: 76%-$54,705,000) (National

Agricultural Statistics Service of USDA, 2012). However, Bexar has higher livestock sales in US dollars, although Bandera has a higher percentage of livestock sales. Therefore, the use of percentage can lead to errors for the vulnerability assessment. In this regard, to use the total market value of products sold in monetary units is more realistic instead of the percentage of the product sold.

Four classes, ranging from the lowest to the highest values, were selected for the indicators which have been discussed above. The natural breaks method was used for grouping the classes. For all the indicator classes, higher values are given higher ratings and vice versa for lower ratings. The natural breaks method counts similar values and classifies similar ranges according to an algorithm that uses the average of each range to distribute the data more evenly across the ranges. ArcMap 10.1 was used to identify and analyze the natural breaks points in the data with the GIS software. The highest rating was 4, while the lowest rating was 1. After the all indicators are given ratings, the composite drought vulnerability index (DVI) of the integrated layers was defined from the indicators as follows:

$$\mathrm{DVI} = \frac{\mathrm{PD_r} + \mathrm{PL_r} + \mathrm{IL_r} + \mathrm{MW_r} + \mathrm{IW_r} + \mathrm{AW_r} + \mathrm{MVOP_r}}{\text{Number of indicators}} \tag{17}$$

The rating of population density (PD) was abbreviated as PD_r, and all other ratings of the indicators were abbreviated similar to PD_r. Based on the DVI calculation in equation (17), the maximum DVI would be 4 (=28/7), and the minimum DVI would be 1 (=7/7). This range was normalized from 1-4 to 0-1 by using equation (16). After normalization of

the values, DVI would be between 0 and 1. Figure 8 shows ranges for the percentage of people living below poverty level in the region for four classes.

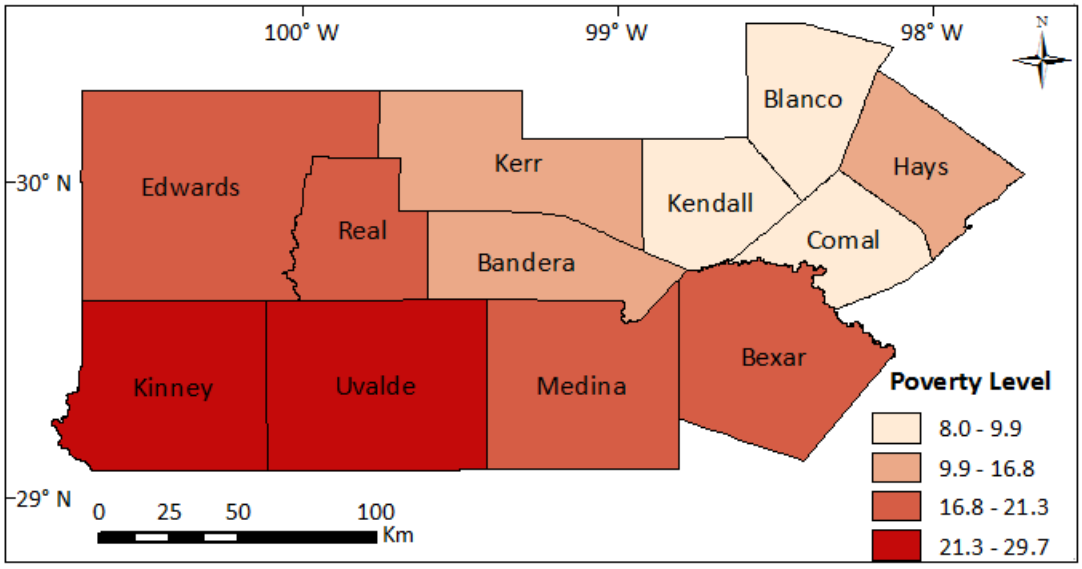

Figure 8. County level drought vulnerability indicator, percentage of people living below the poverty level

Based on this classification, ratings poverty levels in each county are shown in Table 5.

Table 5 Drought vulnerability ratings in county level for percentage of people living below the poverty level

County	Rating
Kinney, Uvalde	4
Bexar, Edwards, Medina, and Real	3
Bandera, Hays, and Kerr	2
Blanco, Comal, and Kendall	1

3.5 Drought risk assessment

In this study, a conceptual risk model was developed by using observed precipitation data and socio-economic data in the EA region. Risk depends on both hazard and vulnerability. Therefore, drought risk index (DRI) was calculated my multiplying drought hazard index (DHI) and drought vulnerability index (DVI) as follows(Blaikie et al., 1994; Downing and Bakker, 2000; Wilhite, 2000):

$$\mathrm{DRI} = \mathrm{DHIxDVI} \tag{18}$$

Four discrete classes were used for both hazard and vulnerability: low (0-0.25), moderate (0.25-0.50), high (0.50-0.75), and very high (0.75-1.00). Correspondingly, risk was classified into four classes using the same description but different value ranges, as shown in Table 6.

Table 6 Classification of hazard (H), vulnerability (V), and risk (R) for the spatial drought risk assessment

Class	R=H×V	H	V
Low	0.000-0.0625	0.00-0.25	0.00-0.25
Moderate	0.0625-0.250	0.25-0.50	0.25-0.50
High	0.250-0.5625	0.50-0.75	0.50-0.75
Very High	0.5625-1.000	0.75-1.00	0.75-1.00

The drought risk can be represented by plotting hazard versus vulnerability (Figure 9). The risk was divided into four classes by using three hyperbolas: H=0.0625/V, H=0.250/V, and H=0.5625/V.

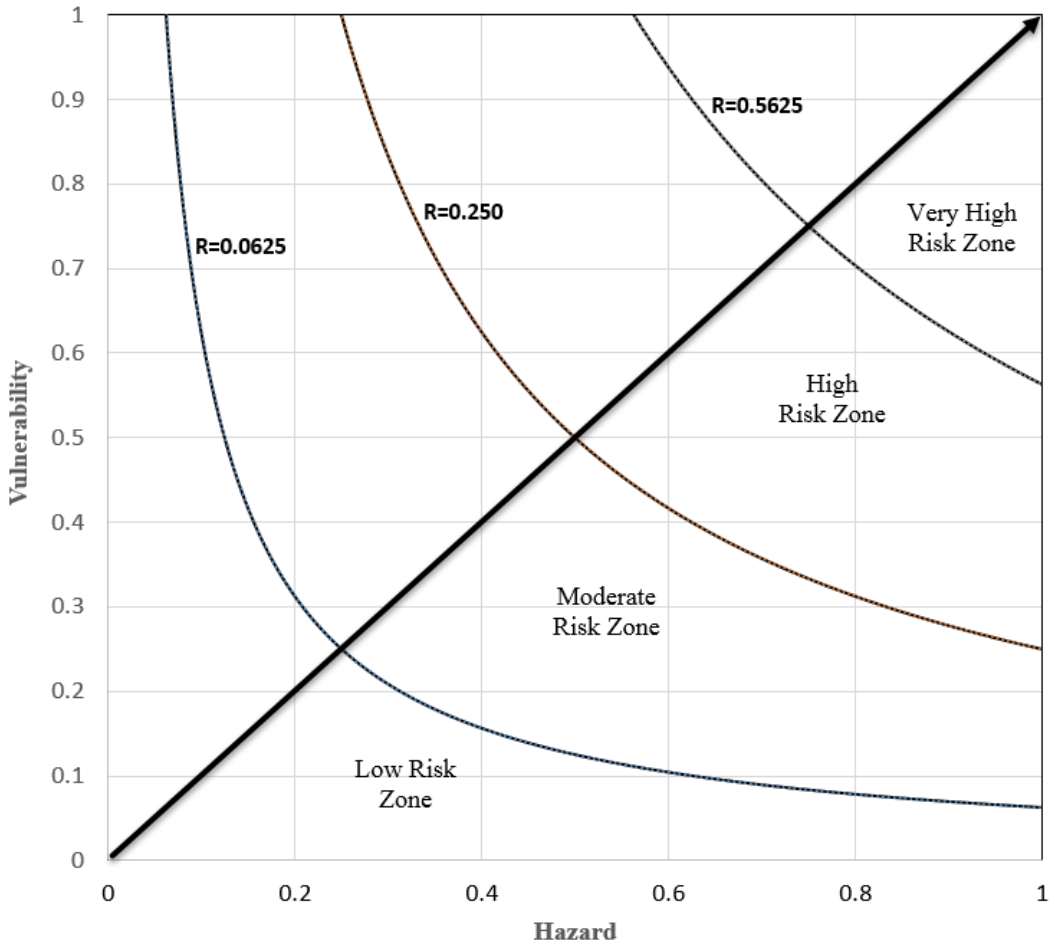

Figure 9. Drought risk classification

4. STUDY AREA AND DATA

4.1 Study area

The Edwards Aquifer (EA), shown in Figure 10, is a unique groundwater system and one of the most prolific artesian aquifers in the world that provides water resources for nearly 2,000,000 people in south-central Texas. Furthermore, the aquifer provides water for agricultural, industrial, recreational and domestic needs throughout the aquifer region; approximately 54 percent is used for municipal supply. The EA which is also known as the Edwards (Balcones Fault Zone) aquifer is located in an area of about 8,000 square miles. This area represents, twelve counties in the EA region.

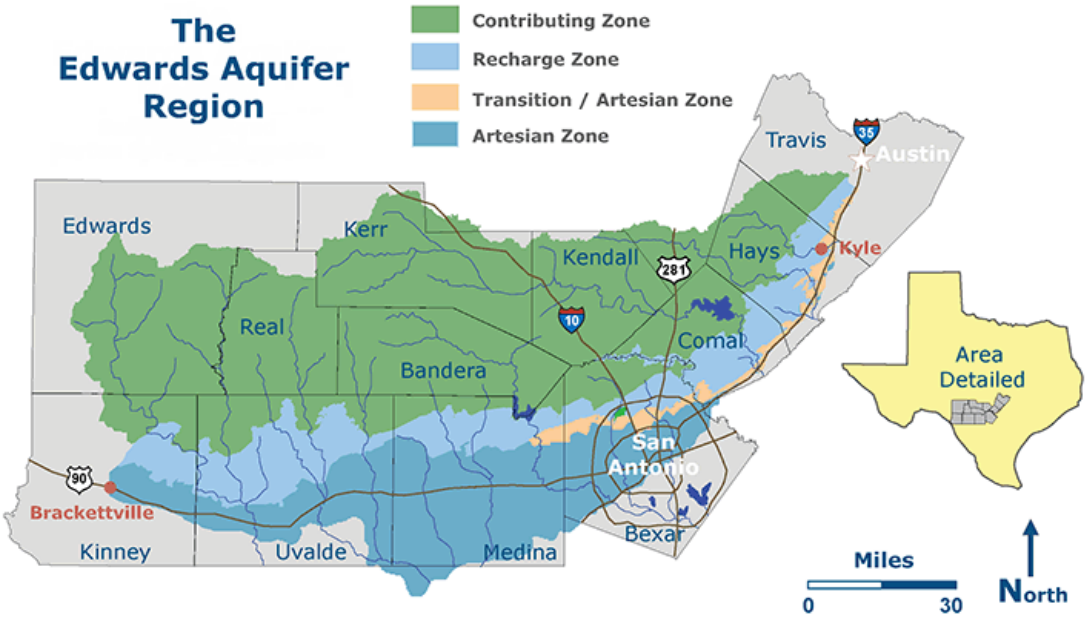

Figure 10. The Edwards Aquifer Region (divided by contributing, recharge, transition and artesian zones). (source: http://www.edwardsaquifer.net/)

4.1.1 Geology

The EA is a karst aquifer which is an intensely faulted and fractured carbonate limestone (Edwards Aquifer Authority, 2013). The dynamics and size of this geologic anomaly make it one of the most miraculous aquifers in the nation, by virtue of its storage capacity, flow characteristics, water producing capabilities and efficient recharging ability. Most of the south-central Texas region is from subjacent cretaceous age, which forms the Edwards Plateau. East and south of the plateau are upper cretaceous chalk, limestone, clay, and dolomite with the extensive EA system, marking the boundary between the Edwards Plateau and the Gulf Coastal Region (Arnow, 1963). The topography consists of a gently rolling plain to the east and moderately hilly country to the west. The altitude of the land surface ranges from about 152.4 m (500 feet) above mean sea level near the Colorado River in Austin to about 457.2 m (1,500 feet) above mean sea level in Uvalde County.

4.1.2. Climate and meteorology

Texas has been divided into 10 separate climatic regions and most of the EA is within the Edwards Plateau. The south-central Texas region consists of three climatic divisions in Texas as the Edwards Plateau, and the South-central and Upper Coast divisions. The climate of the region is classified as humid subtropical. Summers are mostly hot and humid and winters are often near normal and dry. The hot weather is quite persistent from late May through September. The cool season starts beginning about the first of November and extending through March and is typically the driest season of the

year as well. Winters are generally short and mild with most of the precipitation falling as drizzle or light rain. Any accumulation of snow is a rare occurrence. The average annual precipitation ranges from about 559 mm (22 inches) in the west to about 864 mm (34 inches) in the east (USGS).

Most of Texas has pronounced bimodal regimes with peak levels of rainfall occurring both during May-June and September-October based on reports of NDMC (National Drought Mitigation Center, http://drought.unl.edu/). Figure 11 shows the average monthly precipitation for the EA, where peak levels are in May-June and September-October.

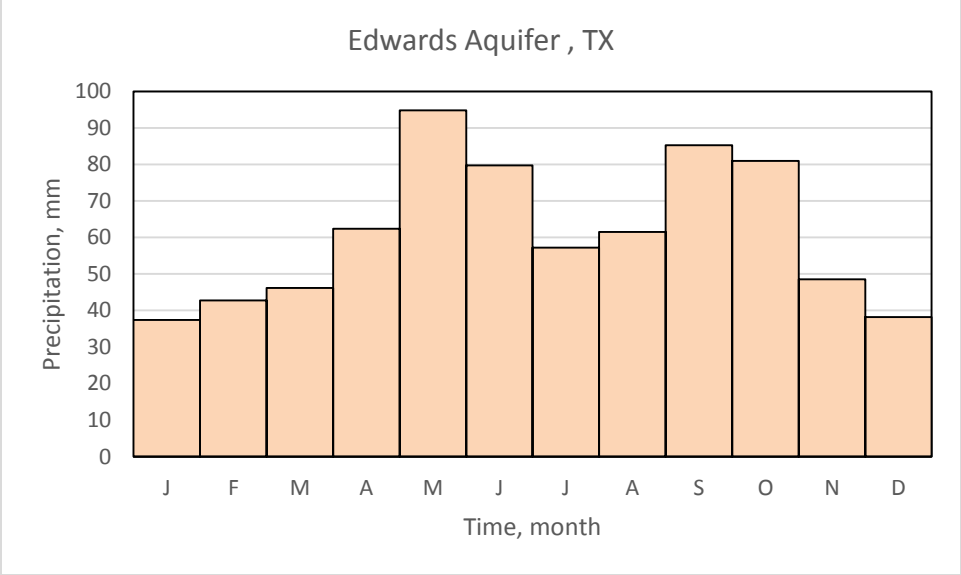

Figure 11. Distribution of precipitation throughout the years, Edwards Aquifer Region

4.2 Data

The material which is used in this study is monthly precipitation data set that pertains to stations which are located in the EA region. Selection of stations is aimed at the thirty-one spatially distributed stations in the EA. There are 12 counties within the EA and there have been more than three hundred stations in these counties, based on the National Oceanic and Atmospheric Administration (NOAA) database system. Some stations, however, are not active and most of the stations started to record in the last ten years. A minimum of 20 years of data is needed for statistical analysis (Guttman, 1994). Wu and Wilhite (2004) say that the longer the length of data set used in drought index calculation, the more reliable drought index values will be. Location of thirty-one stations, shown in Figure 12, were obtained from the NOAA.

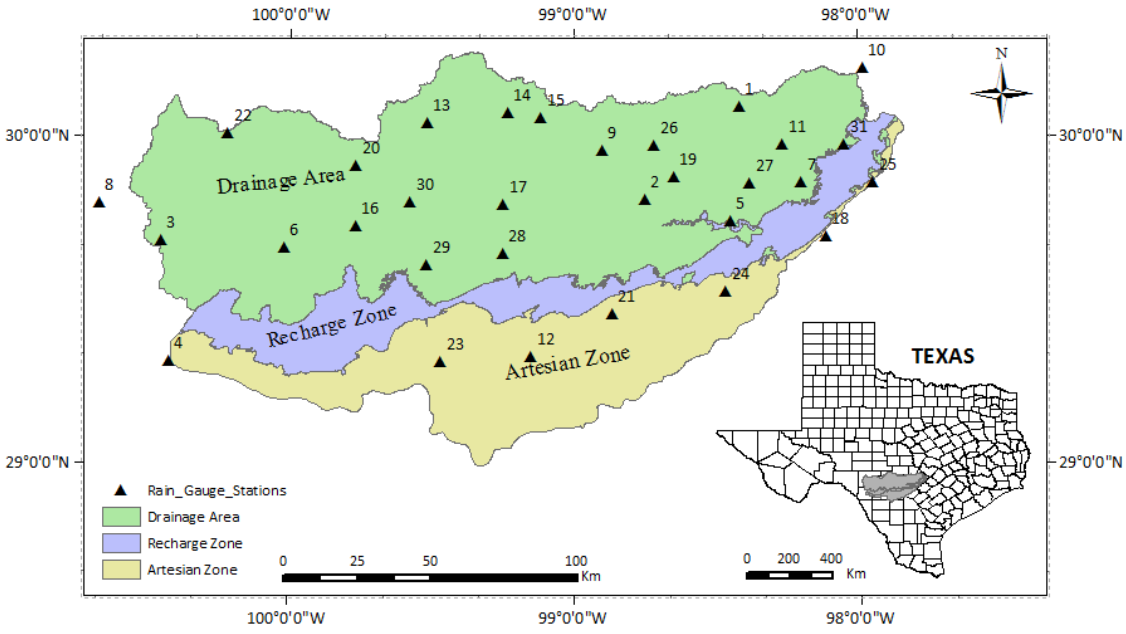

Figure 12. Location of rain gauge stations, Edwards Aquifer, Texas

Not all stations have accurate data, and some of them have missing data. All missing data were filled in by using the normal ratio method which is explained in the next section. Hondo station which is located in the artesian zone of the EA has the longest data of 113 years. Thirteen stations have more than 50 years of data set, while eleven stations have less than 30 years (at least 20 years). All precipitation data have at least 20 years of historical records and all records that have been used are till 2013. While some counties have only one station, such as Kinney, Bexar, and Blanco, other counties have two or more stations. Comal county has the most number of stations as five stations.

4.2.1 Estimation of missing data

Many rain gauge records do not have complete data. Gap lengths may change from one or two days to several years. Estimates of missing data were made, in order to keep continuity of the monthly precipitation time series for this study. Several techniques have been used to fill the gaps (missing observations) in data. Several methods have been used for estimating missing data, including arithmetic mean method, normal ratio method, Inverse distance method, modified inverse distance method, linear programming, areal precipitation ratio method, isohyetal method, and Lagrange method.

The normal ratio method is one of the most popular methods for estimating precipitation data (De Silva et al., 2007). In this study, the normal ratio method has been used to fill in missing data of the rain gauge stations. If any surrounding gauges have the normal annual precipitation exceeding 10 % of the considered gauge, this method is used.

The missing data are estimated as

$$P_x = \frac{1}{m}\left(\frac{N_x}{N_1}\cdot P_1 + \frac{N_x}{N_2}\cdot P_2 + \frac{N_x}{N_3}\cdot P_3 + \cdots + \frac{N_x}{N_m}\cdot P_m\right)$$

$$= \sum_{i=1}^{m}\left(\frac{N_x}{mN_i}\right)P_i \qquad (19)$$

where, P_x = The missing precipitation value for the station X, P_i = The precipitation values at surrounding stations, N_x = The normal annual precipitation of station X, N_i =The normal annual precipitation of surrounding stations, and m = The number of surrounding stations (m is usually 3).

5. RESULTS AND DISCUSSION

In this section, analysis of drought hazard, vulnerability and risk assessment are described. First, drought analysis by using SPI and EDI is explained for each station which is located in the EA region. Then, drought characteristics and probability of drought occurrences are addressed. After that regional drought assessment is illustrated and finally county level hazard and vulnerability quantification is assessed to depict drought risk assessment.

5.1. Drought assessment

Drought is a natural phenomenon detecting its onset and end time. Drought characterizations were detected to analyze drought hazard and next sections discuss drought assessment in the EA region that has been investigated based on the SPI and EDI.

5.1.1. Standardized precipitation index

There are 31 rain-gauge stations located in the EA and SPI calculation was addressed based on these stations. Drought quantifications based on SPI were identified according to the method described in section 3.1.1.1. As an illustration, Blanco rain-gauge station (see Appendix for the stations and referring to numbers) SPI results have been shown in Table 7 and Table 8, respectively, for 12-month and 24-month time scales.

Table 7 Drought characteristics based on SPI-12, Blanco station

Onset		End		D*	M*	I*	Drought Severity	Interarrival Time (month)
Year	**Month**	**Year**	**Month**					
1948	12	1949	4	4	3.52	0.88	Moderate	
1953	11	1957	4	**41**	**65.41**	**1.60**	Extreme	59
1962	7	1965	2	31	25.46	0.82	Severe	104
1966	12	1968	1	13	12.47	0.96	Severe	53
1970	10	1972	5	19	18.96	1.00	Extreme	46
1977	9	1979	1	16	6.89	0.43	Moderate	83
1980	2	1980	11	9	4.34	0.48	Moderate	29
1982	6	1983	8	14	7.41	0.53	Moderate	28
1984	2	1985	3	13	7.8	0.60	Moderate	20
1988	6	1990	9	27	12.4	0.46	Moderate	52
1995	10	1997	2	16	12.93	0.81	Severe	88
1999	9	2000	11	14	21.26	1.52	Extreme	47
2005	10	2007	5	19	25.84	1.36	Extreme	73
2008	5	2010	1	20	31.98	**1.60**	Extreme	31
2011	3	2012	9	18	22.7	1.26	Extreme	34

*Abbreviations refer to "D: Duration in month, M: Magnitude, I: Intensity"

Table 7 explains the drought starting and ending time as a year and month. Duration, magnitude, and intensity identify the drought characteristics and finally interarrival time refers to the period of time between the beginning of a drought and the beginning of the next one. For example, the first drought event begins in December 1948 and the next consecutive drought event begins in November 1953 and the interarrival time is 59 months. Non-drought duration also can be inferred by using "drought duration" and "interarrival time." Interarrival time is the sum of drought duration and non-drought duration. For instance, non-drought duration is 54 (=59-4) months for first consecutive drought event (Table 7). The total drought event is 30 based on 12-month SPI at Blanco station since 1948 to 2013, the drought during 1953-1957 is the longest drought (41

months) with highest magnitude (65.41) and the highest intensity (1.60). This is a coincidental circumstance for all highest values belonging to the same drought event. Since drought event (between 2008 and 2010) has also highest intensity (1.60) even if duration and magnitude don't have the highest value. According to the historical reports, Texas has faced drought problem in the 1950s and the problem appeared in the last decade. Table 7 shows that there were four extreme drought events observed in last 14 years and last two drought event have pretty short non-drought duration. Figure 13 illustrates drought events 12-month and 24-month SPI versus years as visual. Figure 13a shows clearly the extreme drought event between 1953 and 1957 and other severe, moderate and wet conditions. Moderate and extreme drought events have equal occurrences while severe drought occurrence has half of these events.

Table 8 Drought characteristics based on 24-month SPI, Blanco station

onset		end		D*	M*	I*	Drought Severity	Interarrival Time (month)
year	month	year	month					
1951	1	1952	9	20	17.21	0.86	Moderate	
1954	9	1957	11	38	**77.58**	**2.04**	Extreme	44
1963	2	1965	7	29	31.13	1.07	Severe	101
1970	12	1973	2	26	20.18	0.78	Moderate	94
1983	3	1986	5	38	14.35	0.38	Moderate	147
1989	6	1991	9	27	14.85	0.55	Moderate	75
1994	3	1997	6	**39**	21.63	0.55	Moderate	57
1999	9	2001	9	24	18.71	0.78	Moderate	66
2006	6	2007	9	15	17.14	1.14	Extreme	81
2008	4	2010	9	29	30.34	1.05	Extreme	22
2011	4	2013	10	30	26.83	0.89	Severe	36

*Abbreviations refer to "D: Duration in month, M: Magnitude, I: Intensity"

Table 8 illustrates 24-month SPI values and the highest intensity (2.04) and magnitude (77.58) were detected between 1954 and 1957 with 38-month duration as extreme drought. The highest duration was detected in 1994 with 39 months duration and drought character was moderate in that duration.

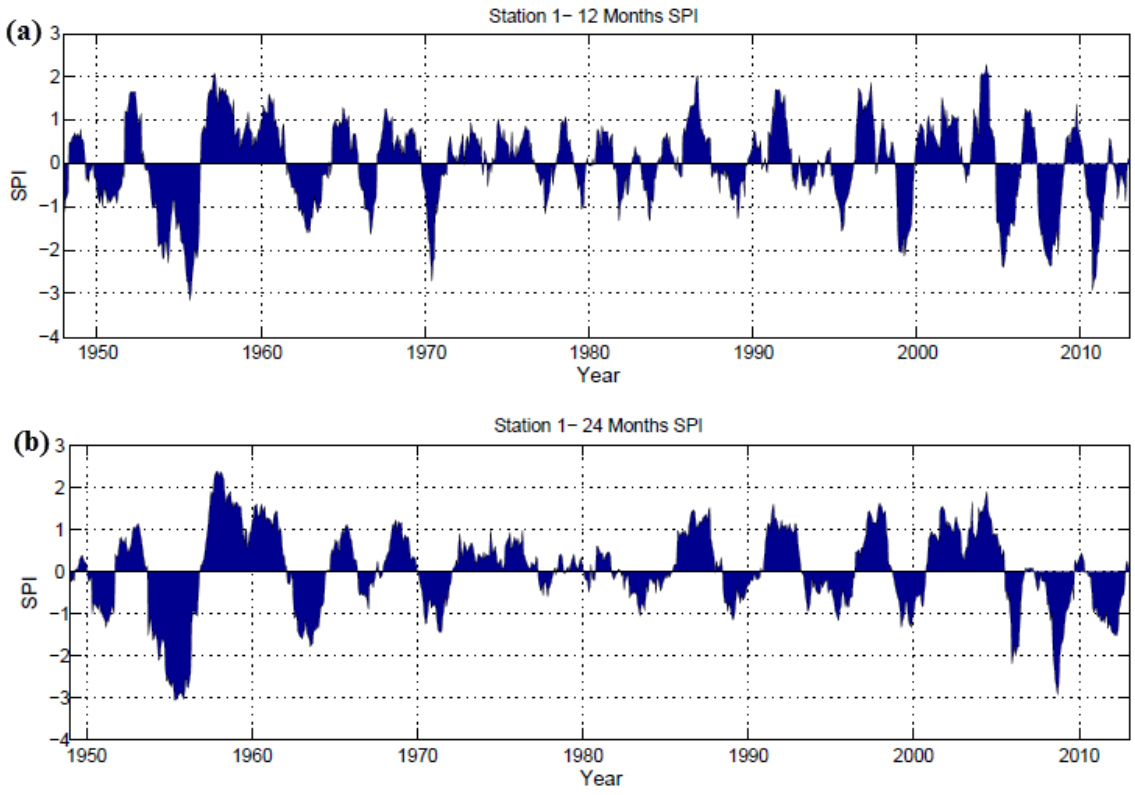

Figure 13. Time series of SPI values for station Blanco for (a) 12-month, (b) 24-month between 1948-2013

The longest interarrival time was monitored between 1970 (December) and 1983 (March) as 147 months for a 24-month SPI, while 104 months was the longest interarrival time observed between 1953 (November) and 1962 (July) for a 12-month SPI. The longest

time interval without drought was observed from February of 1973 to March of 1983 as 121 months for a 24-month SPI while this value was 64 months non-drought from May of 1972 to September of 1977 for a 12-month SPI.

The most drought type which was observed at Blanco based on a 24-month SPI was moderate drought. While severe drought was detected only one in 1963 (29 months), an extreme drought was monitored in 1954, 2006, and 2008 and their durations were 38, 15, and 29 months, respectively. On the other hand, moderate drought and extreme drought were monitored equally for 12-month SPI, while severe drought half of these moderate and extreme droughts. All other SPI calculations for multiple time scales have been shown in Figure 14 for the station Blanco.

Table 7 and Figure 13 show only one station and one SPI time-scale (12-month) results. Here, on the other hand, the regional representative of SPI for the EA region was addressed and analyzed for multiple time-scales for all 31 stations. Due to these results, maps were created by using average drought quantifications such as average magnitude, average duration, and average intensity. The map was created by using the kriging interpolation method in ArcMap 10.1. 24-month SPI, in other words 2-year drought, results which have been shown in Figure 15 are tabulated in Table 9 for all stations to illustrate the average duration, magnitude and intensity.

While west of the region has higher duration and magnitude, the highest intensity seemed in some of the north and south part. The east part of the EA had low average duration and magnitude. Table 9 illustrates the results of calculation for the EA region for

average duration, average magnitude, and average intensity. The highest intensity (1.10) was detected north of the EA (station 15), while the lowest one (0.72) was monitored in

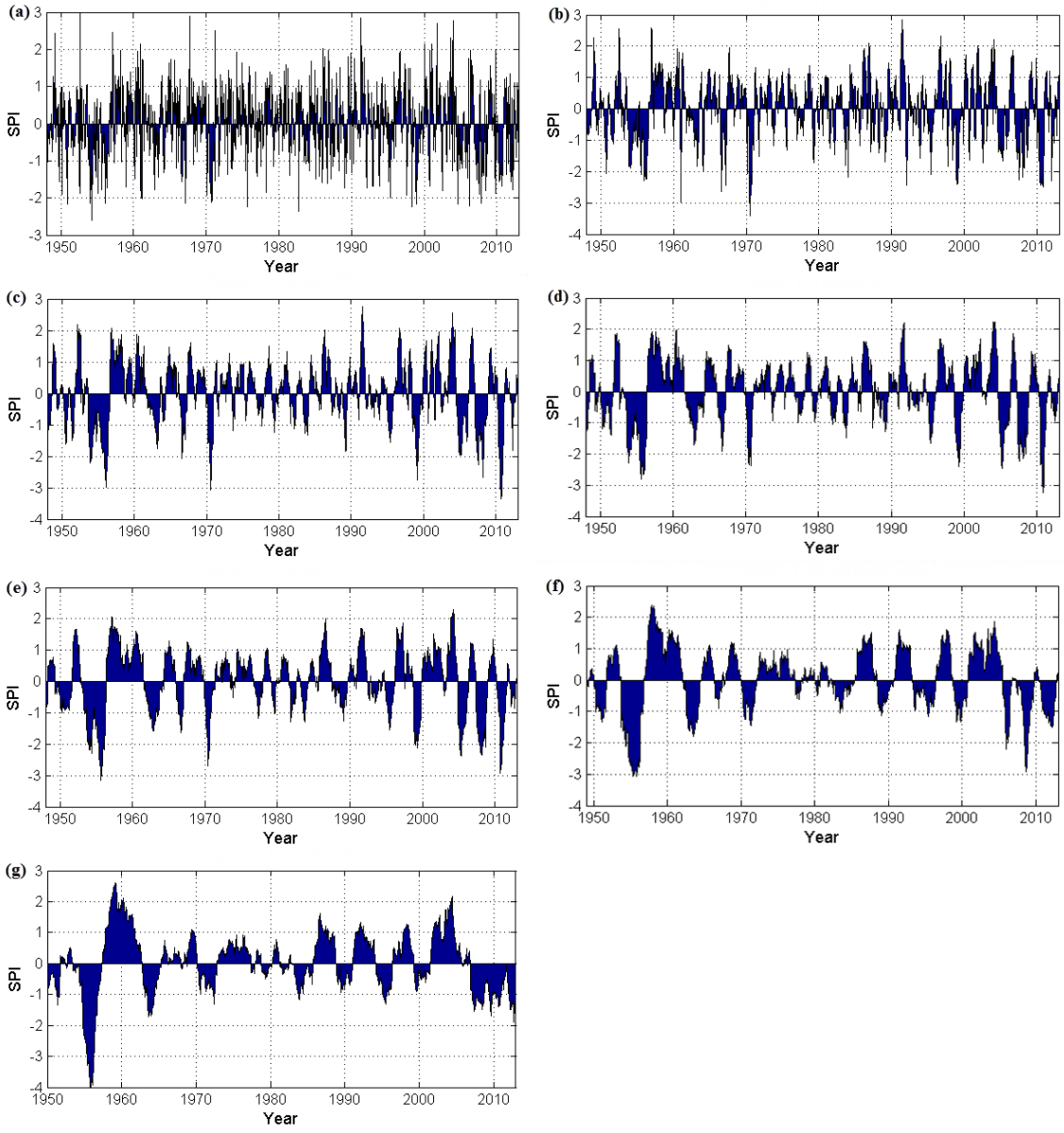

Figure 14. Time series of SPI values for Blanco station in the EA region for (a) 1-month, (b) 3-month, (c) 6-month, (d) 9-month, (e) 12-month, (f) 24- month SPI, and (g) 36- month SPI time scales

the middle of the region (station 30). The longest duration was calculated as 47.25 months in the west of the EA (station 3) and the lowest one (20.50 months) was detected in the north of the EA (station 14). The highest intensity and the lowest duration results have been seen in the same area (Figure 15). While the highest magnitude (43.66) was detected in the middle of the region (Station 29), the lowest magnitude (20.97) was detected in the east of the region (station 31).

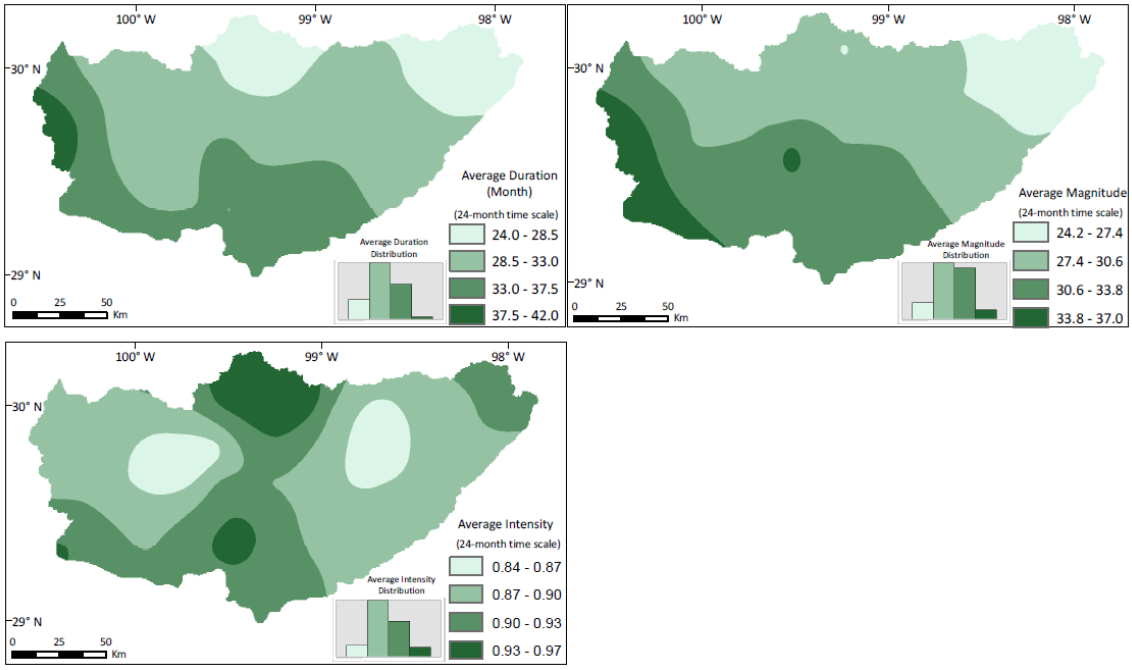

Figure 15. The 24-month SPI drought characterization based on average duration, magnitude, and intensity in the EA region

Table 9 Drought quantification based on 24-month SPI in the EA region for average duration, magnitude, and intensity

Station	Latitude	Longitude	Average		
			Duration (month)	Magnitude	Intensity
1	30.10	-98.42	28.64	26.36	0.92
2	29.82	-98.75	34.50	33.41	0.82
3	29.68	-100.45	**47.25**	42.82	0.85
4	29.32	-100.42	34.80	36.04	1.02
5	29.75	-98.45	32.22	31.21	0.89
6	29.67	-100.02	26.55	26.31	0.85
7	29.87	-98.20	24.91	22.93	0.90
8	29.80	-100.67	40.67	34.02	0.81
9	29.97	-98.90	32.33	31.02	0.83
10	30.22	-97.98	26.80	24.15	0.90
11	29.98	-98.27	26.18	25.10	0.82
12	29.33	-99.15	38.50	36.77	0.92
13	30.05	-99.52	29.33	31.96	1.05
14	30.08	-99.23	**20.50**	22.73	0.98
15	30.07	-99.12	26.80	30.14	**1.10**
16	29.73	-99.77	27.25	26.76	0.72
17	29.80	-99.25	29.25	27.72	0.95
18	29.70	-98.12	32.20	29.57	0.81
19	29.88	-98.65	25.50	21.20	0.84
20	29.92	-99.77	32.57	32.25	0.91
21	29.47	-98.87	33.78	30.20	0.84
22	30.02	-100.22	29.25	26.42	0.88
23	29.32	-99.47	31.22	30.91	0.99
24	29.53	-98.47	28.09	26.37	0.83
25	29.87	-97.95	28.43	27.93	0.88
26	29.98	-98.72	32.33	33.20	0.83
27	29.87	-98.38	27.90	25.13	0.89
28	29.65	-99.25	29.00	28.28	0.84
29	29.62	-99.52	39.50	**43.66**	1.06
30	29.81	-99.58	27.75	25.35	**0.72**
31	29.98	-98.05	20.83	**20.97**	0.99

5.1.2 Effective drought index

The EDI was calculated with historical precipitation data to accurately quantify the exact onset and end of a drought event. Twenty stations were used to calculate the EDI, while thirty-one stations were used in calculation of the SPI. Droughts were identified by EDI according to the method described in section 3.1.1.2 (Table 10).

Table 10 Drought characteristics based on EDI, Blanco station

onset		end		D*	M*	I*	Drought Severity	Interarrival time (month)
year	month	year	month					
1950	9	1952	4	19	16.46	0.87	Severe	
1953	11	1957	3	**40**	**70.47**	**1.76**	Extreme	38
1962	5	1964	3	22	19.46	0.88	Severe	102
1964	4	1965	2	10	5.69	0.57	Moderate	23
1966	10	1968	1	15	13.15	0.88	Moderate	30
1970	10	1971	8	10	14.62	1.46	Severe	48
1977	5	1978	8	15	7.46	0.50	Moderate	79
1982	6	1983	3	9	6.26	0.70	Moderate	61
1983	12	1984	10	10	8.17	0.82	Moderate	18
1988	9	1990	3	18	12.58	0.70	Severe	57
1995	10	1996	9	11	11.1	1.01	Moderate	85
1999	4	2000	10	18	19.24	1.07	Severe	42
2005	6	2007	1	19	21.92	1.15	Severe	74
2007	12	2009	10	22	28.22	1.28	Severe	30
2010	12	2012	3	15	16.87	1.12	Extreme	36
2012	11	2013	5	6	4.43	0.74	Moderate	23

*Abbreviations refer to “D: Duration in month, M: Magnitude, I: Intensity”

All the highest values for drought were detected for the same time interval between 1953 and 1957. The longest drought duration (40 months), the highest magnitude (70.47), and the highest intensity (1.76) were observed for the same extreme drought event. The longest interarrival time was observed between 1953 (November) and 1962 (May) as 102 months, while the shortest one was monitored between 1982 (June) and 1983 (December)

as 18 months. The longest non-drought duration was observed as 62 (=102-40) months between 1957 (March) and 1962 (May), while the shortest non-drought duration was detected between 1964 (March) and 1964 (April) as 1 month (=23-22). Most observed drought types, based on EDI calculation, were severe drought and moderate drought. Both moderate and severe droughts were monitored seven times, while extreme drought was observed only two times (Figure 16).

It can be indicated from Figure 17 that the highest values were observed mostly in the east part of the region (most of the east part of the EA refers to "Region 3" which is explained in section 3.2.3). Average magnitude was observed in more extensive area than average duration and average intensity.

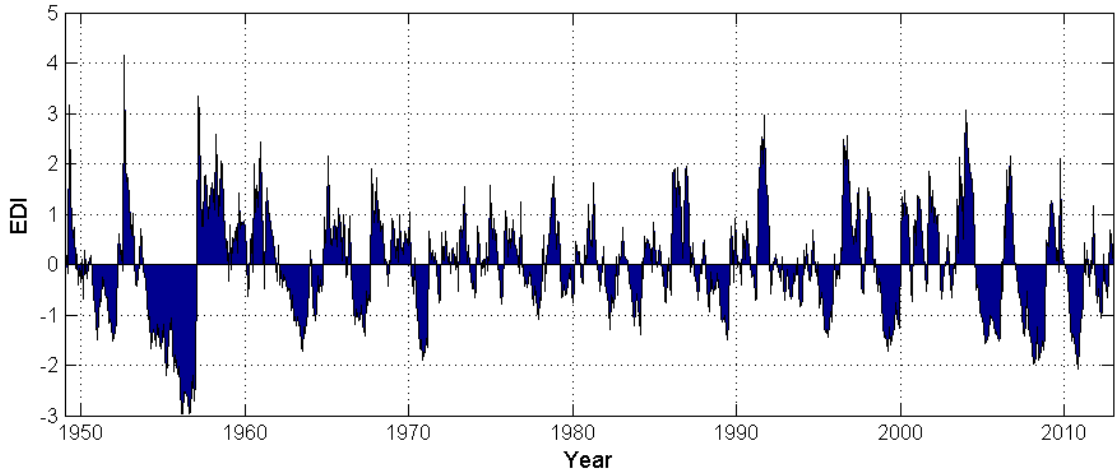

Figure 16. Time series of EDI values for station Blanco in the EA region between 1948 and 2013

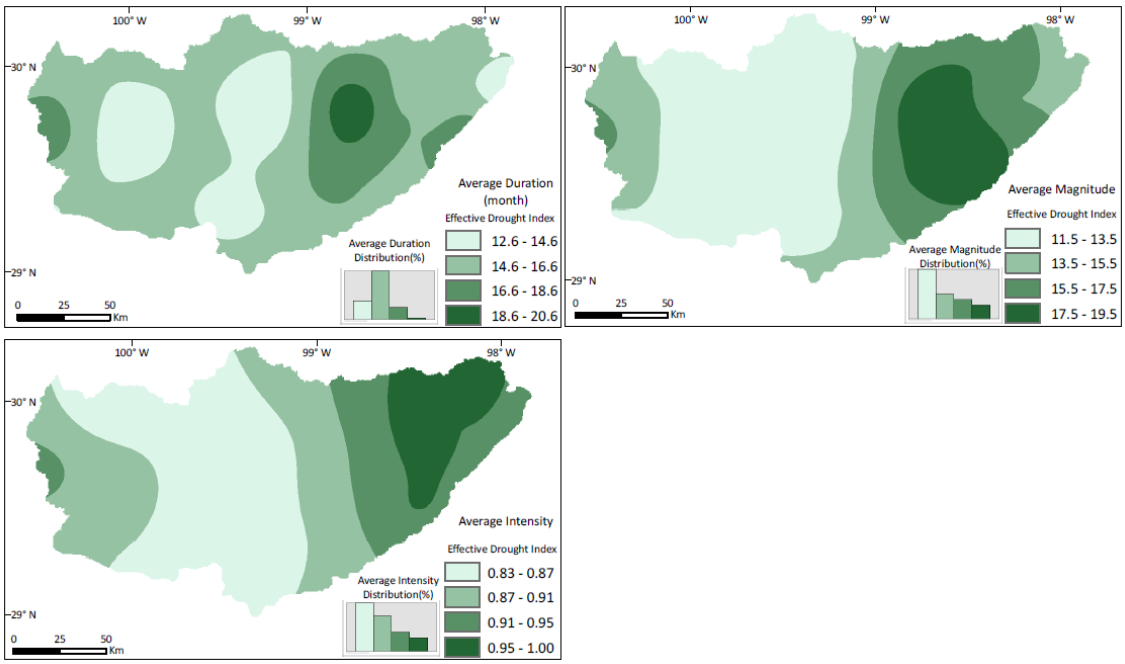

Figure 17. EDI drought characterization based on average duration, magnitude, and intensity in the EA region

Table 11 illustrates the average duration, magnitude, and intensity which were calculated by the EDI for twenty stations in the EA region. The longest average duration and the highest average magnitude were observed as 20.65 months and 21.41, respectively, in the same area (station 2) while the highest intensity (1.04) was detected at station 11. The shortest and the lowest values for average duration, average magnitude, and average intensity were monitored as 12.60 months, 10.64, and 0.81, respectively at station 6, 17, and 22.

Table 11 Drought quantification by EDI in the EA region for average duration, magnitude, and intensity

Stations	Latitude	Longitude	Average		
			Duration (month)	Magnitude	Intensity
1	30.10	-98.42	16.19	17.26	0.97
2	29.82	-98.75	**20.65**	**21.41**	0.92
3	29.68	-100.45	18.10	17.41	0.96
4	29.32	-100.42	14.50	12.75	0.85
5	29.75	-98.45	16.71	17.73	0.95
6	29.67	-100.02	**12.60**	11.61	0.89
7	29.87	-98.20	14.88	13.97	0.91
8	29.80	-100.67	18.88	16.95	0.88
11	29.98	-98.27	16.11	19.50	**1.04**
12	29.33	-99.15	15.04	13.26	0.84
15	30.07	-99.12	14.50	12.90	0.89
17	29.80	-99.25	12.60	**10.64**	0.83
18	29.70	-98.12	18.33	18.45	0.92
20	29.92	-99.77	14.75	12.92	0.86
21	29.47	-98.87	17.63	17.74	0.90
22	30.02	-100.22	15.08	12.40	**0.81**
23	29.32	-99.47	13.68	12.18	0.86
24	29.53	-98.47	16.32	19.24	0.98
25	29.87	-97.95	13.85	13.16	0.92
27	29.87	-98.38	14.86	15.17	1.00

5.2 Probability of drought occurrences

This section focuses on the calculation of the probabilities of drought occurrences (PDO) for different drought categories, such as extreme, severe, and moderate droughts.

5.2.1 PDO based on the SPI

The results of the PDO have been shown in Table 12 as an example for all stations in the EA region for a 24-month period drought.

The highest probability of occurrence for extreme drought (10.20 %) was monitored at station 23. Three stations had a higher percentage than 10 % severe drought occurrence probability and the highest percentage was observed at station 7 as 13.46 % for severe drought, while any severe drought was not monitored at five stations (stations 2, 9, 14, 26, and 30). The highest percentage at the moderate drought was detected as 15.79 % at station 2, while any moderate drought wasn't observed at three stations 13, 15, and 29. Table 12 shows that the occurrence probability of ear normal drought was higher than the wet condition occurrence of probability for all stations.

Table 12 Drought occurrence probability based on a 24-month SPI in the EA region

Stations	Latitude	Longitude	Drought occurrence probability (%)				
			Wet	Near Normal	Moderate	Severe	Extreme
1	30.10	-98.42	31.15	50.82	9.84	3.28	4.92
2	29.82	-98.75	28.95	50.00	15.79	0.00	5.26
3	29.68	-100.45	34.78	47.83	8.70	4.35	4.35
4	29.32	-100.42	29.17	50.00	4.17	12.50	4.17
5	29.75	-98.45	32.73	50.91	9.09	3.64	3.64
6	29.67	-100.02	33.33	49.21	7.94	6.35	3.17
7	29.87	-98.20	28.85	50.00	3.85	13.46	3.85
8	29.80	-100.67	35.14	48.65	5.41	5.41	5.41
9	29.97	-98.90	28.57	50.00	14.29	0.00	7.14
10	30.22	-97.98	26.09	52.17	4.35	8.70	8.70
11	29.98	-98.27	32.26	50.00	8.06	4.84	4.84
12	29.33	-99.15	34.12	49.41	4.71	4.71	7.06
13	30.05	-99.52	36.36	50.00	0.00	9.09	4.55
14	30.08	-99.23	34.78	47.83	8.70	0.00	8.70
15	30.07	-99.12	33.33	50.00	0.00	10.00	6.67
16	29.73	-99.77	34.62	50.00	7.69	3.85	3.85
17	29.80	-99.25	34.00	50.00	6.00	4.00	6.00
18	29.70	-98.12	30.61	48.98	12.24	2.04	6.12
19	29.88	-98.65	28.00	48.00	8.00	8.00	8.00
20	29.92	-99.77	29.41	50.00	8.82	5.88	5.88

Table 12 Continued

Stations	Latitude	Longitude	Drought occurrence probability (%)				
			Wet	Near Normal	Moderate	Severe	Extreme
21	29.47	-98.87	34.00	48.00	6.00	8.00	4.00
22	30.02	-100.22	29.73	48.65	8.11	5.41	8.11
23	29.32	-99.47	32.65	48.98	4.08	4.08	10.20
24	29.53	-98.47	26.09	50.00	10.87	6.52	6.52
25	29.87	-97.95	25.81	51.61	9.68	6.45	6.45
26	29.98	-98.72	36.36	50.00	9.09	0.00	4.55
27	29.87	-98.38	33.33	50.00	6.67	5.00	5.00
28	29.65	-99.25	31.25	50.00	6.25	6.25	6.25
29	29.62	-99.52	41.18	47.06	0.00	5.88	5.88
30	29.81	-99.58	37.93	48.28	10.34	0.00	3.45
31	29.98	-98.05	32.43	51.35	5.41	2.70	8.11

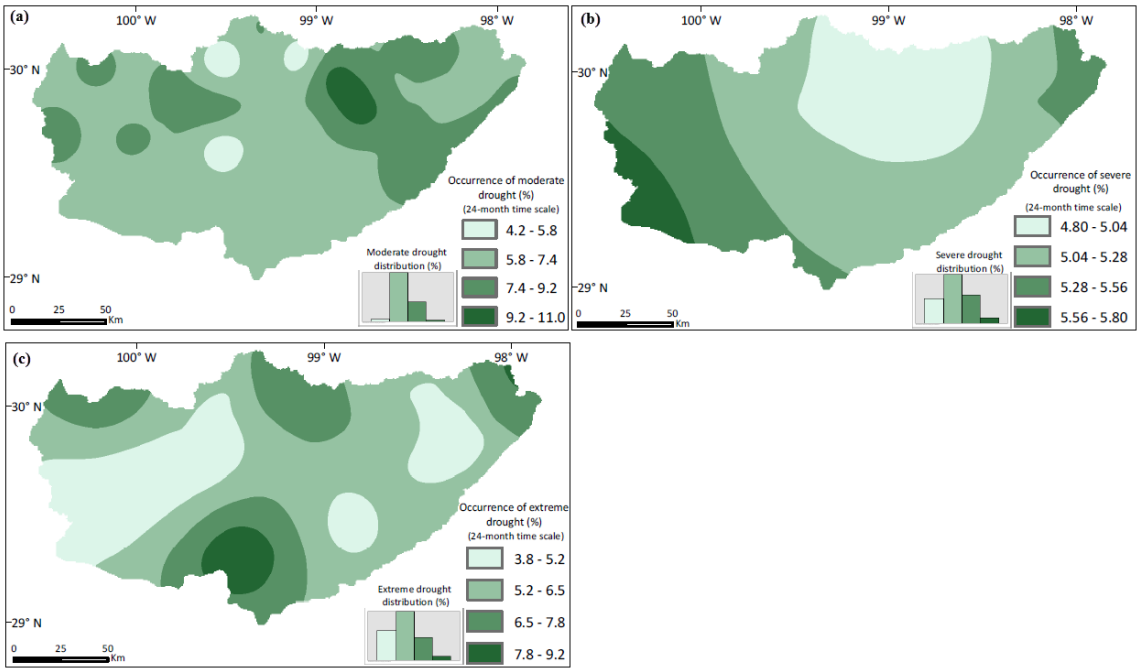

Figure 18. Drought occurrences: (a) moderate, (b) severe, and (c) extreme drought at a 24-month SPI time step

Figure 18c reflects that the higher extreme drought was observed in the south part of the EA in contrast to the west region. A severe drought (Figure 18b) was monitored frequently in the west part of the area, while the highest moderate drought frequency (Figure 18a) was only observed in some part of the northeast of the EA region. The result of drought occurrences at 24-month SPI shows that the central south part of the area was most prone to extreme drought, while the west part of the region was most prone to severe drought. Moderate droughts occurred more frequently in the east part of the area.

5.2.2 PDO based on the EDI

The PDO was calculated for the EDI similar to the SPI based on the event occurrence. As mentioned in the previous sections, the PDO was created only one time because of the time independent index of the EDI. The highest rate of extreme drought was detected by EDI at station 11 (Table 13). Eight stations out of twenty didn't face any extreme drought and the percentage of extreme drought was quite less than any other time step SPI. Figure 19c illustrates the spatial distribution of each moderate, severe, and extreme drought probability and most of the region had less than 0.8 extreme drought probability.

The EDI estimated mostly moderate drought and the highest rate was observed at station 17. The central part of the area was dominated by moderate drought (Figure 19a). All percentages of severe drought probabilities were less than 10% and the highest rate was monitored as 7.76% for severe drought. The highest percentage of severe drought was mostly observed in some part of the northwest (Figure 19b).

Table 13 Drought occurrence probability based on the EDI in the EA region

Stations	Latitude	Longitude	Drought occurrence probability (%)				
			Wet	Near Normal	Moderate	Severe	Extreme
1	30.10	-98.42	36.97	49.58	5.88	5.88	1.68
2	29.82	-98.75	34.04	47.87	11.70	5.32	1.06
3	29.68	-100.45	34.92	49.21	11.11	1.59	3.17
4	29.32	-100.42	35.62	47.95	12.33	4.11	0.00
5	29.75	-98.45	40.77	48.46	4.62	5.38	0.77
6	29.67	-100.02	33.62	49.14	8.62	7.76	0.86
7	29.87	-98.20	35.92	48.54	9.71	5.83	0.00
8	29.80	-100.67	37.70	49.18	6.56	6.56	0.00
11	29.98	-98.27	37.40	47.97	6.50	4.88	3.25
12	29.33	-99.15	36.17	48.94	10.11	4.79	0.00
15	30.07	-99.12	34.33	47.76	11.94	4.48	1.49
17	29.80	-99.25	33.33	46.67	13.33	6.67	0.00
18	29.70	-98.12	37.61	48.62	7.34	5.50	0.92
20	29.92	-99.77	34.69	48.98	10.20	6.12	0.00
21	29.47	-98.87	34.51	48.67	10.62	4.42	1.77
22	30.02	-100.22	34.29	48.57	10.00	7.14	0.00
23	29.32	-99.47	35.88	49.62	9.16	4.58	0.76
24	29.53	-98.47	36.00	48.80	8.00	5.60	1.60
25	29.87	-97.95	35.96	49.44	7.87	5.62	1.12
27	29.87	-98.38	40.46	48.85	4.58	6.11	0.00

Analysis of drought occurrences in different categories indicates that the central part of the region was most prone to severe and moderate droughts. Extreme drought was not observed as much as moderate and severe droughts and it is difficult to say which area is more prone to extreme drought based on the EDI. Figure 19c shows that the highest extreme drought probability was monitored in a small area in the east part and west part at, respectively, stations 11 and 3. (See the Appendix for spatial drought occurrence probability at each time scale SPI)

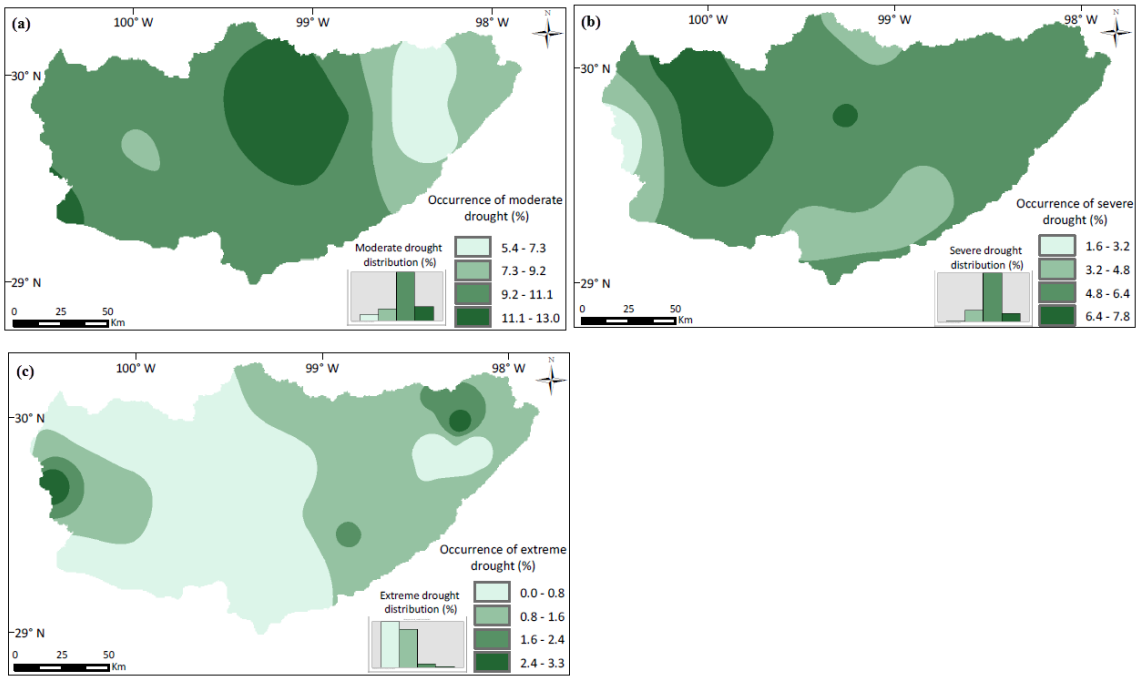

Figure 19. Drought occurrences: (a) moderate, (b) severe, and (c) extreme drought based on EDI

5.2.3 Comparison of SPI and EDI

This section focuses on the comparison of the SPI and the EDI calculations at Blanco station that were explained in the previous sections. Figure 20 and Table 14 briefly explain the drought severity type based on EDI and different time steps of SPI at the Blanco station. The most extreme drought was observed 15 times based on 1-month SPI, while this type of drought was observed only one time based upon 36-month SPI. Even if 1-month SPI has the most observed extreme drought (15), 12-month SPI has the highest occurrence probability for the extreme drought (7.69%) and 9-month SPI follows with 6.45% occurrence of probability. 1-month SPI had greater total drought, severe drought, and moderate drought percentages than any other time step SPI and EDI. The lowest

extreme drought was observed as 1.68% by EDI in comparison with observation of two times of extreme drought. Although 9-month SPI and 12-month SPI have exactly the same event number (for extreme, severe, and moderate), both time scales have different drought occurrence probabilities because of total event occurrences.

Table 14 Comparison of EDI and multiple time scales SPI at Blanco station

Drought	Occurrence Probability			Number of the events		
Index	Extreme	Severe	Moderate	Extreme	Severe	Moderate
EDI	1.68	5.88	5.88	2	7	7
SPI1	4.66	8.70	12.42	15	28	40
SPI3	6.91	5.85	7.45	13	11	14
SPI6	6.00	6.00	7.00	6	6	7
SPI9	6.45	3.23	6.45	6	3	6
SPI12	7.69	3.85	7.69	6	3	6
SPI24	4.92	3.28	9.84	3	2	6
SPI36	2.70	5.41	10.81	1	2	4

*Note: Wet and near normal conditions have not been shown

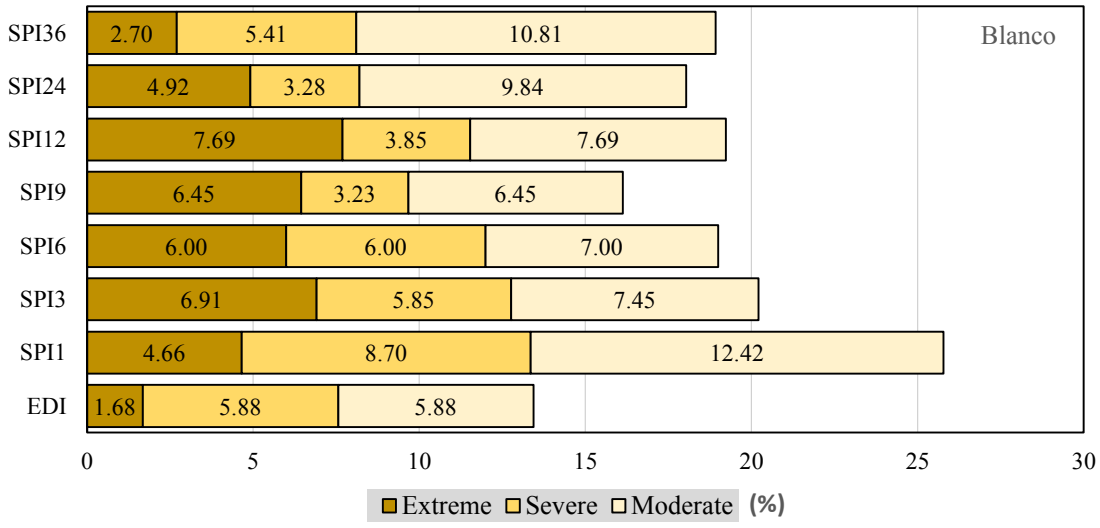

Figure 20. Drought severity percentage by EDI and SPIs at Blanco station

5.3 Spatial drought assessment

This section explains drought characteristics for each region. The natural breaks method was used to create three hydrological boundaries based on monthly rainfall distribution. In this way, accurate average rainfall distribution range was generated for each division by using the natural breaks algorithm. The oldest historical record was used to obtain the average precipitation for each region.

Regions which are named region-1, region-2, and region-3 have 7, 7, and 17 stations, respectively, for SPI analysis and have 6, 5, and 9 stations, respectively, for EDI analysis. Therefore, the number of stations which were used are 31 stations for SPI analysis, while the number of stations are 20 stations for EDI analysis. The mean monthly precipitation in each region has been shown in Figure 21 and shows that region-3 has the highest average monthly precipitation while region-1 has the lowest monthly average precipitation. It can be indicated from Figure 21 that the EA region has bimodal precipitation pattern. May is the wettest month in each region followed by September.

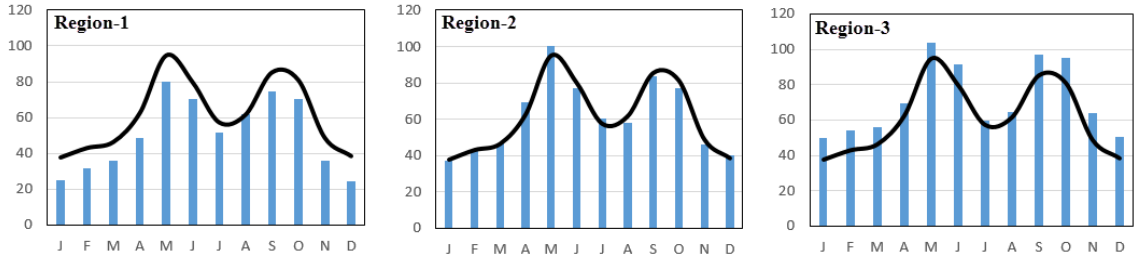

Figure 21. Mean monthly precipitation (mm) in each region between 1951 and 2013. Solid black line represents monthly mean precipitation (mm) for the EA region

5.3.1 Region-1 drought assessment

The mean annual precipitation (608 mm) record range is from 1951 to 2013 years for both SPI and the EDI analyses. SPI for multiple timescales was calculated for region-1 by using the mean areal precipitation (Figure 22). The most extreme 1-month and 3-month SPIs were detected in May 1956 and March 1954, respectively (Figure 22a and Figure 22b). The minimum values for both time scales for 1-month SPI and 3-month SPI were observed as -2.79 and -2.95, respectively. The minimum SPI values for the 6-month SPI and 9-month SPI were monitored within the last five years in February 2009 and June 2011, respectively. The drought severity for both time scales SPI was detected as extreme and SPI values were -2.72 and -2.63 for 6-month SPI and 9-month SPI (Figure 22c and Figure 22d), respectively. The highest drought severities for 24-month and 36-month SPI were detected as extreme in September 2009 (24-month SPI=-2.56) and January 1957 (36-month SPI=-2.46). The SPI values reached the peak 3-month and 12-month time scales as -2.95 and -2.94, respectively, in March 1954 and in September 2011.

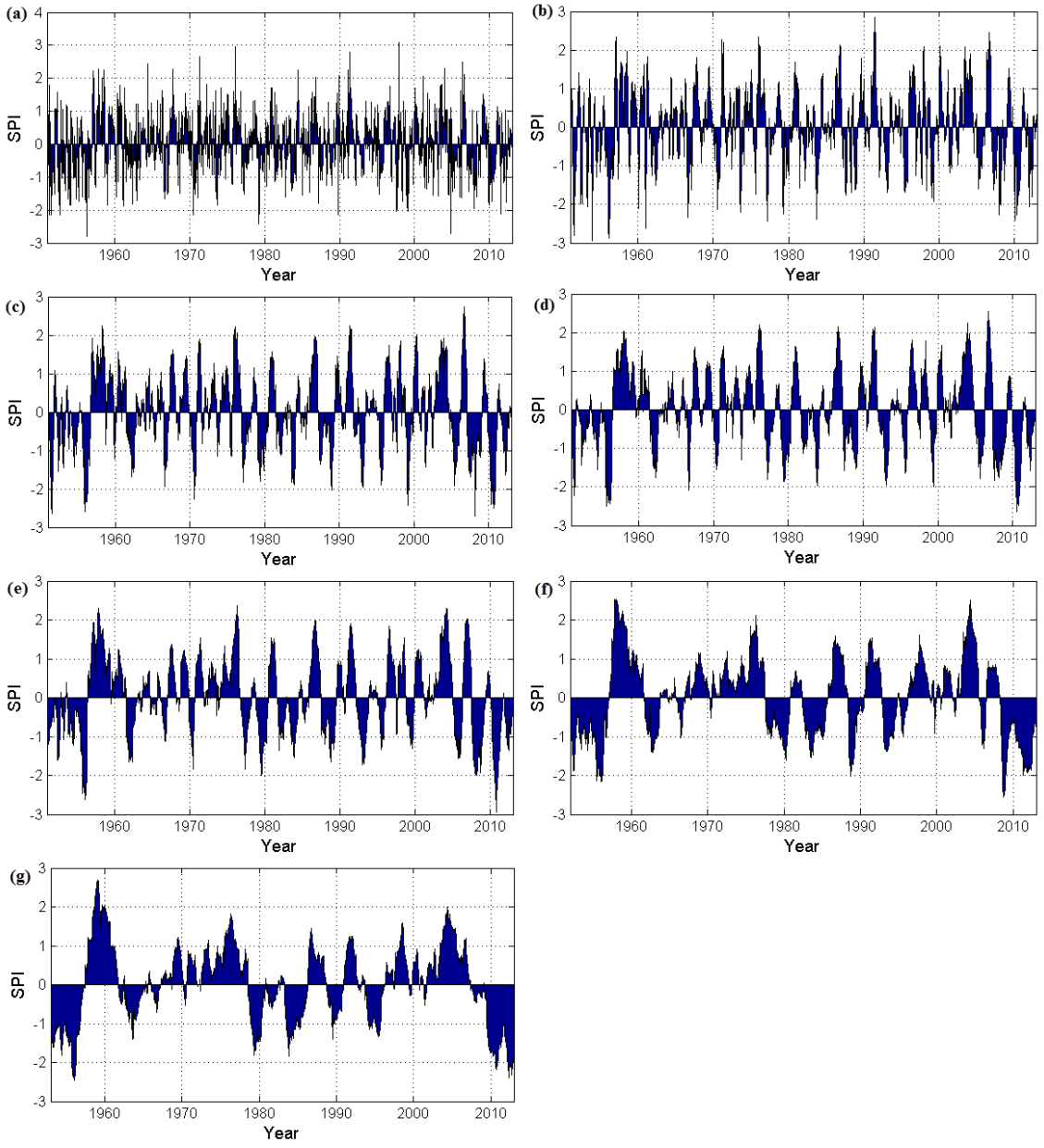

Figure 22. Time series of SPI values for region-1 for (a) 1-month, (b) 3-month, (c) 6-month, (d) 9-month, (e) 12-month, (f) 24- month SPI, and (g) 36- month SPI time scales

Extreme drought event wasn't observed, based upon the EDI analysis in region-1. While five "severe drought" events were detected, the region had faced mostly "moderate

drought" event fifteen times. The lowest EDI value was monitored as -1.96 in January 1957. The longest drought duration was monitored between 1988 (January) and 1990 (March) as 26 months, while the highest intensity was detected between 1955 (October) and 1957 (April) as 1.16. The highest magnitude was observed as a severe drought event between 2008 (February) and 2010 (January) as 23.44. Figure 23 illustrates that drought was detected more frequently during the 1950s and quite intense drought between 2008 and 2012. Furthermore, the lowest interarrival time occurred in the 1950s (1952 and 1954) as 6 and 8 months.

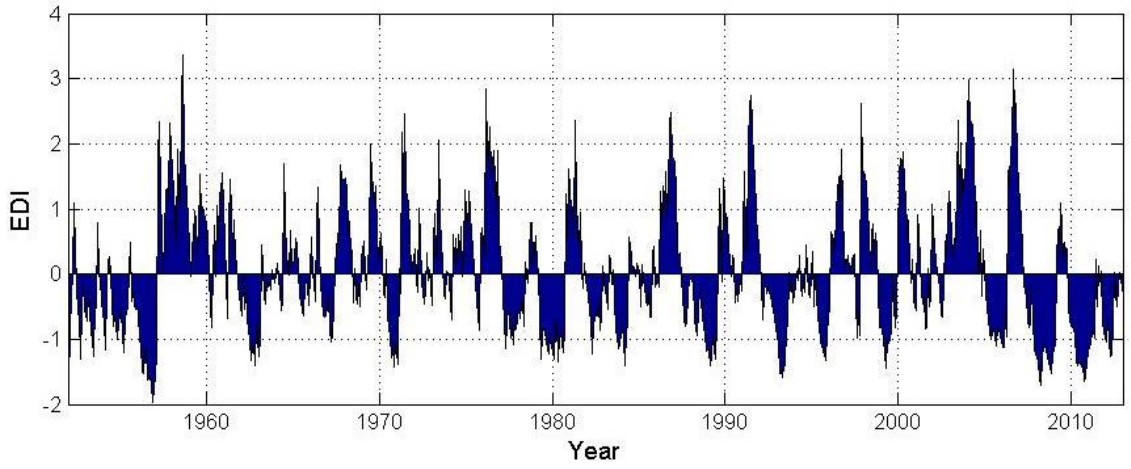

Figure 23. Time series of EDI values for region-1 between 1951 and 2013

Figure 24 depicts the probability of drought occurrences for different drought classes for the EDI and different time-scale SPIs. 1-month SPI had a greater total drought (sum of "Extreme", "Severe", and "Moderate") percentages 25.87% than any time-step SPI and EDI. The highest rate of extreme drought was detected by 3-month SPI, while the

lowest one was detected by 1-month SPI (except EDI). An interesting point of Figure 24 illustrates that EDI underestimated extreme droughts than any SPI and any extreme drought wasn't observed by EDI. Therefore, EDI had the highest rate of moderate drought as 12.50%. Furthermore, EDI had the lowest total drought percentages (16.67%).

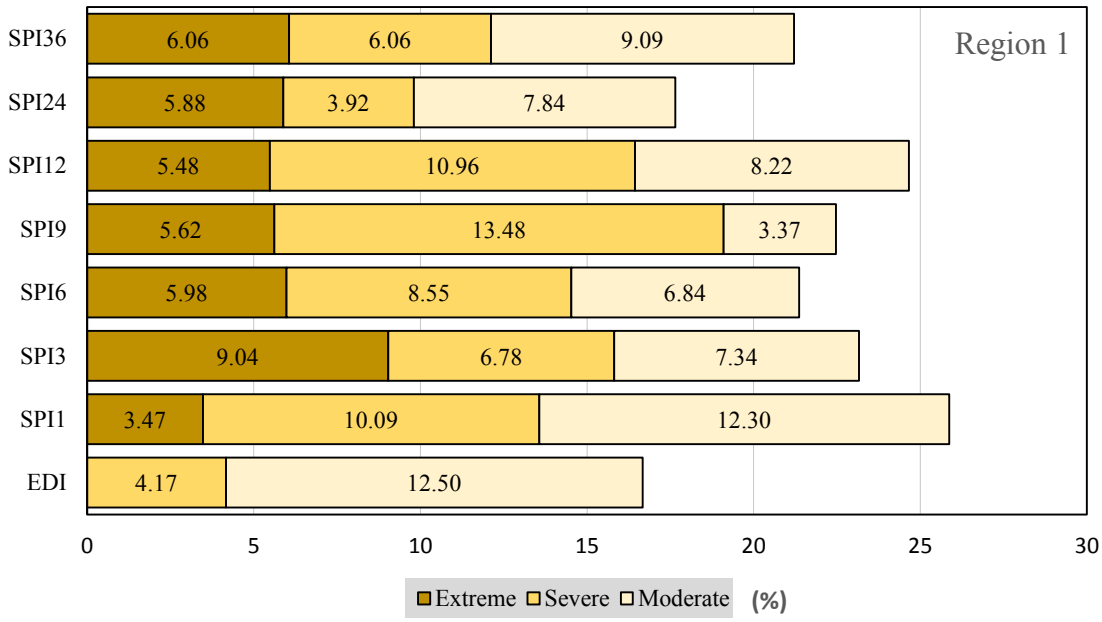

Figure 24. Drought class percentage by EDI and SPIs in region-1 for 1951 and 2013

5.3.2 Region-2 drought assessment

The mean annual precipitation (753 mm) record range is from 1900 to 2013 years for both the SPI and the EDI analyses. The most extreme 1-month and 3-month SPIs were observed in April 1998 and January 1971, respectively (Figure 25a and Figure 25b). The minimum values which were indicated for both time scale SPIs were observed as -2.69 and -3.11, respectively. The minimum 6-month SPI value (=-3.11) which was detected in August 2011 was the same value which was detected by 3-month SPI. The drought severity for three time scale (1, 3, 6 months) SPIs was detected as extreme droughts and their durations were 4, 10, 16 months, respectively (Figure 25a, Figure 25b, and Figure 25c). The most extreme 9-month SPI (=-2.78) occurred in March 1925 and had an 18 month duration (Figure 25d). The drought severity for 12-month and 24-month SPI was evaluated as extreme (12-month SPI=-3.03 and 24-month SPI=-2.98) in June 1925 and June 1956, respectively (Figure 25e and Figure 25f). The peak SPI value was detected as 36-month time scale SPI as -3.63 in January 1957 (85-month extreme drought).

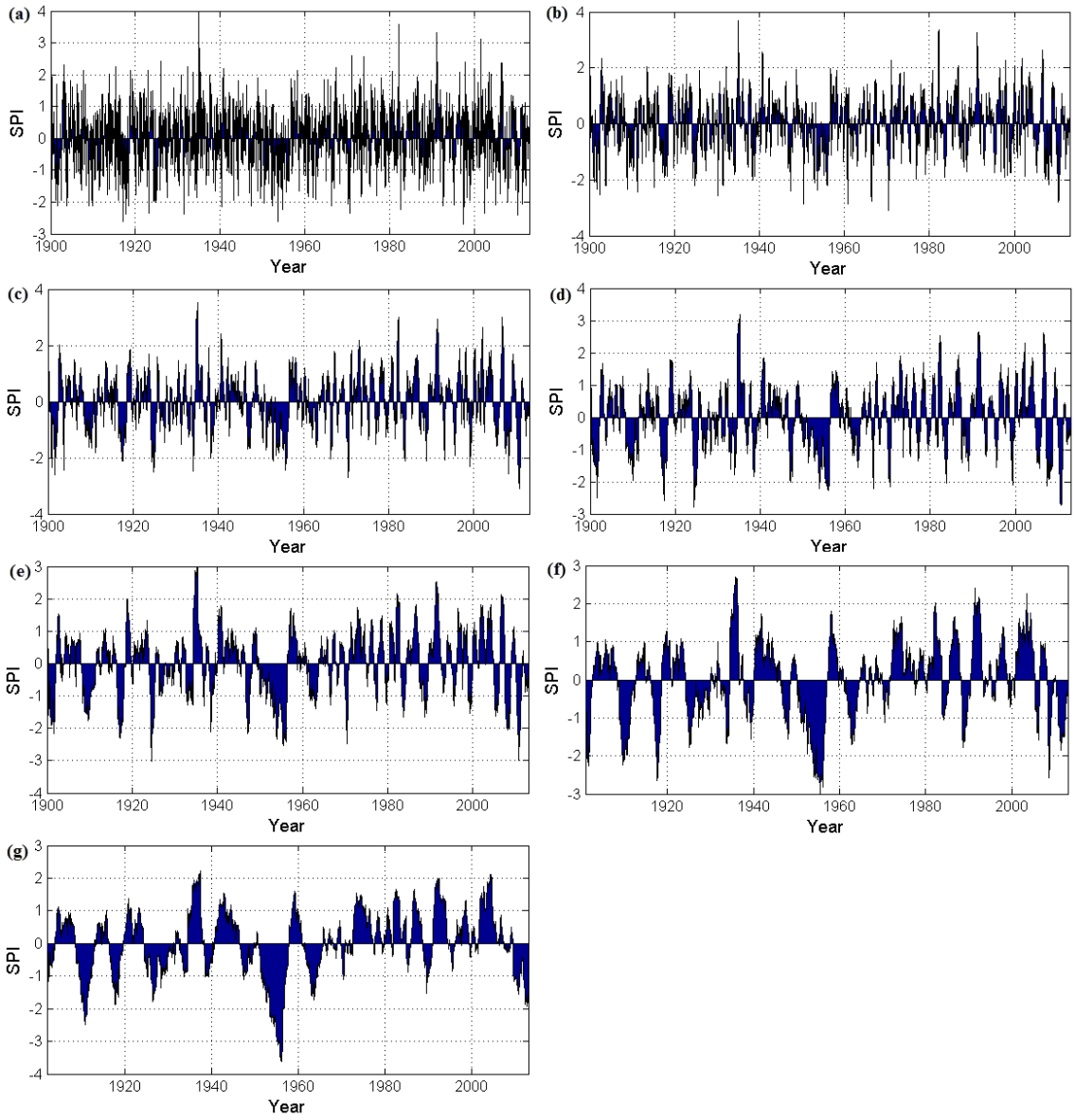

Figure 25. Time series of SPI values for region-2 for (a) 1-month, (b) 3-month, (c) 6-month, (d) 9-month, (e) 12-month, (f) 24- month SPI, and (g) 36- month SPI time scales

Figure 26 clearly depicts that the highest intense drought was observed in the 1950s by EDI. The longest drought, 51-month duration, was observed between 1953

(January) and 1957 (April) as an extreme drought. The peak value was detected as -3.29 by the EDI in January 1957. Furthermore, the highest magnitude and intensity were observed in the same extreme event as 95.83 and 1.88, respectively. Any extreme drought event wasn't observed any more after this extreme drought. Two severe drought events which had high intensity were observed within the last six years between 2008 (February) and 2009 (October) and between 2010 (October) and 2012 (February). Intensities of these consecutive drought events were detected as 1.11 and 1.2, while observed durations were 20 and 16 months, respectively.

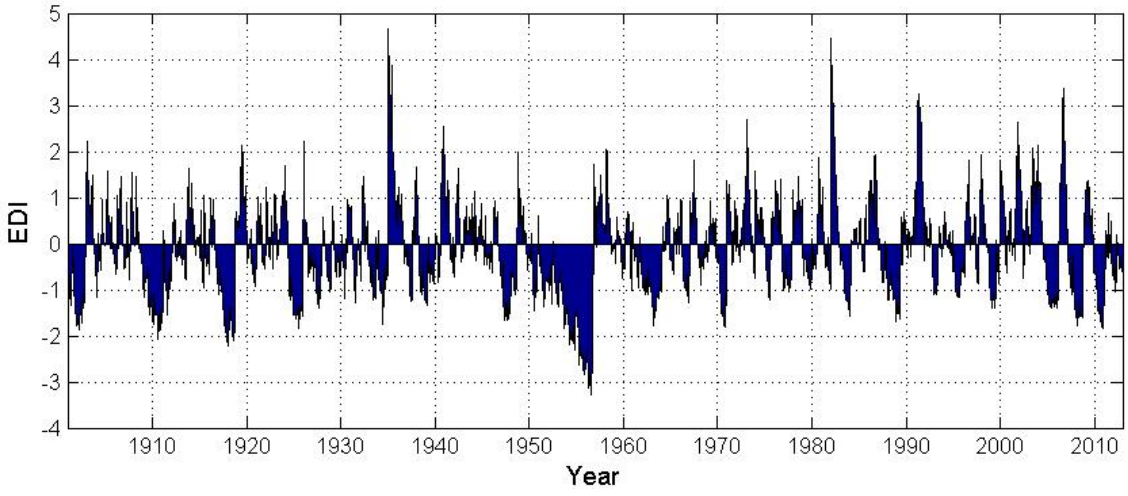

Figure 26. Time series of EDI values for region-2 between 1900 and 2013

Figure 27 reflects the probability of drought occurrences for different drought classes for the EDI and different time-scale SPIs in region-2. The drought event numbers which were detected in region-2 were more than region-1 due to the time series and

average monthly rainfall distribution. 1-month SPI had a greater total drought, severe drought, and moderate drought percentages, respectively, 27.43%, 9.14%, and 13.43%, than any time step SPI and EDI. EDI detected 1.54% extreme drought and underestimated extreme droughts than did any SPI similar to the results in region-1. However, EDI indicated 9.74% the second highest value subsequent to 1-month SPI for moderate drought. The highest rates of extreme drought were detected by 6-month, 9-month, and 12-month SPIs, respectively, as 7.73%, 7.14%, and 7.32%. Extreme drought percentages increased from 1-month SPI to 6-month SPI and then decreased, but 9-month SPI responded differently and out of this trend. 9-month and 36-month SPIs had equal moderate and severe drought percentages in their own time step in contrast to other SPIs and only 24-month SPI had low moderate drought percentage (2.15%) in comparison with severe drought percentage (8.60%).

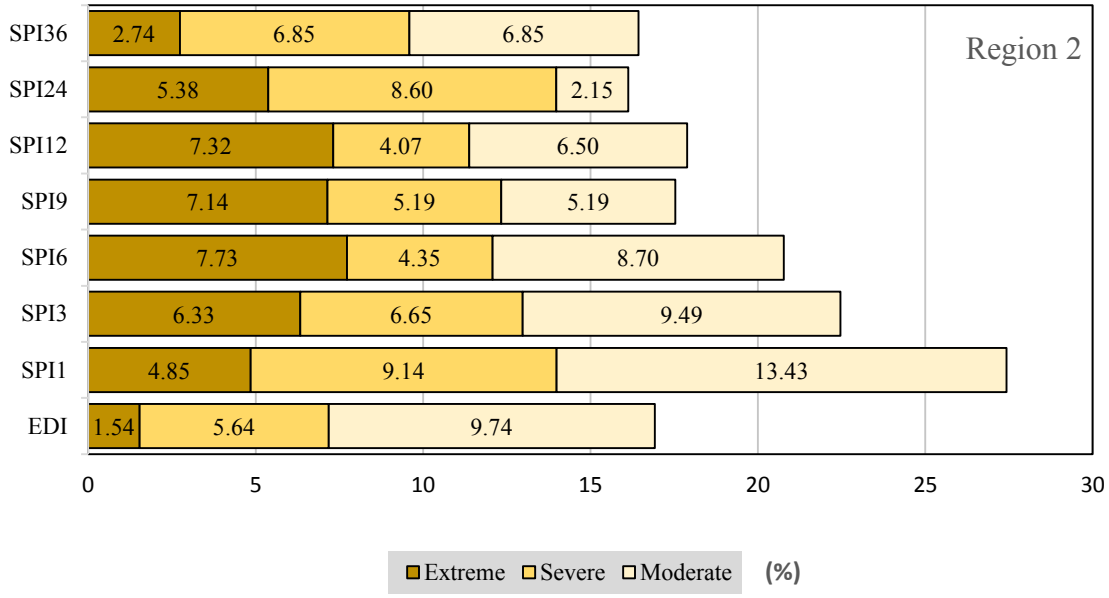

Figure 27. Drought class percentage by EDI and SPIs in region-2 for 1900 and 2013

5.3.3 Region-3 drought assessment

The mean annual precipitation (873 mm) record range is from 1946 to 2013 years for both the SPI and the EDI analyses. The minimum SPI values were detected less than -3.00 for all time step SPIs except 9-month SPI which was -2.98. The peak value was computed by 36-month SPI as -3.83 then 1-month SPI followed with -3.6 SPI value (Figure 28g and Figure 28a). The longest drought based on 1-month SPI was monitored between 1955 (September) and 1956 (August) as a severe drought.

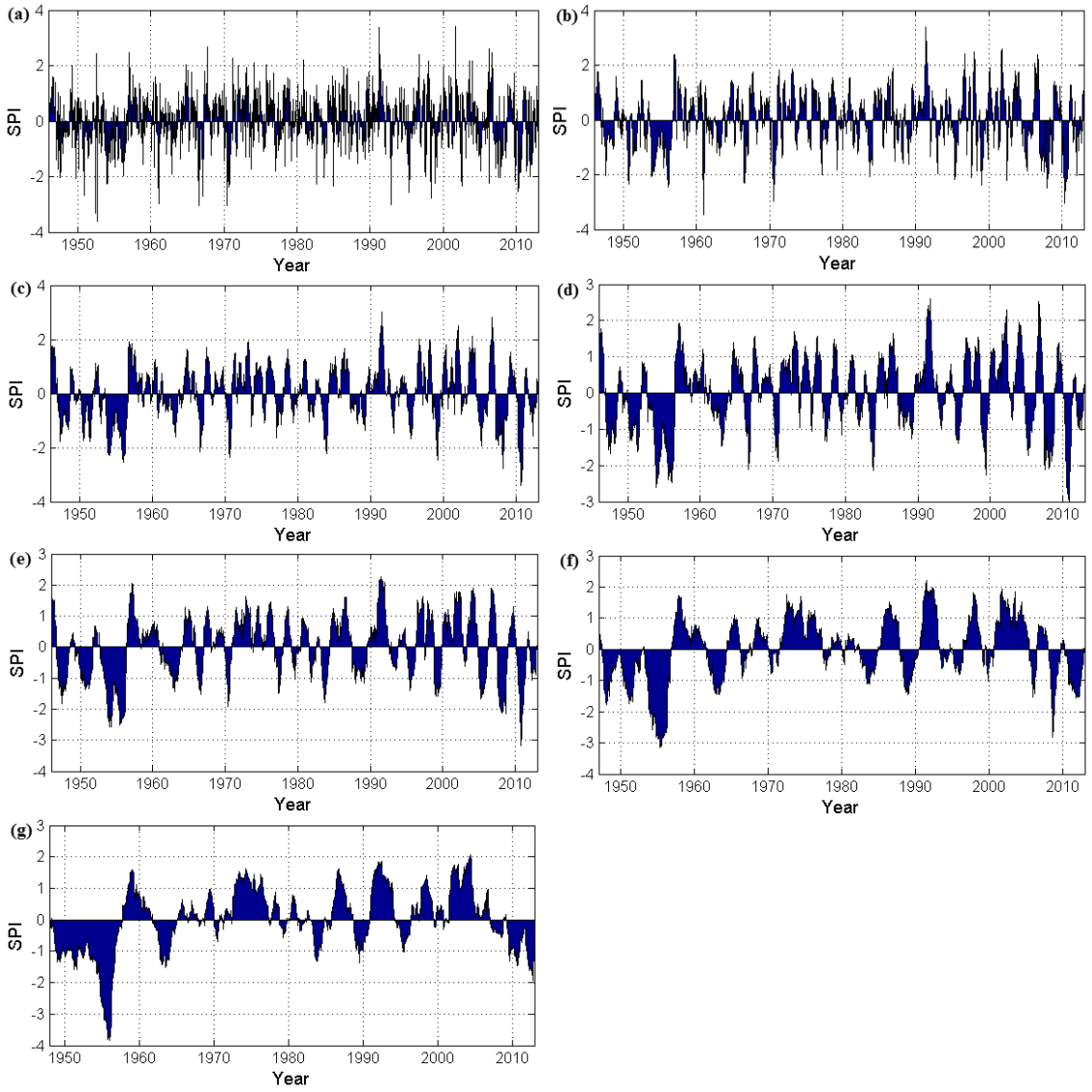

Figure 28. Time series of SPI values for region-3 for (a) 1-month, (b) 3-month, (c) 6-month, (d) 9-month, (e) 12-month, (f) 24- month SPI, and (g) 36- month SPI time scales

The only one extreme drought event was detected by EDI between 1953 (October) and 1957 (April) with 42-month duration. In addition, the highest magnitude and intensity also were detected in this time series. The highest intensity in the EA based on the EDI

was observed in region-3 as 1.93, while the magnitude pretty high (80.86) but less than the magnitude value (95.83) which was observed in region-2.

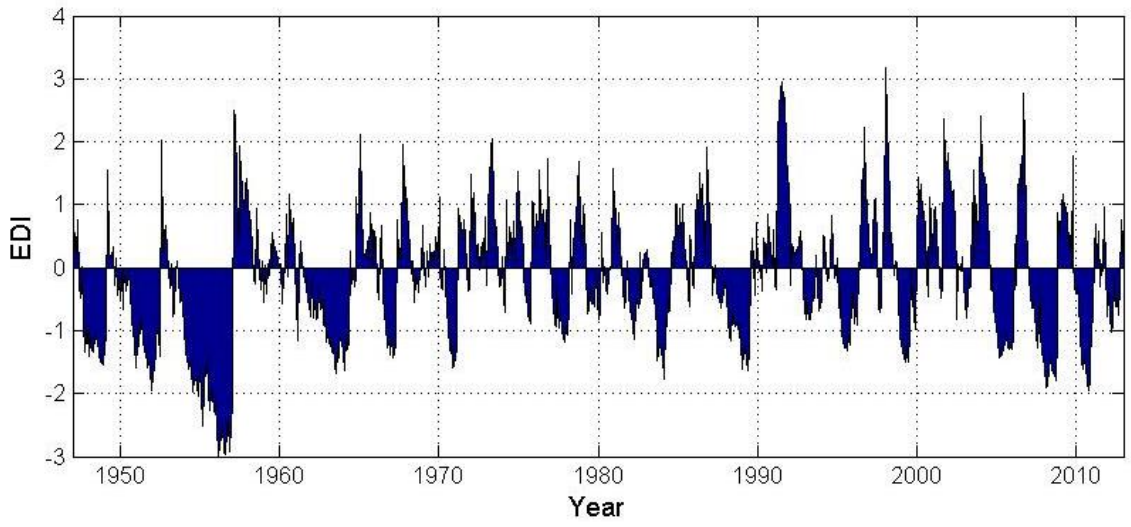

Figure 29. Time series of EDI values for region-3 between 1946 and 2013

The probability of drought occurrences for different drought classes have been shown in Figure 29 for the EDI and different time-scale SPIs in region-3. 12-month SPI had equal severe and moderate drought percentage as 7.78%. Similar to region-1 and region-2, 1-month SPI had the highest rate of total drought event percentages 24.76% in region-3. EDI had the highest severe drought percentage (7.83%) when compared with other regions. In addition, EDI had the lowest extreme drought percentage (0.87%) similar to region-1 and region-2. 3-month SPI and 1-month SPI had the most extreme drought percentages, respectively, 8.15% and 7.62%. Not only were extreme drought event percentages fluttered from 1-month SPI to 36-SPI but other drought severities (severe and

moderate drought) also were undulated for any time step SPI so there is no any specific trend and there is a fluctuation.

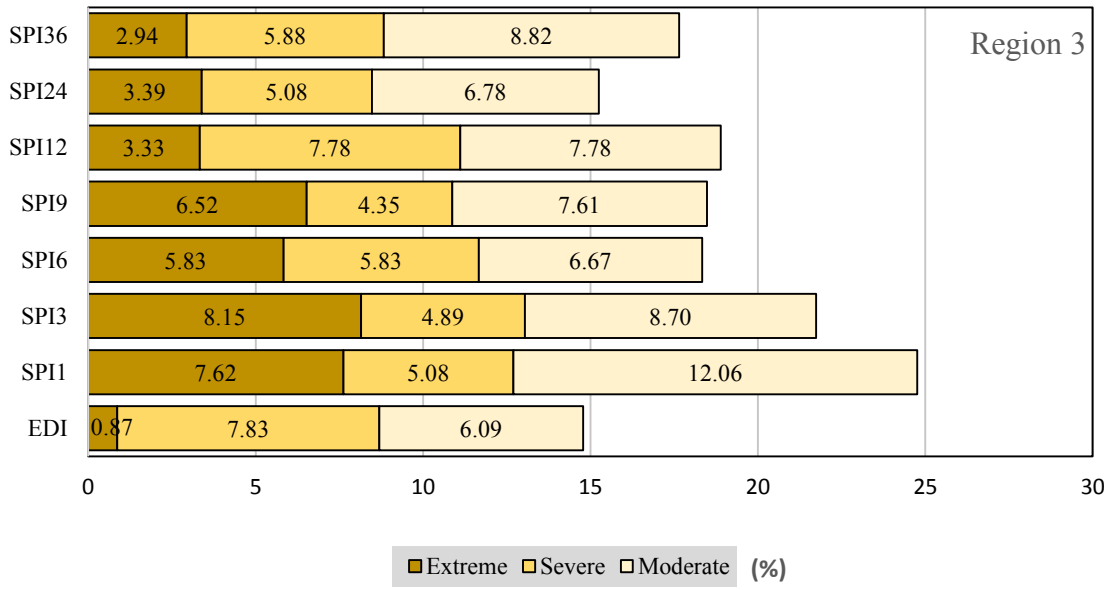

Figure 30. Drought class percentage by EDI and SPIs in region-3 for 1946 and 2013

A variety of drought severity has been changing from region to region and Figure 31 illustrates the spatial distribution of drought severities in the EA at different time step SPIs and EDI. It can be indicated from Figure 31 that EDI only drought index detected extreme drought less than any time steps SPI for each region. Region-1 has lower average rainfall and 3-month SPI found this region having the highest rate of extreme drought (9.04%) and the highest rate of severe drought was found by 9-month SPI with 13.48%. The highest percentage of moderate drought was detected by EDI (12.50%). Region-2 has the average rainfall and extreme drought was found 7.73% by 6-month SPI. 1-month SPI

had the highest severe and moderate drought percentages, respectively of 9.14% and 13.43% in region-2. Region-3 has higher average precipitation than other regions and the highest rate of extreme drought was found 8.15% by 3-month SPI similar to region-1. EDI detected the highest severe drought percentage (7.83%) in contrast to the lowest rate of extreme drought (0.87%). 1-month SPI had the highest total drought (sum of "extreme", "severe", and "moderate") percentage for region-1, region-2, and region-3, respectively, of 25.87%, 27.43%, and 24.76%.

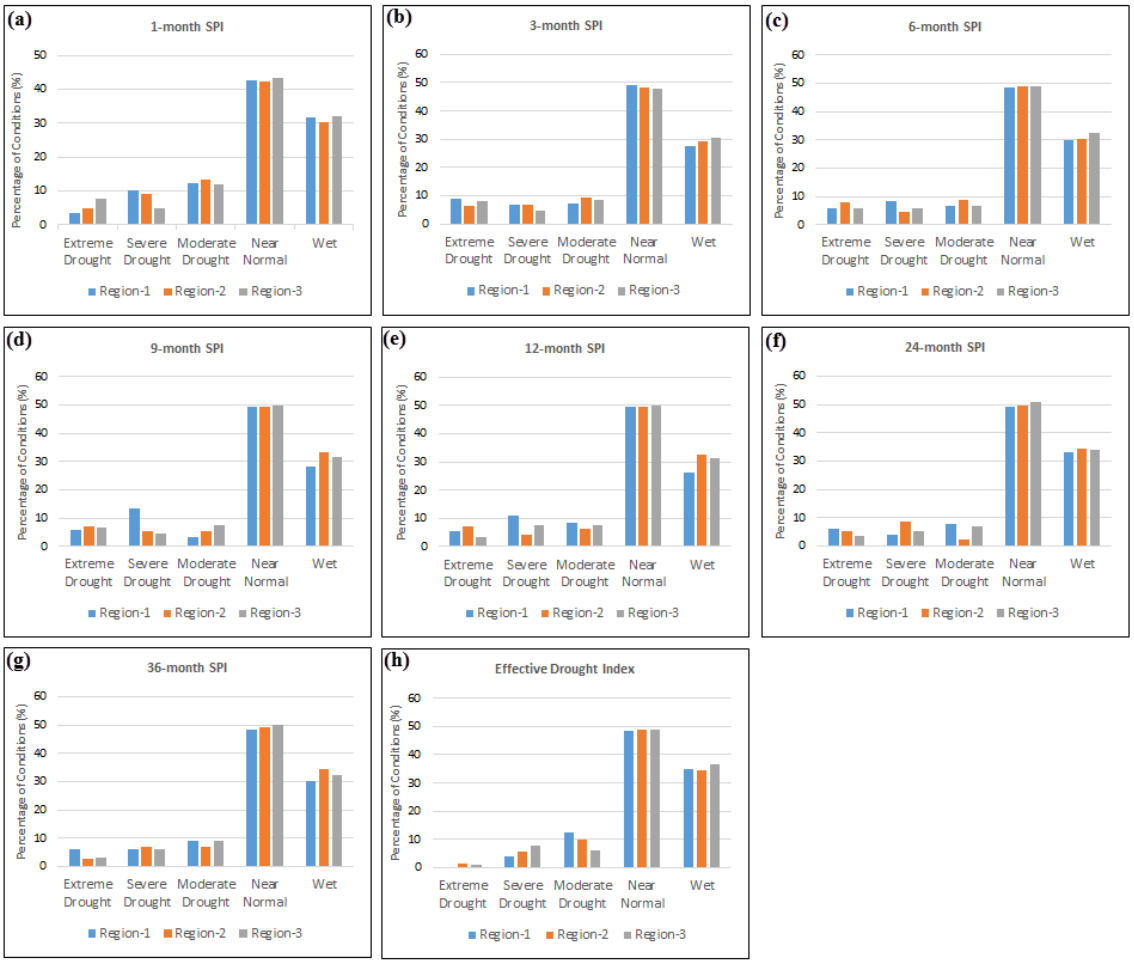

Figure 31. Regional droughts found by (a) 1-month SPI, (b) 3-month SPI, (c) 6 month SPI, (d) 9-month SPI, (e) 12-month SPI, (f) 24-month SPI, (g) 36-month SPI, and (h) EDI

5.4 Spatial drought hazard assessment

Drought hazard assessment, in this study, was calculated by using the probability of occurrence and severity based upon weight and ratings, as mentioned in section 3. The weights were assigned according to the SPI and EDI drought severity, while the ratings were assigned a range of drought occurrence probability. An effective area for each station was created by using the Thiessen polygon method and ratios were obtained by dividing

the area of station by the total area. For example, region-1 has seven stations and their ratios based on Thiessen polygons are 11.91%, 11.31%, 25.07%, 1.56%, 7.67%, 17.53%, and 24.94%, and their drought occurrence probabilities of near normal drought (NND) (24-month SPI) are 47.83%, 50.00%, 49.21%, 48.65%, 50.00%, 48.65%, and 48.98%, respectively. Hence, the occurrence probability (OP) of NND based on 24-month SPI for region-1 is 49.033 (=11.91x47.83+11.31x50.00+25.07x49.21+1.56x48.65+7.67x50.00+17.53x48.65+24.94 x48.98). Thus, OP of each condition NND, MD, SD, and ED are 49.033%, 6.021%, 6.272%, 6.185%, respectively for region-1. The same computing was applied for each occurrence probability of MD, SD, and ED for each region for each time scale SPI and EDI. After these calculations, the EA region had OP's range from 49.166% to 50.105% for the NND condition based on 24-month SPI (Table 16). OP's ranges which were created by dividing the range into 4 for the MD, SD, and ED, have been shown in Table 15.

Table 15 Occurrence probability for DHI based on a 24-month SPI

Region	NND	MD	SD	ED
1	49.033	6.021	6.272	6.185
2	48.854	6.076	5.450	5.892
3	50.105	9.149	3.616	5.714

Table 16 Weight and rate for drought severity for DHI (ex: 24-month SPI, region-1)

Severity	Weight	Occurrence probability (%)	Rating
Near Normal	1	OP<49.166	4
		49.166≤OP<49.479	3
		49.479≤OP<49.792	2
		49.792≤OP<50.105	1
Moderate	2	OP<6.803	4
		6.803≤OP<7.585	3
		7.585≤OP<8.367	2
		8.367≤OP<9.149	1
Severe	3	OP<4.280	4
		4.280≤OP<4.944	3
		4.944≤OP<5.608	2
		5.608≤OP<6.272	1
Extreme	4	OP<5.831	4
		5.831≤OP<5.949	3
		5.949≤OP<6.067	2
		6.067≤OP<6.185	1

The ratings for region-1 are 4, 4, 1, and 1, based on 24-month SPI of NND, MD, SD, and ED, respectively. As an illustration of this, NND of region-1 is 49.033% (Table 15) and rating of NND is 4 (Table 16). Table 17 briefly summarizes the results of ratings and weights for each region based on the 24-month SPI.

Table 17 Ultimate ratings and weights of regions for DHI (ex: based on 24-month SPI)

Drought Severity	Weights	Ratings		
		Region 1	Region 2	Region 3
NND	1	4	4	1
MD	2	4	4	1
SD	3	1	2	4
ED	4	1	3	4

Finally, DHI was generated by using equation (10) as follows:

$$DHI = (4 \times 1) + (4 \times 2) + (1 \times 3) + (1 \times 4)$$

$$DHI = 19$$

As a result, DHI was determined as 19 for region-1. Then, DHI was re-scaled through from 10 to 40 to obtain the range 0 to 1, and 0.3 was computed by using equation (11).

DHI which was generated for all regions and for all time scales such 1, 3, 6, 9, 12, 24 and 36-month SPIs and EDI has been shown DHI and DHI classification in Table 18 and Table 19, respectively.

The regions were classified according to the DHI index into four classes, such as "Very High" between 0.75 and 1.0, "High" between 0.50 and 0.75, "Moderate" between 0.25 and 0.50, and "Low" between 0 and 0.25.

Table 18 Drought hazard index for each region and for each time-scales SPI and EDI

Region	Drought Hazard Index							
	SPI 1	SPI 3	SPI 6	SPI 9	SPI 12	SPI 24	SPI 36	EDI
Region-1	0.70	0.33	0.20	0.30	0.60	0.30	0	0.40
Region-2	0.40	0.27	0.57	0.67	0.67	0.67	0.70	0.73
Region-3	0.50	0.70	0.20	0.60	0.30	0.70	0.30	0.30

"Low" drought hazard class was no detected in region-2, and region-2 had relatively "High" drought classification compared to other regions (Table 19). Region-1 and region-3 had "Low" drought hazard based on 6-month SPI. Region-1 had faced "Low" drought hazard based on 36-month SPI. Only region-1 had two "Low" drought classes

which were observed in SPI-6 and SPI-36. Table 18 illustrates that the highest DHI was detected as 0.73 by EDI in region-2 and the highest DHI was detected as 0.70 for 1, 3, 24, and 36-month SPI in region-1, region-3, region-3, and region-2, respectively. Therefore, "Very High" drought class was not observed for any time scale SPI and EDI in any regions.

Table 19 Drought hazard index classifications for each region and for each time-scale SPI and EDI

Region	DHI classifications							
	SPI 1	SPI 3	SPI 6	SPI 9	SPI 12	SPI 24	SPI 36	EDI
Region-1	H	M	L	M	H	M	L	M
Region-2	M	M	H	H	H	H	H	H
Region-3	H	H	L	H	M	H	M	M

*Abbreviations refer to: L: Low, M: Moderate, and H: High

Figure 32 depicts the spatial drought hazard map for the EA region. It can be signified from Figure 32 that although region-3 (east part of the EA) normally receives more than average precipitation of the study area, high level hazard was observed more than region-1 which has the lowest average rainfall in the area. It has been indicated that there exists no relation between the precipitation distribution and proneness to drought zones.

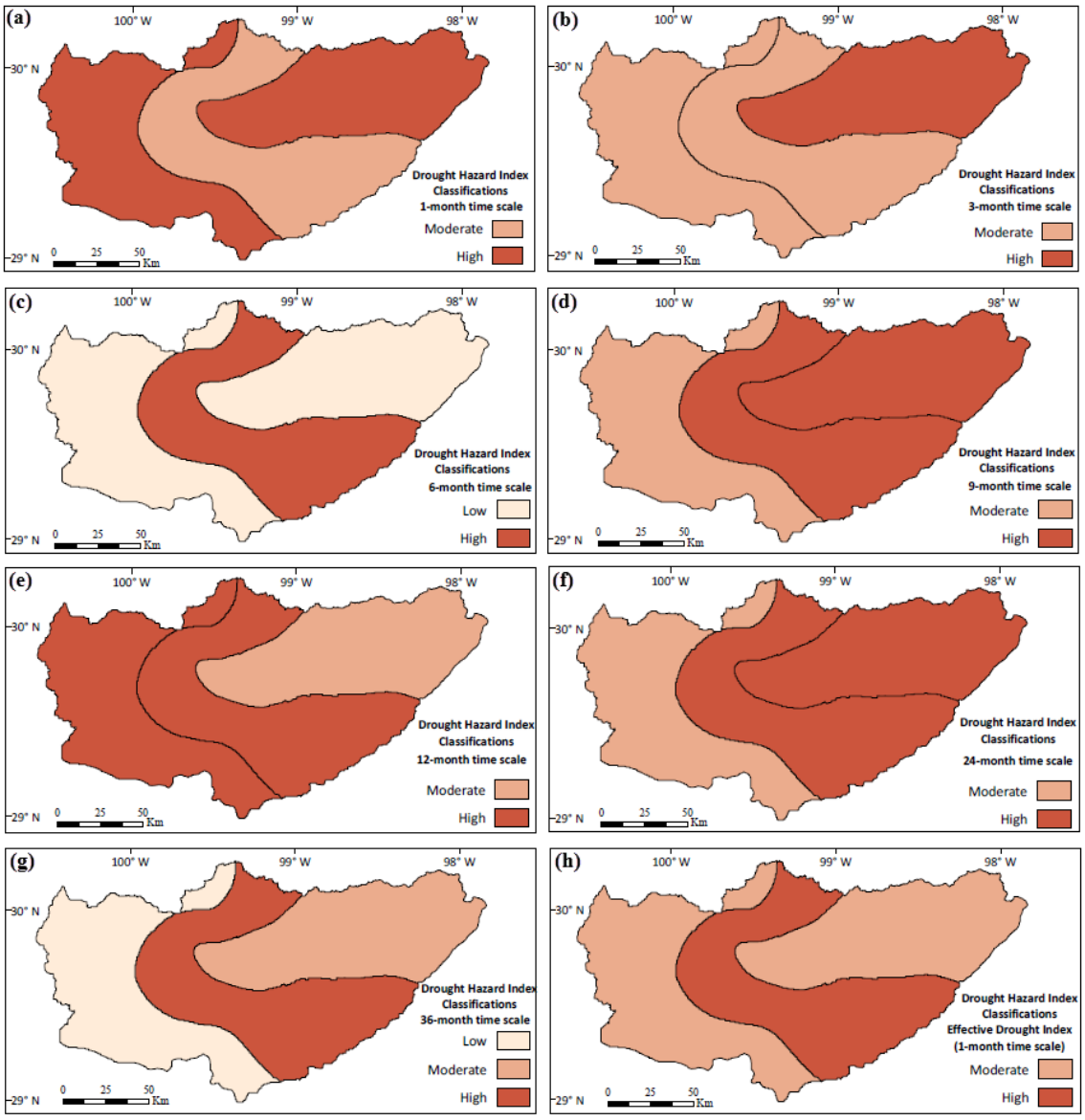

Figure 32. Drought hazard map for the Edwards Aquifer region, based on (a) 1-month SPI, (b) 3-month SPI, (c) 6-month SPI, (d) 9-month SPI, (e) 12-month SPI, (f) 24-month SPI, (g) 36-month SPI, and (h) EDI

5.5 County level drought hazard index

Edwards Aquifer is located within different climatic divisions and it makes difficult to analyze observed precipitation data for the regional drought assessment.

Therefore, the EA was divided into three hydrological regions, based on the monthly average precipitation distribution. The region boundaries which were created accurately to analyze drought assessment is relative and the virtual hydrological divisions were transformed from region to county level. The first reason for this conversion is to address specifically county-based drought assessment, since county level has significant political, agricultural, and environmental decision making. The other reason is to overlay and intersect drought hazard and vulnerability in order to obtain the best matching drought risk map, since drought vulnerability assessment is discussed and analyzed in county level.

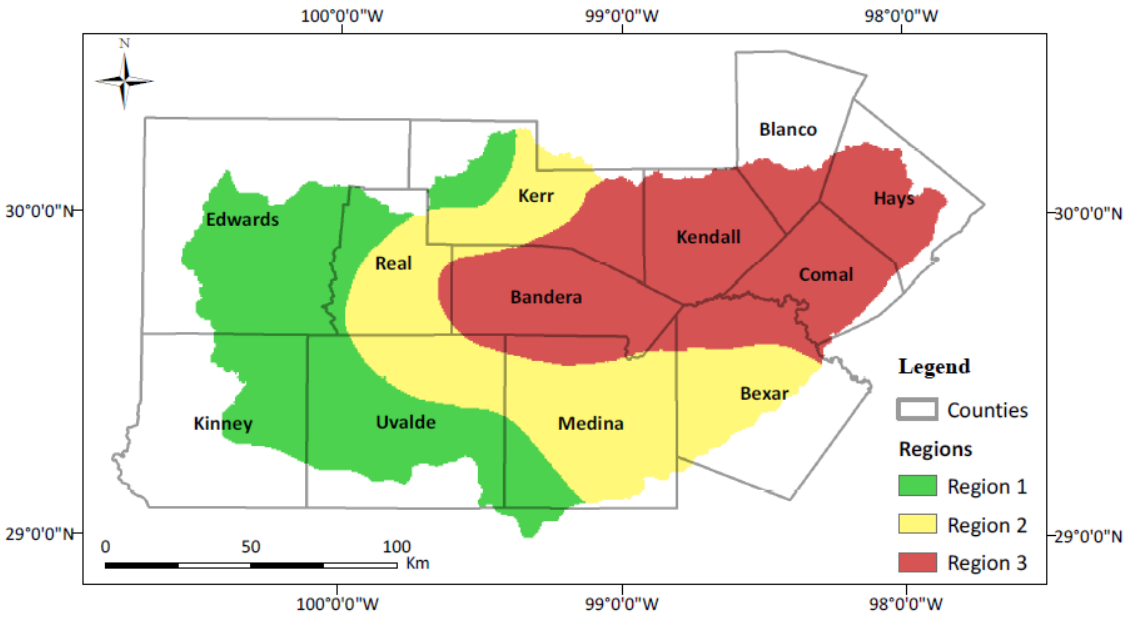

Figure 33. Edwards Aquifer region and located counties

The fundamental concept used is the combination of the area ratio and the DHI which have counties to transform from region to county level. The main assumption in this process is that Edwards and Kinney counties were assumed totally located in Region-1 (see the Appendix on the spatial average precipitation distribution at the county level). Thus, DHI belongs to Region-1 and was applied to these counties. The same assumption was applied for Blanco, Comal, Hays, and Kendall for Region-3. To compare regional DHI and county based DHI see Table 18 and Table 20.

As an illustration, the how DHI computed at the county level is explained for Bandera as follows:

Bandera is totally located within Region-2 and Region-3 (Figure 33). The area ratios for Bandera in Region-2 and Region-3 are 0.17 and 0.83, respectively. The DHI (12-month SPI) is 0.67 and 0.30 for Region-2 and Region-3, respectively. The adjusted ultimate DHI for Bandera is 0.36 (=0.67x0.17+0.30x0.83). All adjusted DHIs, based on equation (10), for each county, have been shown in Table 20.

Table 20 Adjusted drought hazard index at county level at each time-scale SPI and EDI

County	SPI 1	SPI 3	SPI 6	SPI 9	SPI 12	SPI 24	SPI 36	EDI
Bandera	0.48	0.63	0.26	0.61	0.36	0.69	0.37	0.37
Bexar	0.41	0.32	0.53	0.66	0.63	0.67	0.65	0.68
Blanco	0.50	0.70	0.20	0.60	0.30	0.70	0.30	0.30
Comal	0.50	0.69	0.21	0.60	0.31	0.70	0.31	0.31
Edwards	0.70	0.33	0.20	0.30	0.60	0.30	0.00	0.40
Hays	0.50	0.70	0.20	0.60	0.30	0.70	0.30	0.30
Kendall	0.50	0.70	0.20	0.60	0.30	0.70	0.30	0.30
Kerr	0.47	0.36	0.44	0.59	0.59	0.61	0.50	0.60
Kinney	0.70	0.33	0.20	0.30	0.60	0.30	0.00	0.40
Medina	0.48	0.30	0.46	0.57	0.64	0.57	0.50	0.63
Real	0.52	0.29	0.42	0.52	0.64	0.52	0.42	0.60
Uvalde	0.63	0.32	0.29	0.39	0.62	0.39	0.17	0.48

The Drought Hazard Index (DHI) classification of drought hazards is illustrated in Figure 34, Figure 35, and Figure 36 for different time scale SPIs and EDI.

It can be seen from Figure 34 that 1-month SPI found higher DHI in the study area by comparing to 3-month and 6-month SPIs. The western and north-east parts of the region have high level DHI while the middle of the area detected moderate DHI based on 1-month SPI which represents a short-term drought. Besides, the east part of the study area has the highest average rainfall while the west part has the lowest one. The probability of drought occurrence of 1-month SPI (Figure 30) detected quite high level and even region-3 has more than average rainfall and it is highly prone to short-term drought. 3-month SPI reflects short and medium term moisture conditions and seasonal estimation of precipitation. High level DHI of 3-month SPI bears a resemblance to 1- month SPI result for the north-east part. Blanco, Comal, Hays, and Kendall counties have the high level DHI based on 1-month and 3-month SPI. 6-month SPI, interestingly, has mostly different hazard classes than 1-month and 3-month SPI. The high DHI of 6-month drought was observed only in Bexar county, while the west and north-east part of the region faced a low hazard class. Moderate DHI of 6-month SPI was found mainly in the central part of the region.

Figure 35 shows that 9-month and 24-month SPIs perfectly matching for all DHI classes at the county level and DHI was detected mostly at the high level in the study area for both SPIs. Bexar, Medina, Kerr, and Real have high level DHI for all 9, 12, and 24-month time scale SPIs. Any low DHI class was not observed and regions dominated by high DHI based on 9, 12, and 24 month SPIs.

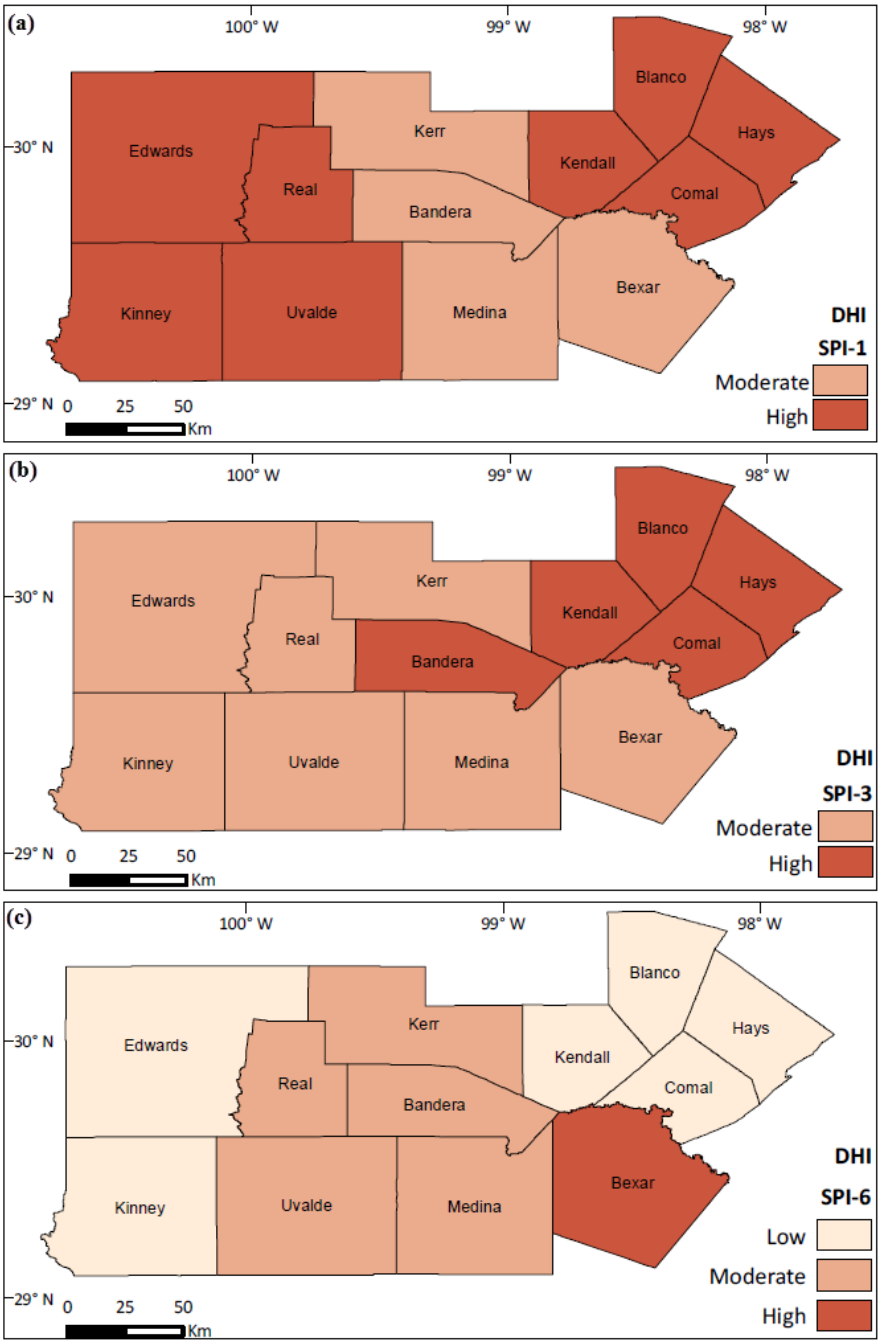

Figure 34. Drought hazard map: (a) 1-month, (b) 3-month, and (c) 6-month time scale SPIs

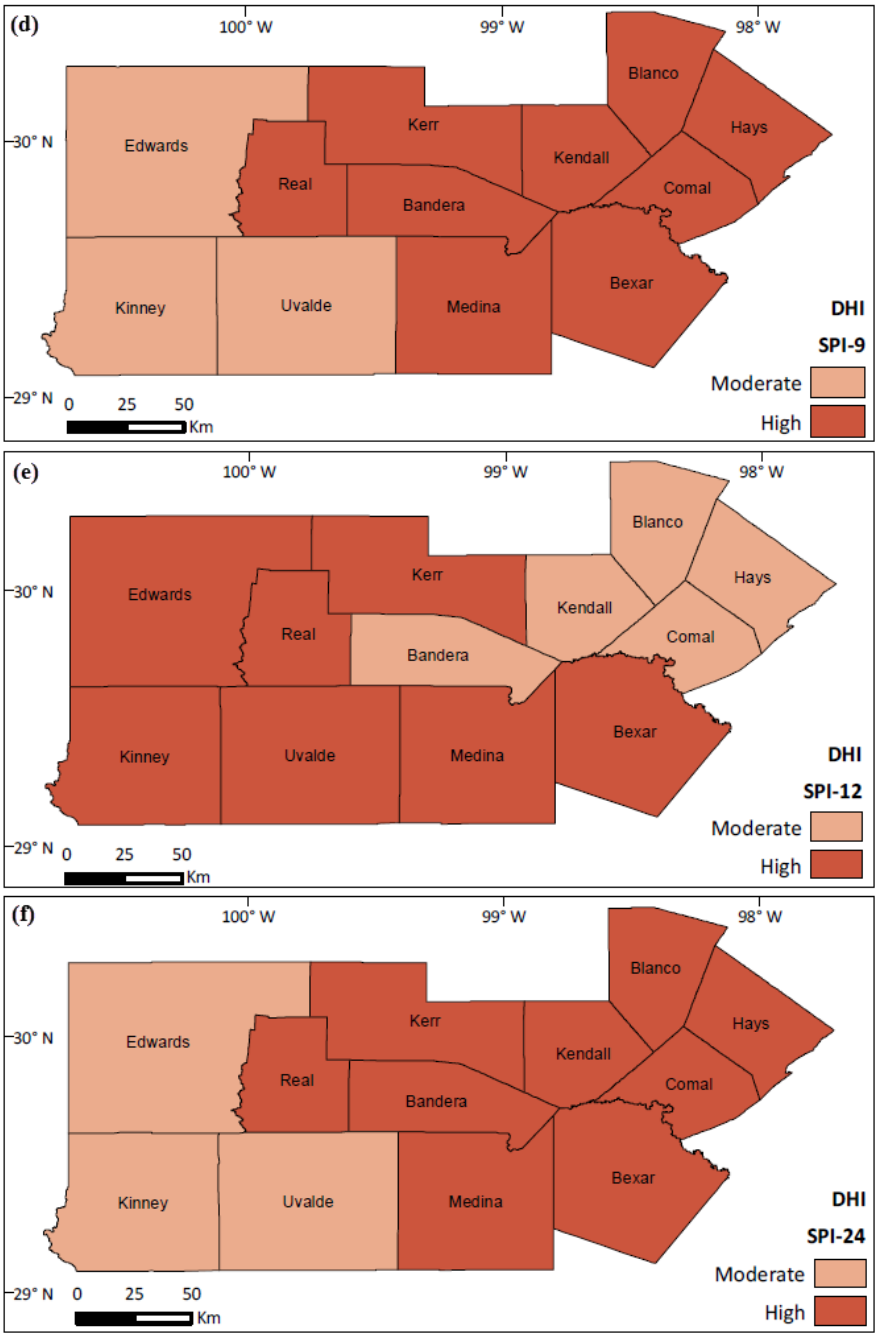

Figure 35. Drought hazard map: (d) 9-month, (e) 12-month, and (f) 24-month time scale SPIs

Figure 36 illustrates that 36-month SPI has three types of DHI as low, moderate, and high level. Low DHI was detected in the west part of the region, similar to 6-month SPI (except Uvalde), and moderate DHI similar to 12-month SPI (except Real). High level DHI was observed in only three counties, such as Bexar, Kerr, and Medina. EDI didn't detect any low DHI in the region and mostly moderate DHI was observed. The high DHI was detected by EDI for Bexar, Kerr, Medina, and Real counties.

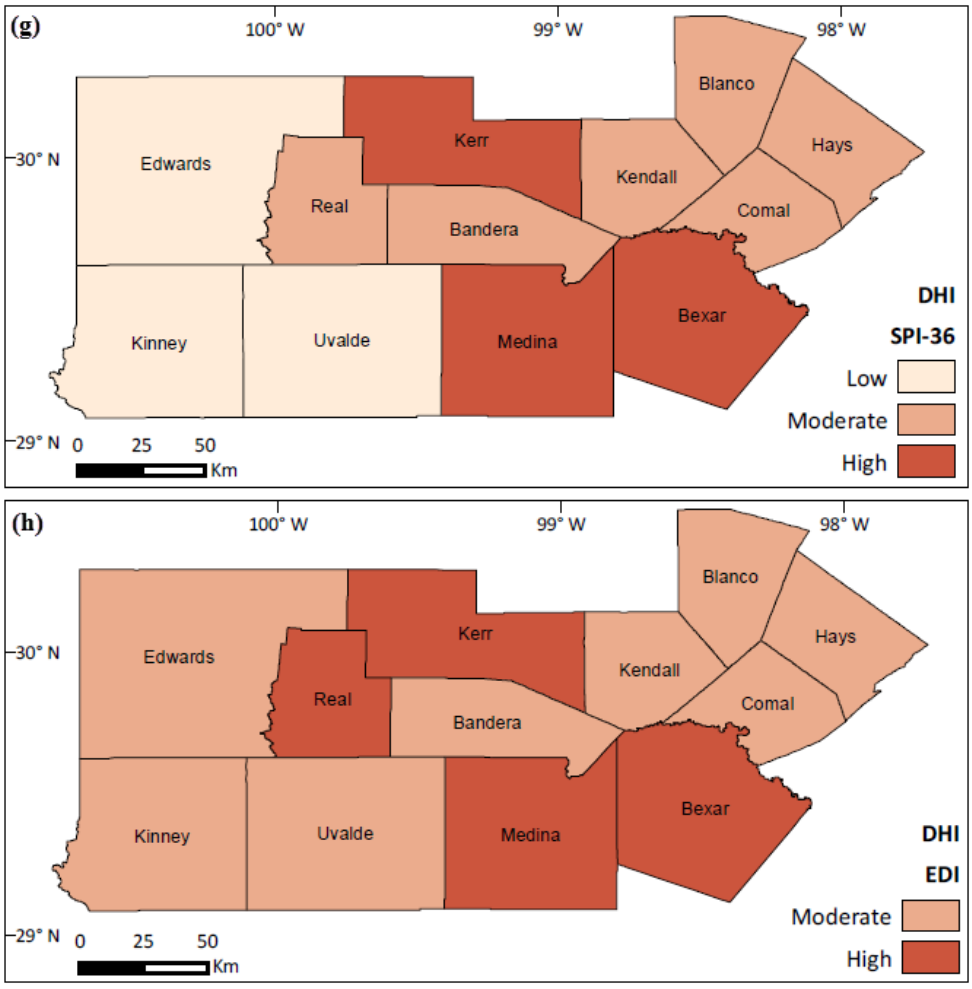

Figure 36. Drought hazard map: (g) 36-month time scale SPI and (h) EDI

Generally, high DHI was observed, based on 1, 9, 12, and 24-month time scale SPIs and spatial variations of DHI differ from each other, except 9-month and 24-month SPIs. Bexar had the high DHI which was detected by 6, 9, 12, 24, and 36-month SPIs and EDI. Very high level DHI was not detected for any time scale SPI and EDI. EDI detected high DHI less than 1, 9, 12, and 24-month SPIs based on county level and moderate DHI was detected by EDI more than any time scale SPI.

5.6 Drought vulnerability assessment

Ground water is the major water resource in the region for agricultural, municipal, manufacturing, irrigation, livestock water use, and so on. Most of water supply for the region is from the groundwater source and regional water use percentage is 81% groundwater while the surface water use is 19% (Figure 37). Hays had the highest rate of surface water use as 51% in the region. Kerr, Kendall, and Comal follow with 42%, 32%, and 30% surface water use, respectively. The other counties had less than 30% surface water use in the EA.

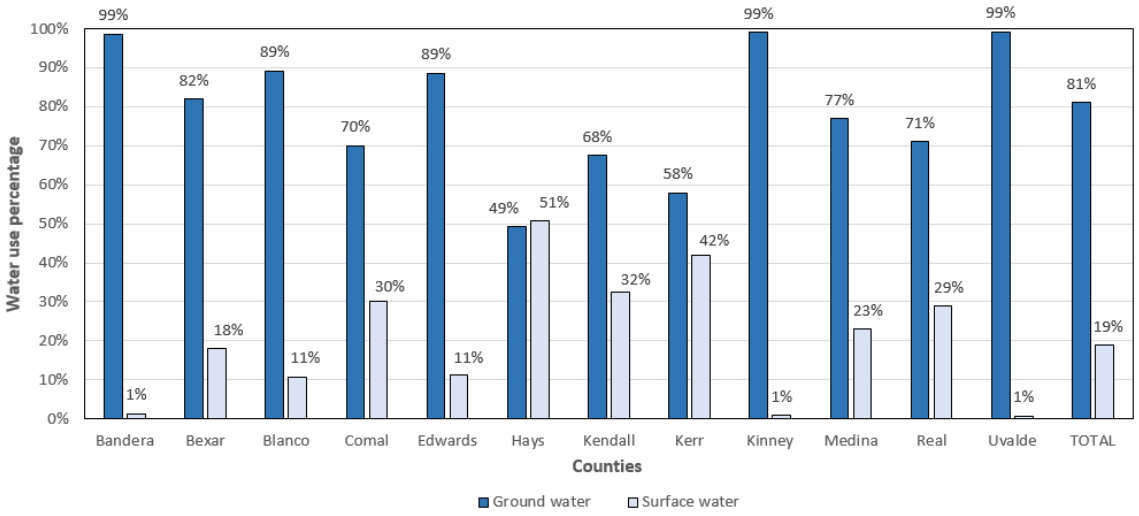

Figure 37 Water use summaries for counties located in the EA (TWDB, 2012)

5.6.1 Drought vulnerability indicators

Figure 38 depicts spatial patterns of different vulnerability indicators which were integrated using the natural break method. Then, the Drought Vulnerability Index (DVI) values were classified into four classes based on the natural break classification. The ultimate DVI was generated by using equation (17).

It can be observed from Figure 38a, c, and d that the percentage of population density, municipal water, and industrial water are the highest in the Bexar county. Higher percentage of people who live below the poverty level is detected mostly in the west part of the region that has lower population density (Figure 38a, b). Not only Kinney and Uvalde have low population density, but they also have the highest percentage of people living below the poverty level (Figure 38b). The most vulnerable counties in terms of

agricultural water and irrigated land were detected as Medina and Uvalde (Figure 38e,f). Furthermore, the percentage of market value of products was observed to be at the highest level for Medina and Uvalde with Bexar (Figure 38g).

5.6.2 Drought vulnerability index

DVI was calculated, based on 7 vulnerability indicators which have been shown in Figure 38, then thematic map was generated for 12 counties by using the GIS environment (Figure 39). DVI was classified into four groups and only one "very high" level was detected in Bexar county. In other words, Bexar is the most vulnerable county to drought in the region. Medina and Uvalde were observed by DVI as "high" level vulnerable counties. Some of these counties are located in the south-east parts of the region and the west and central part of the region was detected with "low" level vulnerability. It can be seen from Figure 39 that there exists no any specific trend to illustrate vulnerable regions such as east, west and so forth and it could be explained only by differences between vulnerability indicators which were different from county to county.

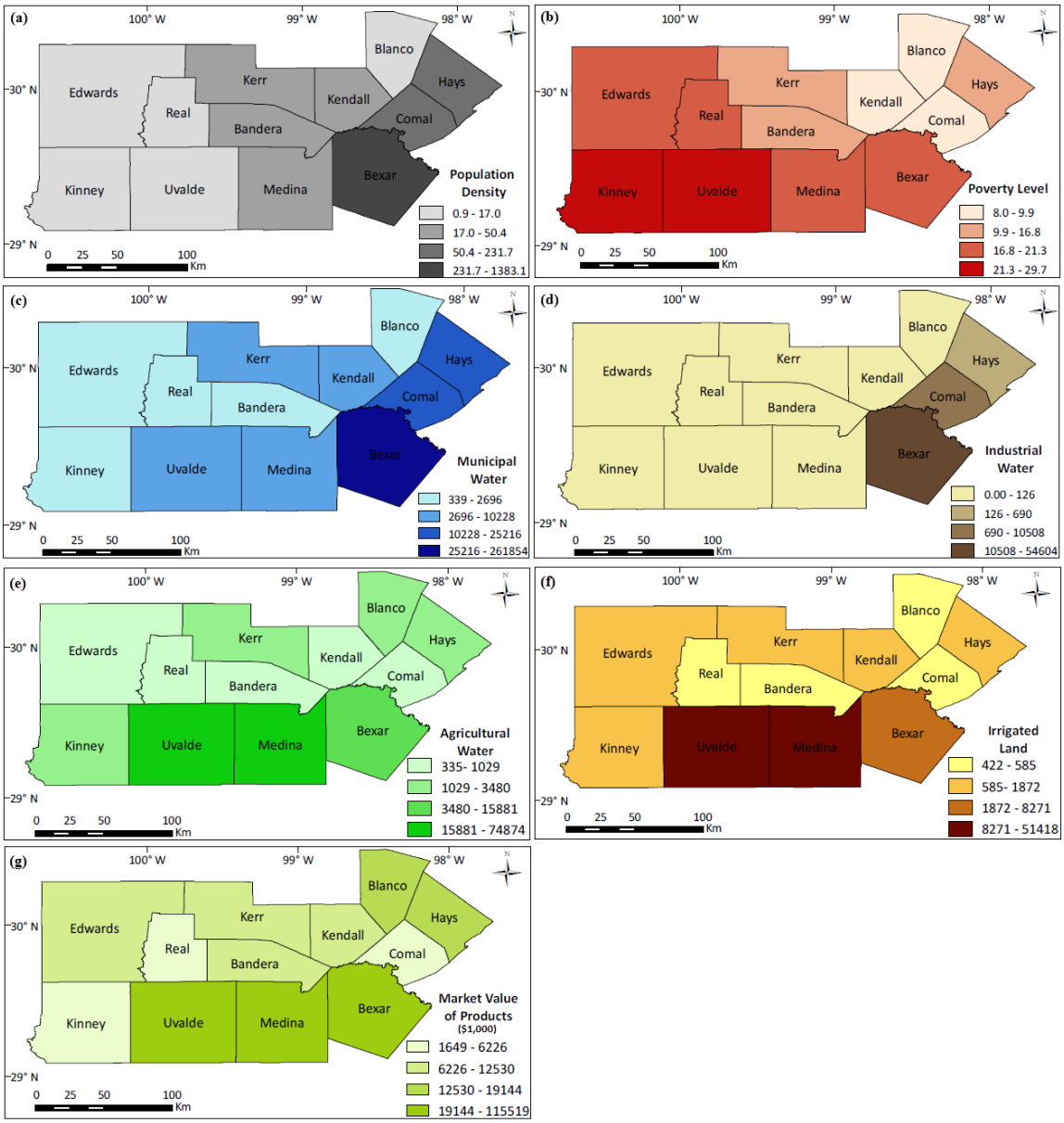

Figure 38. County level maps of drought vulnerability indicators: (a) population density, (b) poverty level, (c) municipal water, (d) industrial water, (e) agricultural water, (f) irrigated land, (g) market value of products (Note: (b) poverty level represents percentage of people who living below the poverty level)

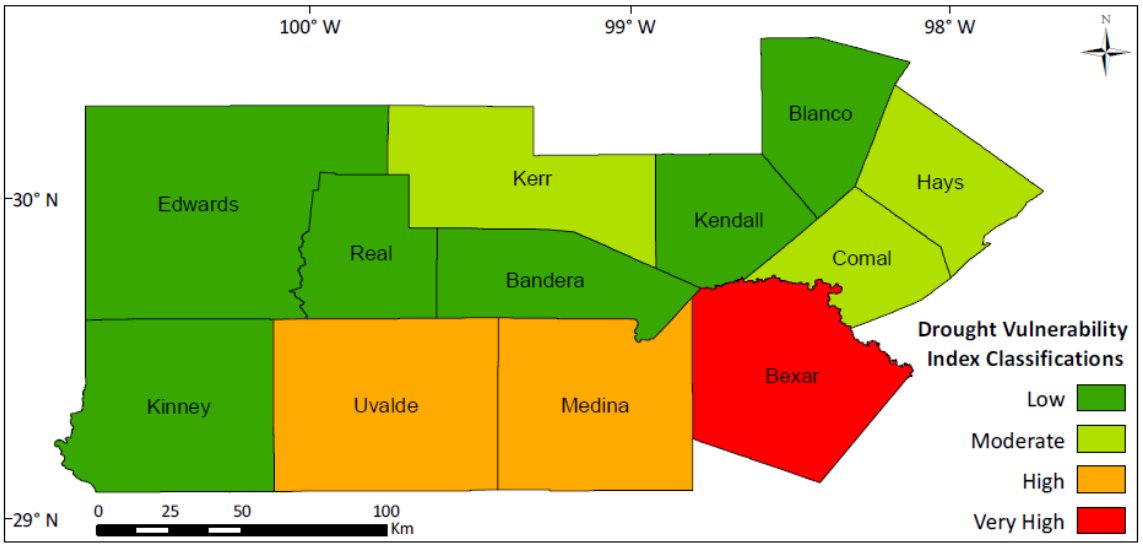

Figure 39. Spatial distribution of composite drought vulnerability map for the counties in the EA region

The DVI values should be grasped to analyze the vulnerability map, since the map shows only the intervals and classes. Therefore, Figure 40 illustrates in detail the DVI values and classes. It can be identified from Figure 40 that there are critical values for Hays and Kinney counties. Although Hays and Kinney counties were detected, respectively, as "moderate" and "low" vulnerability classes, the DVI values are quite close to the limit values. The DVI value was detected as 0.48 (limit value=0.50) and 0.24 (limit value=0.25) for Hays and Kinney, respectively. Their classes could be thought "high" and "moderate" depending on the point of view and the type of assessment to take notice of safety coefficient. As a result, the DVI and thematic map should be addressed together to eliminate errors on the drought risk evaluation. On the other hand, the original values, in this study, are used to assess DVI and stick to the original results.

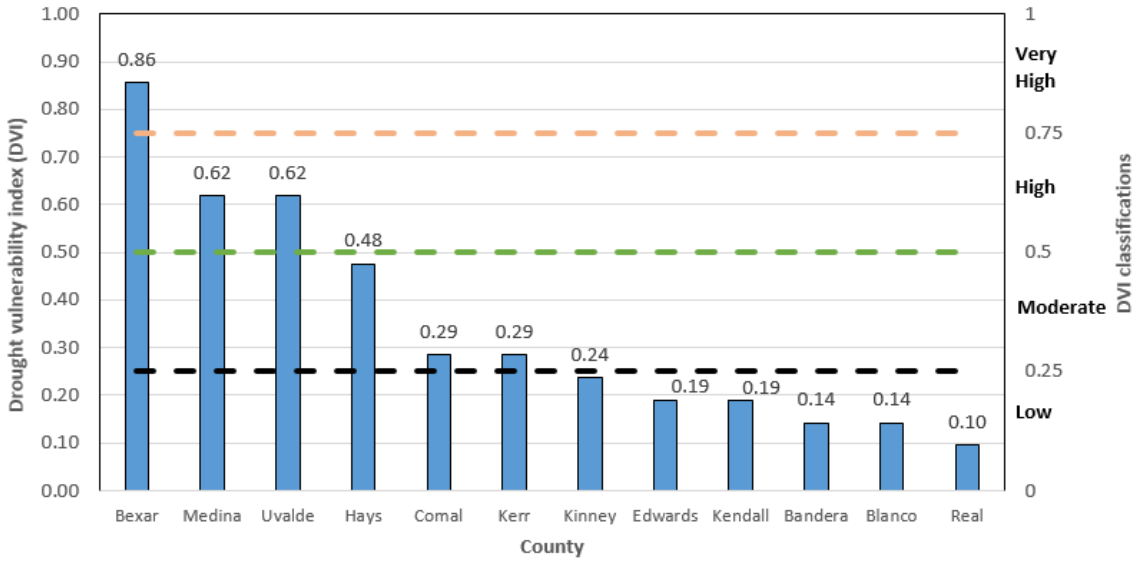

Figure 40. Drought vulnerability index values by county

5.7 Drought risk assessment

Drought Risk Index (DRI) was generated by integrating DHI and DVI by using equation (18). However, a different classification was used for DRI which is different from DHI and DVI classifications (see Table 6 and Figure 9).

Figure 41a shows that high drought risk of 1-month SPI was detected for three counties, Bexar, Medina, and Uvalde, which are located in the southern parts of the region. It can be indicated from Figure 41b that the spatial risk distribution of droughts with a time scale of 3-month SPI is similar to the drought risk of a 1-month time scale SPI. On the other hand, the number of counties characterized by high DRI decreased and most of the counties were dominated by moderate DRI. Table 21 clearly shows the percentage of area under different drought risk categories and it can be understood that 3-month time scale SPI detected mostly moderate risk level in the region. The spatial distribution of the

drought risk of 6-month SPI indicates mostly different classification results, as shown in Figure 41c. The region was detected with mainly low drought risk level (53.9%) based on 6-month time period drought. Very high level DRI was not observed for 1, 3, and 6-month

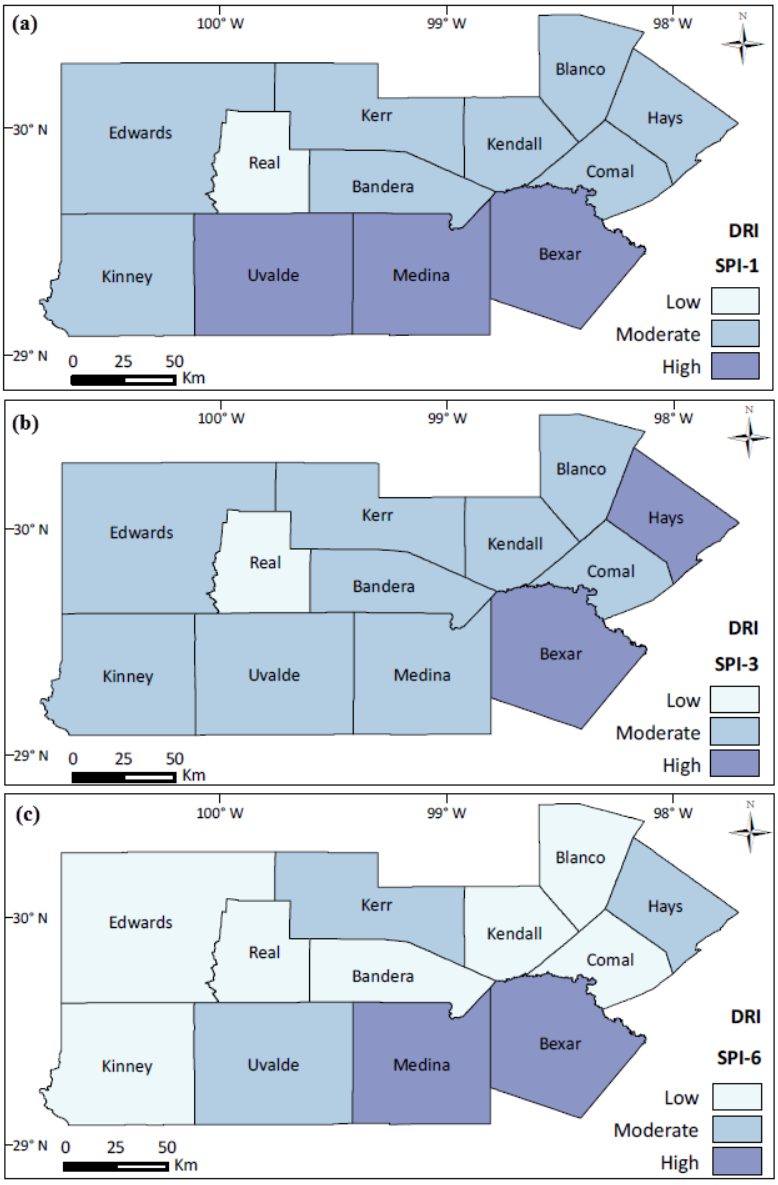

Figure 41. Risk maps of droughts at (a) 1-month, (b) 3-month, and (c) 6-month time scale SPIs

SPIs in the region and Table 21 shows that 32.3% of the area was exposed to high risk, 62.3% of the area to moderate risk at 1-month time step drought. Moreover, 15% of the area observed high drought risk, 79.5% of the area moderate drought risk as a 3-month time period drought.

Table 21 Percentage of area under different drought risk categories for 1, 3, and 6-month time scale SPIs

Time scales (month)	Percentage of area (%)			
	Very High	High	Moderate	Low
1	-	32.3	62.3	5.4
3	-	15.0	79.5	5.4
6	-	20.1	26.0	53.9

Figure 42d shows that only Bexar county was exposed to very high drought risk with 9-month time droughts. However, 9 and 24-month droughts had the same percentage for all types of drought risk categories (Figure 42d, f and Table 22) due to the same DHIs. Table 22 illustrates that 9.8% of the area was exposed to very high drought risk, 15.7% of the area to high drought risk, and 52.7% of the area to moderate drought risk for both 9 and 24-month time period droughts. However, 32.3% of the area was exposed to high drought risk and 45.4% of the area to moderate drought risk with 12-month SPI. The percentage of area for low drought risk was found for each 9, 12, and 24-month droughts, respectively, quite near as 21.9%, 22.3%, and 21.9% (Table 22).

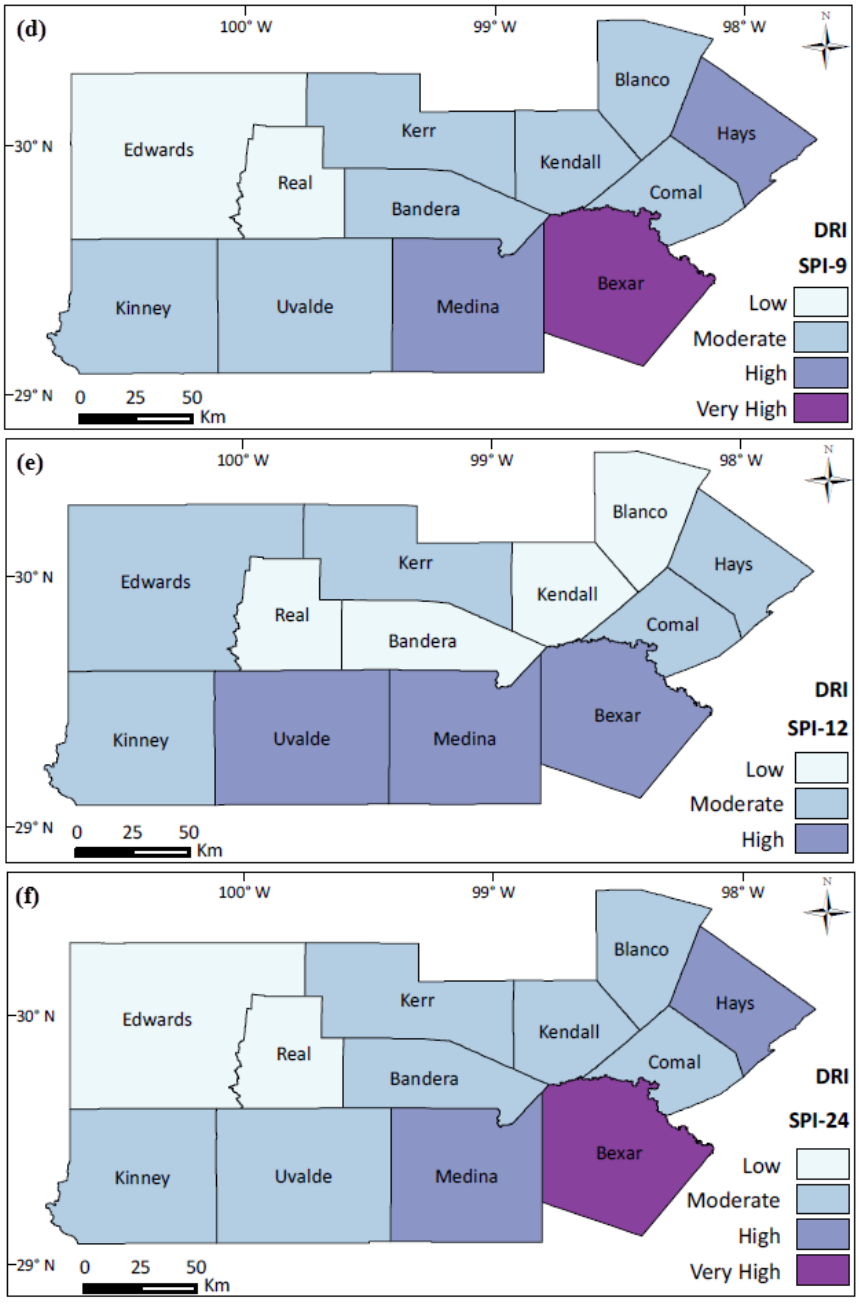

Figure 42. Risk maps of droughts at (d) 9-month, (e) 12-month, and (f) 24-month time scale SPIs

Table 22 Percentage of area under different drought risk categories for 9, 12, and 24-month time scale SPIs

Time scales (month)	Percentage of area (%)			
	Very High	High	Moderate	Low
9	9.8	15.7	52.7	21.9
12	-	32.3	45.4	22.3
24	9.8	15.7	52.7	21.9

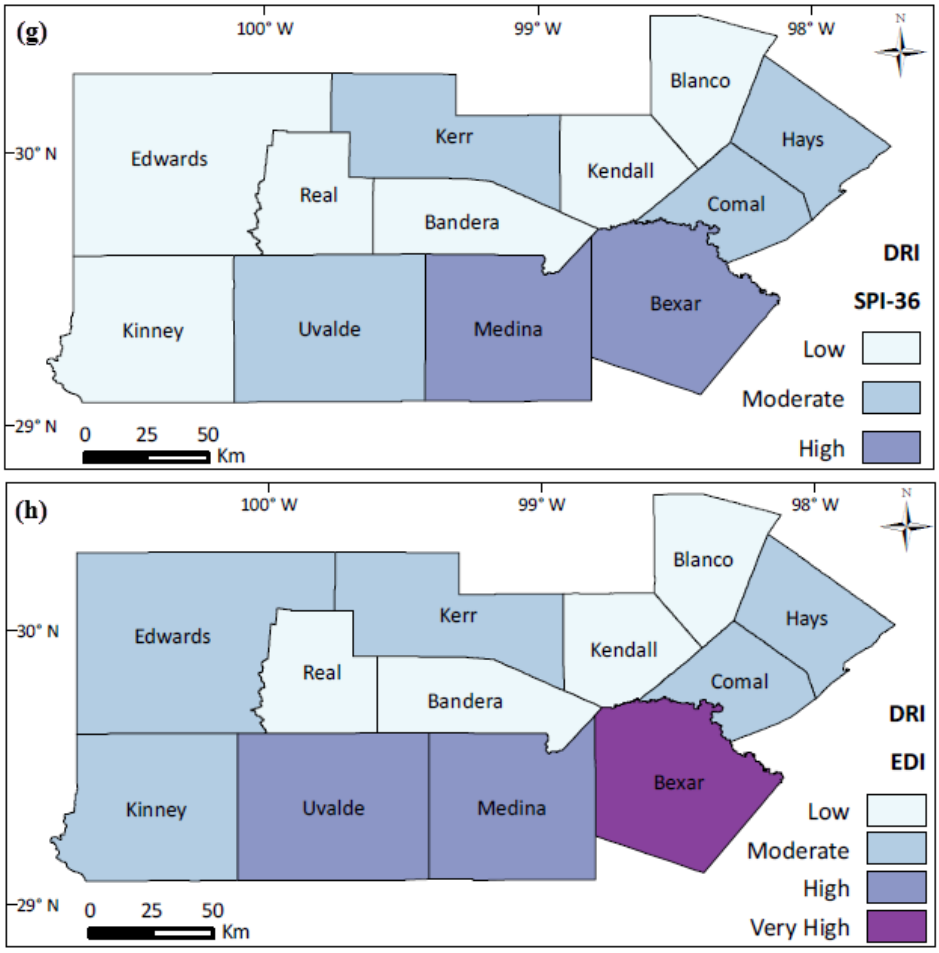

Figure 43. Risk maps of droughts at (g) 36-month time scale SPI and (h) EDI

The drought risk classification for 36-month drought can be seen from Figure 43g that most of the region was found under the low drought risk. Very high drought risk wasn't observed and 20.1% of the area was found under high drought risk, 30.5% of the area under moderate drought risk based on a 36 month time period drought (Table 23). On the other hand, 9.8% of the region was exposed to very high level risk, 22.5% of the region to high level risk, and 45.4% of the region to moderate level risk, based on the Effective Drought index (EDI). The spatial distribution of drought risk categories with a 12-month time scale SPI was similar to the drought risk of EDI except for Bexar county (Figure 42e and Figure 43h). Real, interestingly, was the only county detected as low DRI for any time scale SPI and EDI.

Table 23 Percentage of area under different drought risk categories for 36-month SPI and EDI

	Percentage of area (%)			
	Very High	High	Moderate	Low
36-month SPI	-	20.1	30.5	49.4
EDI	9.8	22.5	45.4	22.3

The same concern should be thought for evaluating the DRI similar to the DVI. For example, Bexar county was found under high drought risk category for 36-month SPI with DRI=0.56 and this value is pretty close to the limit value (0.5625) of DRI. Therefore, this county could be settled in "very high" risk category due to the safety coefficient for the decision making of drought. As mentioned in the vulnerability assessment part, however, original results are used to analyze and stick to the all original values.

When all things considered, very high drought risk was found by 9 and 24-month SPI and EDI in Bexar county (9.8% of the area). The highest percentage of the area in high level drought risk was detected by 1 and 12-month SPI as 32.3% of the area and 3-mont SPI found the highest moderate percentage of the area (79.5%). Bexar county was found under drought risk based on all time scale SPI and EDI (very high drought risk based on 9, 24-month SPIs and EDI). Medina, furthermore, was detected in high drought risk in terms of all time scale SPI (except 3-month SPI) and EDI.

6. CONCLUSIONS AND RECOMMENDATIONS

6.1 Conclusions

The study investigates spatial extent and impacts of droughts in the Edwards Aquifer region. Three main considerations were examined to assess drought risk. First, a non-dimensional conceptual index for drought hazard can be identified using drought frequency and severity. Second, drought vulnerability can be simplified by determining social/physical vulnerability factors on water demand and supply. Third, drought risk can be quantified by integrating both hazard and vulnerability. Therefore, a major outcome of this study is to produce a drought hazard/risk map of the Edwards Aquifer region.

In general, drought risk is higher in counties of the southern part of the area. The only one county, Real, has low drought risk at Effective Drought Index (EDI) and all time scale (1,3, 6, 9, 12, 24, and 36-month) Standardized Precipitation Index (SPI) and shows that lower drought vulnerability mostly corresponds to lower drought risk, since Real has the lowest Drought Vulnerability Index (DVI) in the area. Besides, Bexar has the highest DVI and the only county is found in very high level drought risk. It can be seen from the results that it is difficult to propound a relation between potential drought zone and rainfall distribution, since region-3 has faced higher level drought hazard than region-1 and region-2 has faced the most high level drought hazard. The results confirmed that higher drought risks are found where both high hazard and high vulnerability coincide. Most of the regions both east and west are found more or less prone to short term (based on 1 and 3- month SPI) and long term drought (9, 12, and 24-month SPIs). 9-month SPI can be

thought of as a bridge from a short term seasonal drought to long term drought. Some part of the south and west part of the area are found prone to drought based on the EDI. Therefore, hydrological drought can be thought of as a risk for the region due to the results of meteorological drought analysis. Groundwater level measurements (in J-17 index well used by the Edwards Aquifer Authority) reflect that there is a decreasing trend in last decades, especially within last ten years and twenty years (Figure A.10a and b).

6.2 Recommendations

Recommendations for the future work are listed below:

- Precipitation observations and length of data play a key role to analyze drought and the more number of stations and longer historical data set used, the more reliable results and the confidence level with which drought risk is measured.
- While both SPI and EDI can be used to monitor drought, EDI is found simpler than SPI. Thus, drought indices which are used to analyze drought should be multiple indices (more than one drought index) to compare and evaluate the results and EDI is getting to be a popular drought index because of its reliable results and simplicity.
- Drought occurrence probability should be calculated as event-based such as in this study in order to compare effectively the results.
- Drought vulnerability is a tricky part of drought risk assessment and indicators which are chosen for the vulnerability that has changed and varied from region to region. Therefore, it is essential to detect obtainable and quantifiable vulnerability

indicators. If it is possible, at least seven drought vulnerability indicators are suggested and indirect drought impacts also can be thought of for the vulnerability assessment. What is more, it is strongly suggest that DVI and the vulnerability map must be addressed together otherwise vulnerability can be misleading because of the values which are close to the critical level.

REFERENCES

Abramowitz, M., Stegun, I.A., 1965. Handbook of Mathematical Functions with Formulas, Graphs, and Mathematical Tables. Dover Publications, Inc., New York, New York, pp. 1046.

Agrilife, T.A.M.U., 2011. Available at: http://today.agrilife.org/2011/08/17/texas-agricultural-drought-losses-reach-record-5-2-billion/.

Akhtari, R., Morid, S., Mahdian, M.H., Smakhtin, V., 2009. Assessment of areal interpolation methods for spatial analysis of SPI and EDI drought indices. Int. J. Climatol., 29(1), 135-145.

American Heritage Dictionary, 1976. Houghton Mifflin, Boston.

American Meteorological Society (AMS), 2004. Statement on meteorological drought. Bull. Am. Meteorol. Soc. 85, 771–773.

Arnow, T., 1963. Ground-water geology of Bexar County, Texas. US Government Printing Office.

Blaikie, P.M., Cannon, T., Davis, I., Wisner, B., Blaikie, P., 1994. At risk: natural hazards, people's vulnerability, and disasters. Routledge, New York.

Bryant, E.A., 1991. Natural Hazards. Cambridge University Press, Cambridge, United Kingdom, pp. 294.

Byun, H.R., Wilhite, D.A., 1999. Objective quantification of drought severity and duration. J. Clim., 12(9), 2747-2756.

Chen, C.C., Gillig, D., McCarl, B.A., 2001. Effects of climatic change on a water dependent regional economy: A study of the Texas Edwards Aquifer. Clim. Change, 49(4), 397-409.

De Silva, R., Dayawansa, N., Ratnasiri, M., 2007. A comparison of methods used in estimating missing rainfall data. J. Agric. Sci., 3(2), 101-108.

Delhomme, J.P., 1978. Kriging in the Hydrosciences. Adv. Water Resour., 1(5), 251-266.

Dilley, M., Chen, R.S., Deichmann, U., LernerLam, A.L., Arnold, M., 2005. Natural disaster hotspots: A global risk analysis. World Bank Inst., Washington, 1-134

Dogan, S., Berktay, A., Singh, V.P., 2012. Comparison of multi-monthly rainfall-based drought severity indices, with application to semi-arid Konya closed basin, Turkey. J. Hydrol., 470, 255-268.

Dogan, S., 2013. Spatio-temporal analysis of drought characterization in Konya closed basin, Ph.D. Thesis, Selcuk University, Konya, Turkey

Dracup, J.A., Lee, K.S., Paulson, E.G., 1980. On the definition of drought. Water Resour. Res., 16(2), 297-302.

Du, X.Y., Lin, X.F., 2012. Conceptual model on regional natural disaster risk assessment. 2012 International Symposium on Safety Science and Technology, 45, 96-100.

Edwards Aquifer Authortiy, 1996. Edwards Aquifer Hydrogeologic report for 1996. Available at: http://www.edwardsaquifer.org/scientific-research-and-reports/hydrologic-data-reports

Edwards Aquifer Authority, 2013. Hydrologic Data Report. Report No. 14-02. Available at: http://www.edwardsaquifer.org/documents/2014_Tramallo-etal_2013HydrologicData.pdf

Ferrier, N., Haque, C.E., 2003. Hazards risk assessment methodology for emergency managers: A standardized framework for application. Nat. Hazards, 28(2-3), 271-290.

Fohn, J., 1996. Agricultural Column, San Antonio Express News, San Antonio, Texas, 21 August.

Gumbel, E.J., 1963. Statistical forecast of droughts. Bull. Int. Assoc. Sci. Hydrol. 8(1), 5-23.

Guttman, N.B., 1994. On the sensitivity of sample-L moments to sample-size. J. Clim., 7(6), 1026-1029.

Guttman, N.B., 1999. Accepting the standardized precipitation index: A calculation algorithm. J. Am. Water Resour. Assoc., 35(2), 311-322.

Hagman, G., 1984. Prevention better than cure: Report on human and natural disasters in the third world, Swedish Red Cross, Stockholm

Hennessy, K. et al., 2008. An assessment of the impact of climate change on the nature and frequency of exceptional climatic events. Report by Climate and Ocean Services Bureau of Meteorology, CSIRO Climate Adaptation Flagship and Drought Policy Review Climate Change Division Department of Agriculture Fisheries and Forestry, Melbourne, Australia.

Hisdal, H., Tallaksen, L.M., 2003. Estimation of regional meteorological and hydrological drought characteristics: a case study for Denmark. J. Hydrol., 281(3), 230-247.

Kates, R.W., Kasperson, J.X., 1983. Comparative risk analysis of technological hazards. Proceedings of the National Academy of Sciences of the United States of America-Physical Sciences, 80(22), 7027-7038.

Keyantash, John & National Center for Atmospheric Research Staff (Eds). Last modified 28 Mar 2014. "The Climate Data Guide: Standardized Precipitation Index (SPI)." Retrieved from https://climatedataguide.ucar.edu/climate-data/standardized-precipitation-index-spi.

Kim, D.W., Byun, H.R., Choi, K.S., 2009. Evaluation, modification, and application of the Effective Drought Index to 200-Year drought climatology of Seoul, Korea. J. Hydrol., 378(1-2), 1-12.

Kim, H., Park, J., Yoo, J., Kim, T.-W., 2013. Assessment of drought hazard, vulnerability, and risk: A case study for administrative districts in South Korea. J. Hydro-environ. Res., http://dx.doi.org/10.1016/j.jher.2013.07.003

McKee, T.B., Doesken, N.J., Kleist, J., 1993. The relationship of drought frequency and duration to time scales. In: Proceedings of the 8th Conference on Applied Climatology, Anaheim, CA, USA, 179–184.

Mishra, A.K., Singh, V.P., 2010. A review of drought concepts. J. Hydrol., 391(1-2), 204-216.

Mishra, A.K., Singh, V.P., 2011. Drought modeling - A review. J. Hydrol., 403(1-2), 157-175.

National Agricultural Statistics Service of USDA, 2012. available at http://www.agcensus.usda.gov/Publications/2012/Online_Resources/County_Profiles/Texas/index.asp.
National Drought Mitigation Center, University of Nebraska-Lincoln, USA. Available at: http://drought.unl.edu/DroughtBasics/TypesofDrought.aspx.
O'Brien, M., 2000. Making better environmental decisions: An alternative to risk assessment, The MIT Press, Cambridge, MA.
Palmer, W.C., 1965. Meteorological Drought. US Department of Commerce, Weather Bureau, Research Paper No. 45.
Pandey, R.P., Dash, B.B., Mishra, S.K., Singh, R., 2008. Study of indices for drought characterization in KBK districts in Orissa (India). Hydrol. Process., 22(12), 1895-1907.
Random House Dictionary, 1969. Random House, New York.
Redmond, K.T., 2000. Integrated climate monitoring for drought detection, in drought: A Global Assessment, edited byWilhite, D. A., Routledge, 145–158, 2000, London.
Schneider, S.H., 1996. Encyclopaedia of Climate and Weather. Oxford University Press, New York.
Smith, K., 1996. Environmental Hazards: Assessing risk and reducing disaster, 2nd edn., Routledge, London.
Sonmez, F.K., Komuscu, A.U., Erkan, A., Turgu, E., 2005. An analysis of spatial and temporal dimension of drought vulnerability in Turkey using the standardized precipitation index. Nat. Hazards, 35(2), 243-264.
Texas Water Development Board, TWDB, 2012. Available at: http://www.twdb.state.tx.us/publications/state_water_plan/2012/2012_SWP.pdf
Texas Water Development Board, TWDB, 2014. Available at: http://www.twdb.state.tx.us/groundwater/.
Thom, H.C.S., 1958. A note on the gamma distribution. Monthly Weather Rev. 86, 117-122.
Thom, H.C.S., 1966. Some methods of climatological analysis. WMO Technical Note Number 81, Secretariat of the World Meteorological Organization, Geneva, Switzerland, pp. 53.
U.S. Water News Online, 1996. Drought alert sounded in Edwards Aquifer Region of Texas, March.
UN Secretariat General, 1994. United Nations convention to combat drought and desertification in countries experiencing serious droughts and/or desertification, particularly in Africa, Paris, France.
United Nations Development Programme, 2004. Reducing Disaster Risk: A challenge for development. A Global Report, New York: UNDP-Bureau for Crisis Prevention and Recovery (BRCP).
Wilhite, D.A., 1992. 'Drought', Encyclopaedia of Earth System Science, Vol. 2, 81-92, San Diego, CA: Academic Press.
Wilhite, D.A., 2000. Drought as a natural hazard: concepts and definitions. In: Wilhite DA (ed) Drought: a global assessment. hazards and disasters: a series of definitive major works. Routledge Publishers, New York, USA.

Wilhite, D.A., Buchanan-Smith, M., 2005. Drought as hazard: understanding the natural and social context. In: Wilhite DA (ed) Drought and water crises: science, technology, and management issues. CRC Press, Taylor & Francis Group, Florida, 3–29.

Wilhite, D.A., Glantz, M.H., 1985. Understanding the drought phenomenon: the role of definitions. Water Int 10, 111–120.

Wilhite, D.A., Glantz, M.H., 1987. 'Understanding the drought phenomenon: The role of definitions', in D.A. Wilhite and W.E. Easterling (eds), Planning for Drought: Toward a Reduction of Societal Vulnerability, Boulder, CO: estview Press, 11-27.

Wilson, R., Crouch, E.A.C., 1987. Risk assessment and comparisons - An introduction. Science, 236(4799), 267-270.

World Meteorological Organization (WMO), 1986. Report on drought and countries affected by drought during 1974–1985, WMO, Geneva, pp. 118.

Wu, H., Wilhite, D.A., 2004. An operational agricultural drought risk assessment model for Nebraska, USA. Nat. Hazards, 33(1), 1-21.

Yevjevich, V., 1967. An objective approach to definitions and investigations of continental hydrologic droughts. Hydrology papers / Colorado State University; no. 23. Colorado State University, Fort Collins.

Zelenakova, M., Gargar, I., Purcz, P., 2012. Drought risk assessment in Libya by statistical methods, 12th International Multidisciplinary Scientific GeoConference, www.sgem.org, SGEM2012 Conference Proceedings/ ISSN 1314-2704, June 17-23, 2012, Vol. 3, 633 – 640.

APPENDIX

Table A.1 Station names and referring to numbers in Edwards Aquifer region

Station number	Station name	Latitude	Longitude
1	Blanco	30.10	-98.42
2	Boerne	29.82	-98.75
3	Brackettville 22 N	29.68	-100.45
4	Brackettville	29.32	-100.42
5	Bulverde	29.75	-98.45
6	Camp wood	29.67	-100.02
7	Canyon dam	29.87	-98.20
8	Carta valley	29.80	-100.67
9	Comfort 2	29.97	-98.90
10	Dripping springs 6 E	30.22	-97.98
11	Fischers store	29.98	-98.27
12	Hondo	29.33	-99.15
13	Hunt 10 W	30.05	-99.52
14	Ingram number 2	30.08	-99.23
15	Kerrville 3 NNE	30.07	-99.12
16	Leakey	29.73	-99.77
17	Medina 1 NE	29.80	-99.25
18	New braunfels	29.70	-98.12
19	Northington ranch	29.88	-98.65
20	Prade ranch	29.92	-99.77
21	Riomedina	29.47	-98.87
22	Rocksprings	30.02	-100.22
23	Sabinal	29.32	-99.47
24	San Antonio International Airport	29.53	-98.47
25	San Marcos	29.87	-97.95
26	Sisterdale	29.98	-98.72
27	Spring branch 2 SE	29.87	-98.38
28	Tarpley	29.65	-99.25
29	Utopia	29.62	-99.52
30	Vanderpool 4 N	29.81	-99.58
31	Wimberley 1 NW	29.98	-98.05

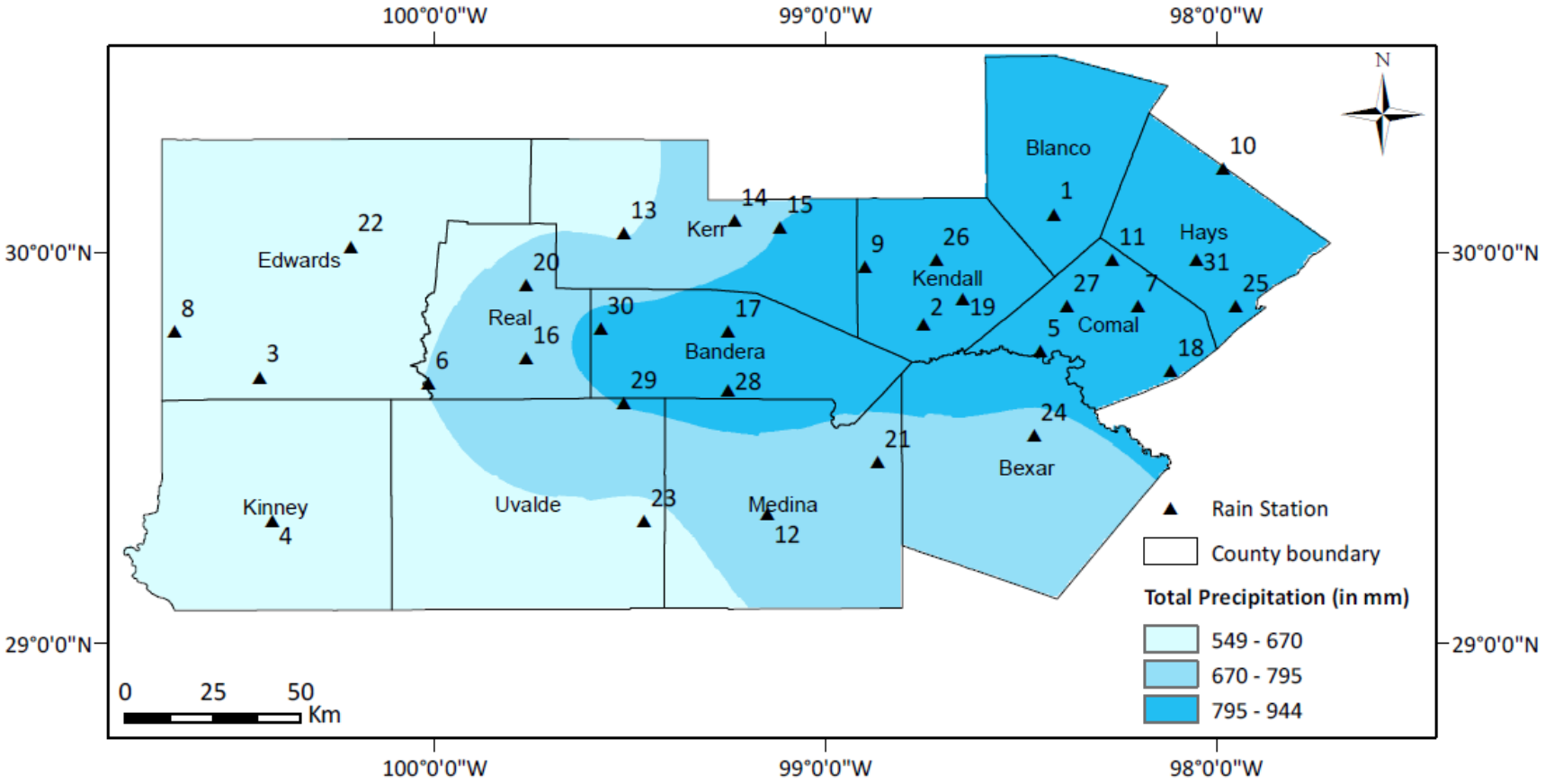

Figure A.1. Spatial distribution of average precipitation at the county level in Edwards Aquifer region

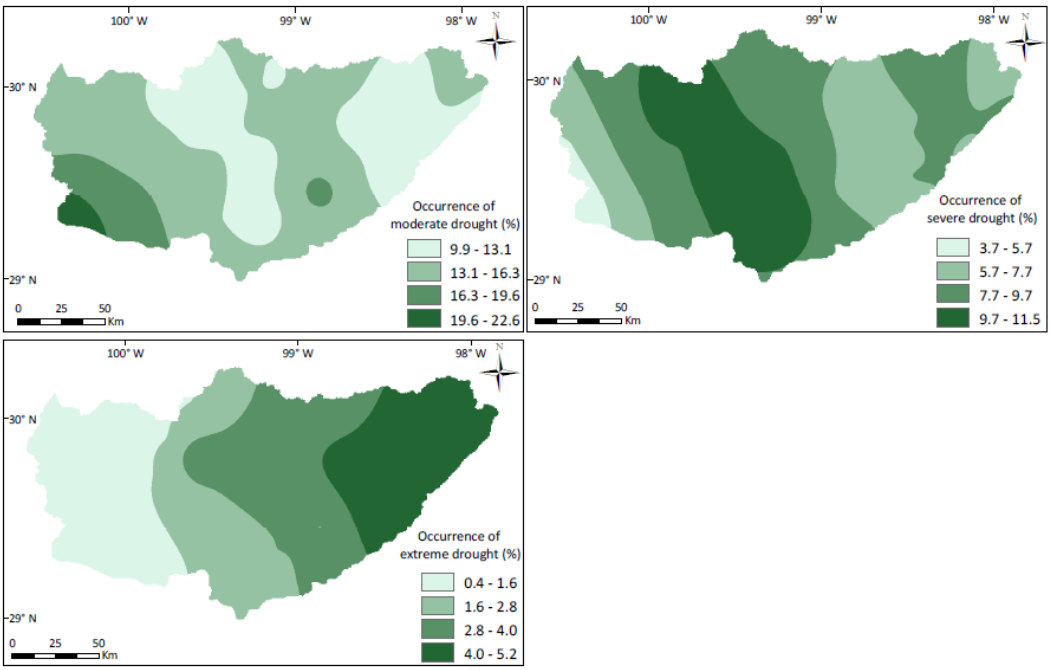

Figure A.2. Drought occurrences: (a) moderate, (b) severe, and (c) extreme drought at a 1-month SPI time step

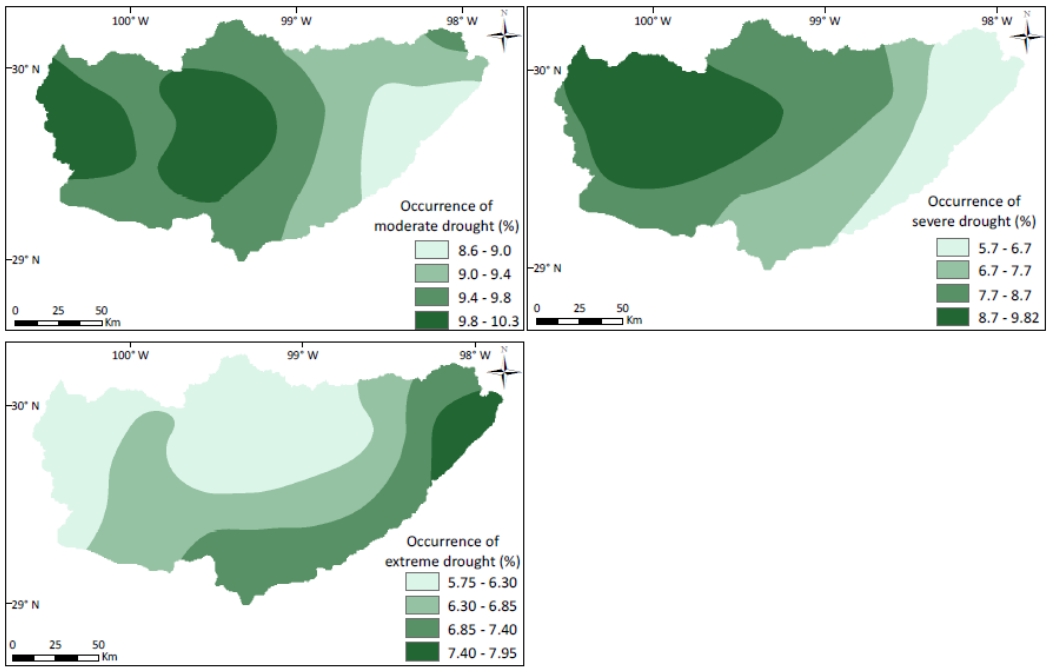

Figure A.3. Drought occurrences: (a) moderate, (b) severe, and (c) extreme drought at a 3-month SPI time step

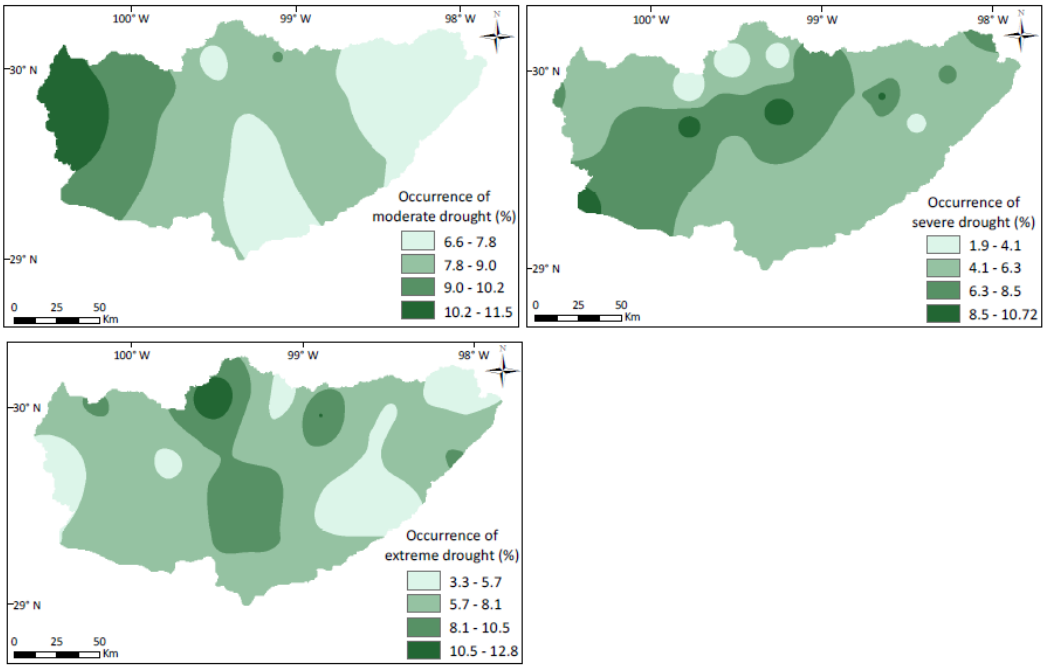

Figure A.4. Drought occurrences: (a) moderate, (b) severe, and (c) extreme drought at a 6-month SPI time step

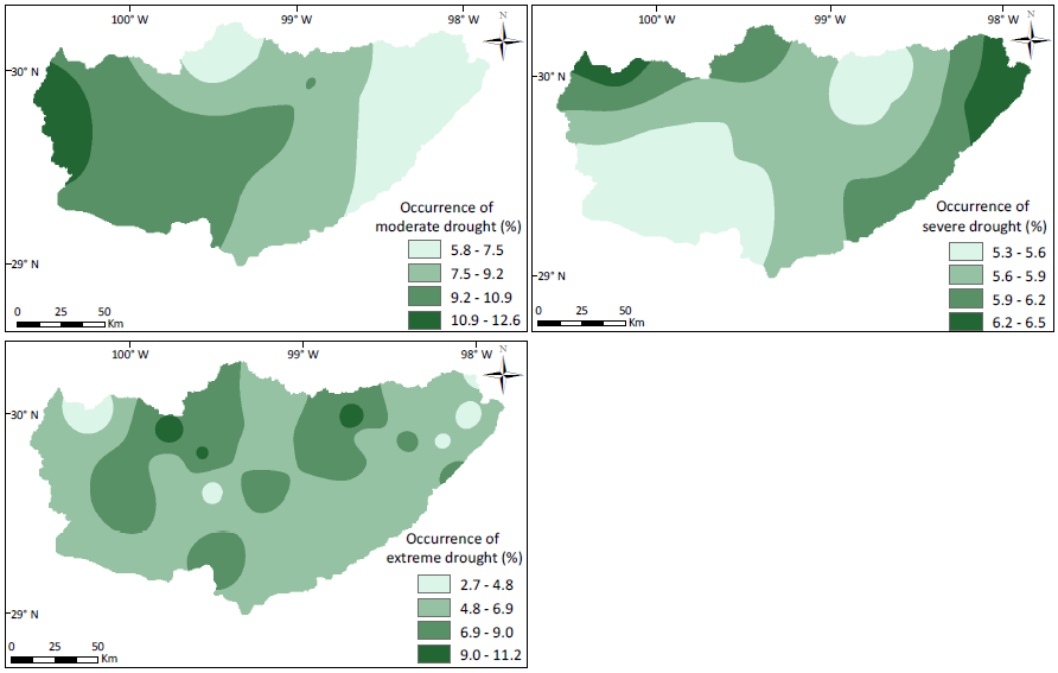

Figure A.5. Drought occurrences: (a) moderate, (b) severe, and (c) extreme drought at a 9-month SPI time step

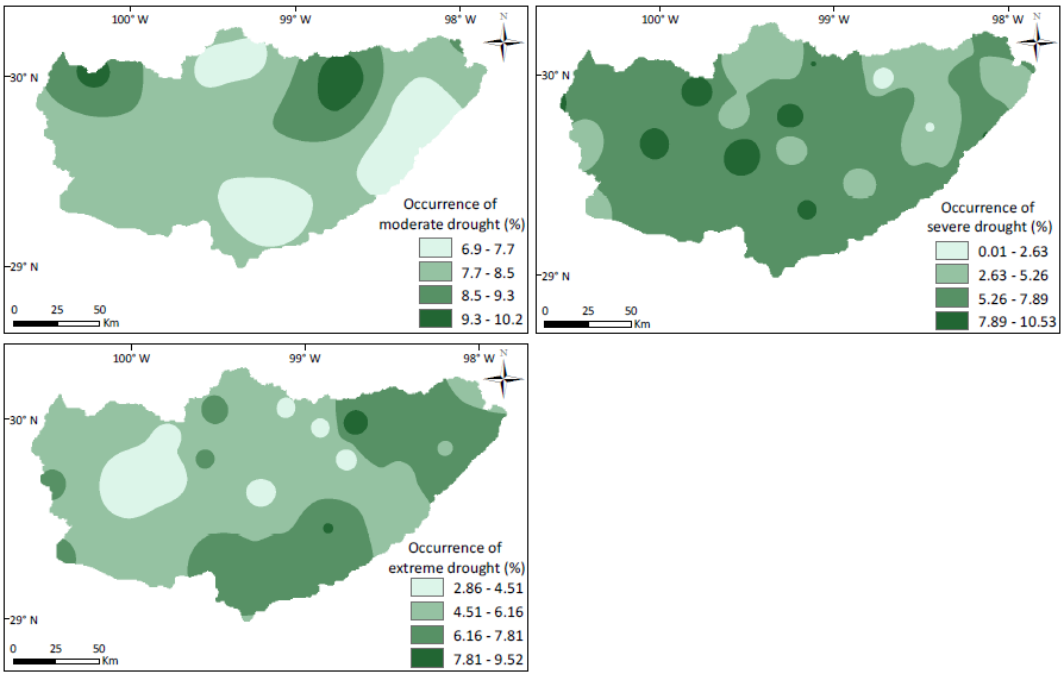

Figure A.6. Drought occurrences: (a) moderate, (b) severe, and (c) extreme drought at a 12-month SPI time step

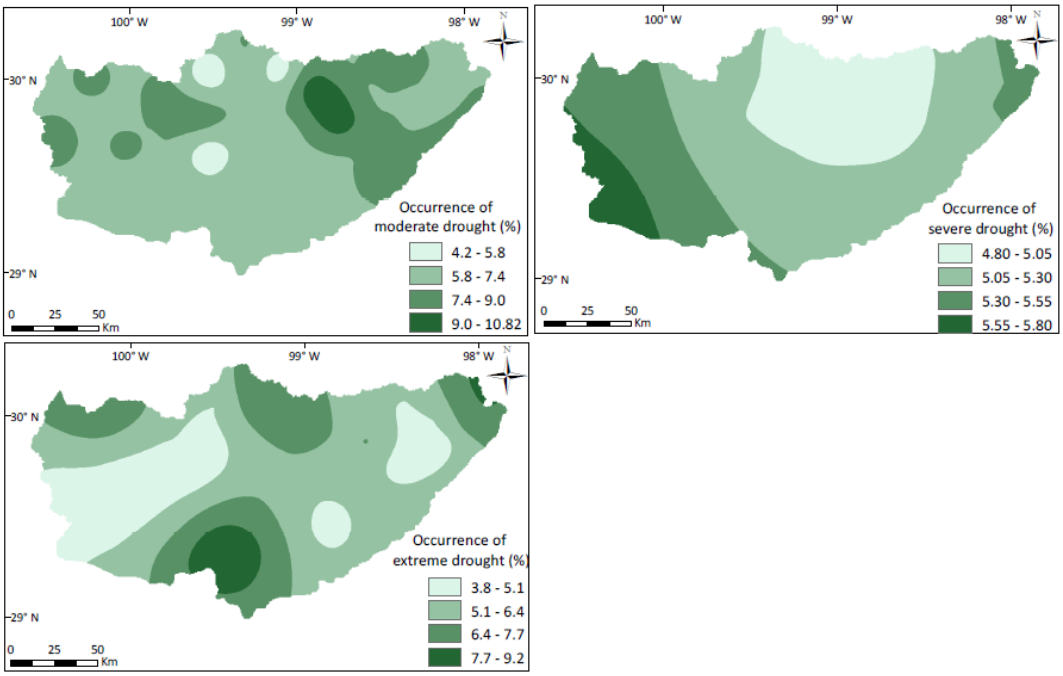

Figure A.7. Drought occurrences: (a) moderate, (b) severe, and (c) extreme drought at a 24-month SPI time step

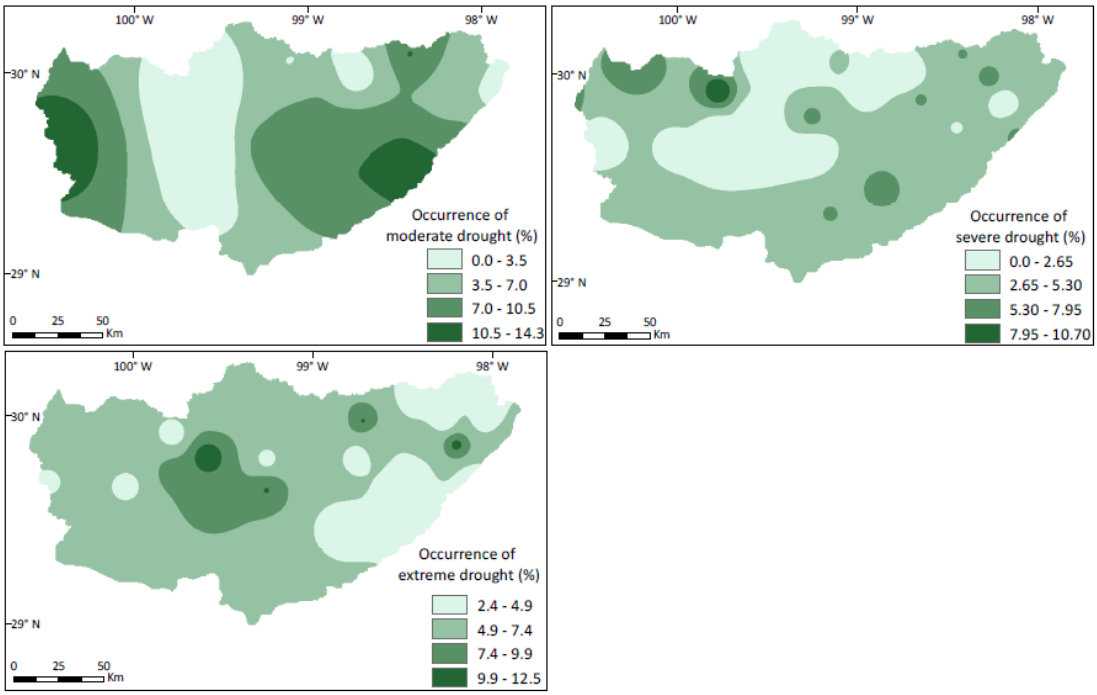

Figure A.8. Drought occurrences: (a) moderate, (b) severe, and (c) extreme drought at a 36-month SPI time step

(Note: Spatial distribution of severe and extreme drought occurrences at 36-month SPI was mapped based on the inverse distance method because of the difficulties of kriging interpolation method similar to Figure A.6)

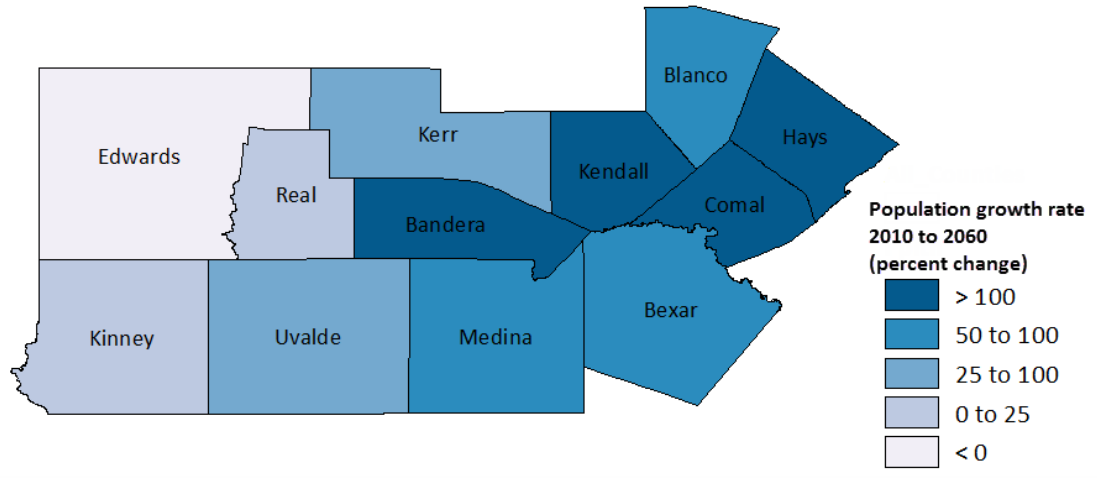

Figure A.9. Projected population growth in Edwards Aquifer region counties (Source: modified from "Water for Texas 2012 State Water Plan", TWDB, 2012)

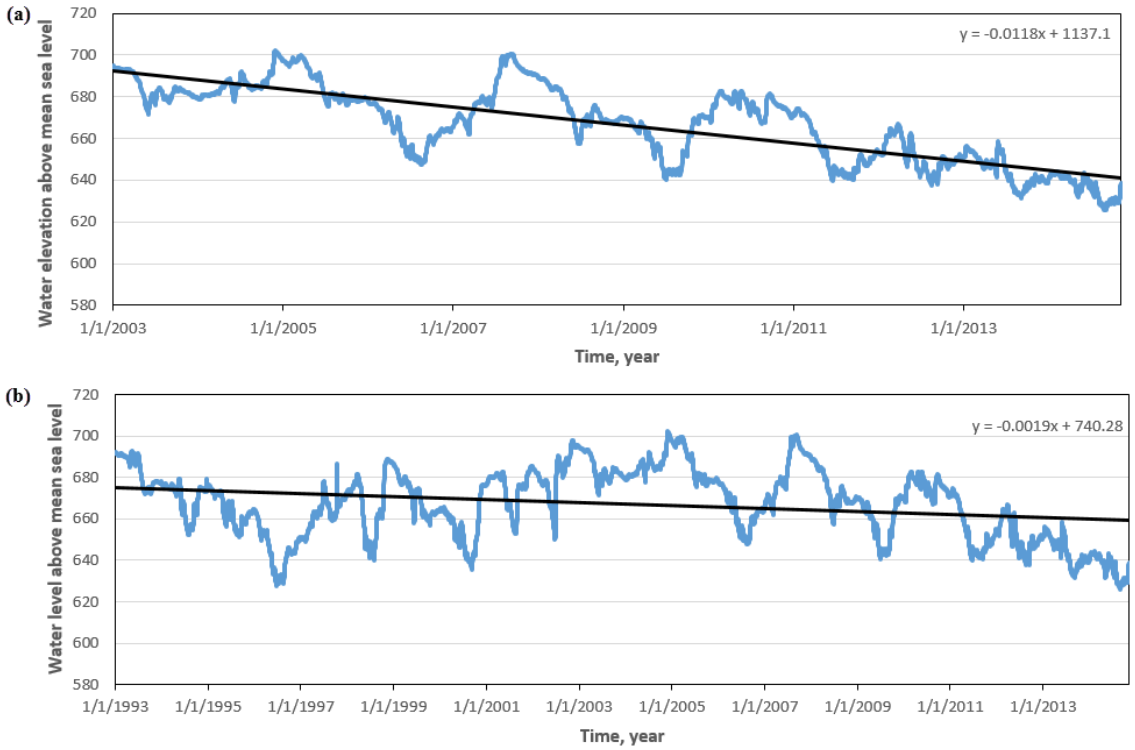

Figure A.10. Groundwater hydrograph in the Edwards Aquifer (J-17 index well)